involve

a journal of mathematics

mathematical sciences publishers

2010 vol. 3, no. 1

involve

pjm.math.berkeley.edu/involve

See inside back cover or http://pjm.math.berkeley.edu/involve for submission instructions and subscription prices.
Subscriptions, requests for back issues from the last three years and changes of subscribers address should be sent to Mathematical Sciences Publishers, Department of Mathematics, University of California, Berkeley, CA 94704-3840, USA.

Involve, at Mathematical Sciences Publishers, Department of Mathematics, University of California, Berkeley, CA 94720-3840 is published continuously online. Periodical rate postage paid at Berkeley, CA 94704, and additional mailing offices.

For production workflow, Involve uses EditFLOW from Mathematical Sciences Publishers.

PUBLISHED BY

mathematical sciences publishers

http://www.mathscipub.org

A NON-PROFIT CORPORATION

Typeset in LaTeX

INVOLVE 3:1(2010)

On the relationship between volume and surface area

Joseph N. Krenicky and Jan Rychtář

(Communicated by Kenneth S. Berenhaut)

We show that the statement that the surface area is the derivative of the volume, which is well known for a ball, can be generalized and stated in a proper way for any set with finite volume and surface area. We also provide a specific statement for star-shaped sets.

1. Introduction

The well known connection between the area of a disk $A = \pi r^2$ and its circumference $C = 2\pi r$ is

$$\frac{\mathrm{d}A}{\mathrm{d}r} = C.$$

The same type of formula,

$$\frac{\mathrm{d}V}{\mathrm{d}r} = S, \tag{1}$$

holds for a volume V of a ball and its surface area S. In fact, it holds for Euclidean balls in any dimension. Indeed, as derived in [Kendall 1961], the n-dimensional volume of an n-dimensional ball of radius r is

$$V_n(r) = \frac{r^n \pi^{n/2}}{\Gamma\left(\frac{n}{2}+1\right)}, \tag{2}$$

where $\Gamma(z) = \int_0^\infty t^{z-1} e^{-t}\,\mathrm{d}t$ is the gamma function [Abramowitz and Stegun 1972, Chapter 6], while the $(n-1)$-dimensional volume of a surface of the ball is [Coxeter 1963, p. 125]

$$S = \frac{2r^{n-1}\pi^{n/2}}{\Gamma\left(\frac{n}{2}\right)} = \frac{nr^{n-1}\pi^{n/2}}{\Gamma\left(\frac{n}{2}+1\right)} = \frac{\mathrm{d}V_n(r)}{\mathrm{d}r}.$$

MSC2000: 28A75, 51M25.

Keywords: volume, surface, star-shaped sets.

J. N. Krenicky was an undergraduate research assistant supported by the Office of Undergraduate Research of The University of North Carolina at Greensboro.

Emert and Nelson [1997] generalized Equation (1) for regular n-dimensional polytopes. First they showed that

$$\frac{\mathrm{d}}{\mathrm{d}r}\lambda_n(P_r) = \lambda_{n-1}(\partial P_r), \tag{3}$$

where r is the inner radius of the polytope, that is, the minimal distance from a center to the boundary ∂P_r. Theorem 2 of their paper is a generalization of the formula in (3) to any polytope P_r that circumscribes a ball of radius r.

The main aim of this paper is to generalize (3) to a larger family of sets. We show that when formulated properly, (3) holds for any set with finite volume and surface area.

2. Definitions and preliminaries

Let $n \geq 2$ be a fixed natural number. All sets considered will be subsets of $\mathbb{R}^n$. The n-dimensional Lebesgue measure on $\mathbb{R}^n$ will be denoted by λ_n.

We recall the notion of *similarity* between sets in $\mathbb{R}^n$, which is an equivalence relation. Two subsets S_1 and S_2 of $\mathbb{R}^n$ are *similar*, and we write $S_1 \sim S_2$, if there exist $c \in \mathbb{R}^n$ and $\alpha > 0$ such that the image of S_1 under the map defined by

$$f_{c,\alpha}(x) = c + \alpha(x - c), \quad x \in \mathbb{R}^n, \tag{4}$$

is congruent to S_2 — that is, there is an isometry of $\mathbb{R}^n$ taking $f_{c,\alpha}(S_1)$ to S_2. The map $f_{c,\alpha}$ is the *homothety* or *scaling* of center c and ratio α. It preserves the point c and dilates or contracts distances between any two points by a factor of α.

An equivalence class of $\sim$ will be called a *shape*. A *ball* is an example of a shape. One can shift, rotate, or resize it, and always get a ball.

Let $d > 0$ be any positive real number. The d-dimensional *Hausdorff measure* [Federer 1969; Morgan 2000] of a set E is defined by

$$H^d(E) = \limsup_{\delta \to 0+} H^d_\delta(E)\,,$$

where $H^d_\delta(E)$ is the infimum, over all countable covers of E by sets A_i of diameter at most δ, of a measure of volume associated with the cover:

$$H^d_\delta(E) = \inf\left\{ \sum_{i=1}^{\infty} V_d\left(\frac{\operatorname{diam} A_i}{2}\right) : E \subset \bigcup_{i=1}^{\infty} A_i,\ \operatorname{diam} A_i < \delta \right\}.$$

Here the summand is the Lebesgue measure of a ball of radius $\frac{1}{2}\operatorname{diam} A_i$; see (2). On Borel sets of $\mathbb{R}^n$, $H^n = \lambda_n$ [Morgan 2000, Corollary 2.8]. For any set S and any point c,

$$H^d\big(f_{c,\alpha}(S)\big) = \alpha^d H^d(S)\,. \tag{5}$$

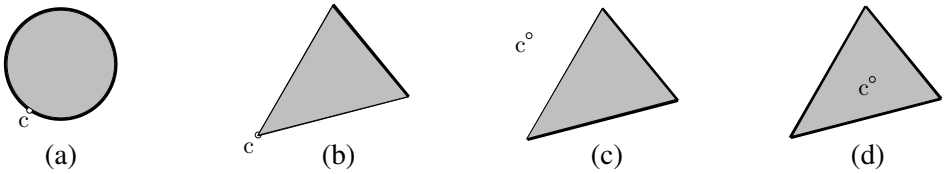

Figure 1. Horizons of c visibility (in bold) for different sets (in gray) and different positions of point c.

The *Hausdorff dimension* [Morgan 2000] of a nonempty set E is defined by

$$\dim_H E = \inf\{\, d \geq 0 : H^d(E) < \infty\}.$$

For $c \in \mathbb{R}^n$ we will call a map ∂_c the *generalized boundary* if it maps subsets of $\mathbb{R}^n$ to subsets of $\mathbb{R}^n$, assigns measurable sets to measurable sets, and satisfies

$$\partial_c(f_{c,\alpha}(S)) = f_{c,\alpha}(\partial_c(S)), \tag{6}$$

for all $\alpha > 0$ and all $S \subset \mathbb{R}^n$. It means that the boundary grows and shrinks together with the set S, but it is not necessarily invariant under translations or other isometries, nor connected to S in any sense. For example, the topological boundary is a generalized boundary.

If S is a set and $c \in \mathbb{R}^n$ any point, we define the *horizon of c-visibility* $\partial_c^* S$ by

$$\partial_c^* S = (\mu_{S,c})^{-1}(1),$$

where $\mu_{S,c} : \mathbb{R}^n \mapsto [0, \infty]$ is the *Minkowski functional* [Fabian et al. 2001, p. 42] given by

$$\mu_{S,c}(x) = \begin{cases} \inf\{r > 0,\ x \in f_{c,r}(S)\}, & \text{if } x \in f_{c,r}(S) \text{ for some } r < \infty, \\ \infty, & \text{otherwise.} \end{cases}$$

It follows directly from the definition that $\partial_c^* S$ is measurable when S is. Yet $\partial_c^* S$ does not have to be closed (Figure 1a); it does not coincide with the topological boundary ∂ even if it is closed (Figure 1a–c), and ∂_c^* is not preserved by shifts (Figure 1b–d). On the other hand, it satisfies (6). Thus ∂_c^* is a generalized boundary.

A set S is called *star-shaped* if there is a point $c \in S$ such that for every point $p \in S$ the line segment $\overline{cp}$ is contained in S. Such a point c is called a *center* of S. A star-shaped set can have many centers; for example, every convex set C is star-shaped and every point $c \in C$ is its center. However, not all star-shaped sets are convex; see, for instance, the drawing at the end of this section.

A set S is called *flat* if S is contained in an affine subspace $p + \mathbb{R}^{\lceil \dim_H S \rceil}$ for some point $p \in \mathbb{R}^n$, where $\lceil\ \rceil$ denotes the ceiling function (least integer not less than). If c is a point and S a flat set, we define $d_f(c, S)$ to be the distance from c

to the affine space $p + \mathbb{R}^{\lceil \dim_H S \rceil}$ that witnesses the flatness of S. Here we see a flat and a nonflat subset of $\mathbb{R}^2$ of dimension 1:

We say that a star-shaped set S *circumscribes a ball of radius* r *in a generalized sense* if there is a center c of S and the decomposition of $\partial_c^* S$ into countably many pairwise disjoint measurable sets F_i, $i \geq 0$, such that

(a) $\operatorname{dist}(f, c) = r$, for any $f \in F_0$,

(b) the sets F_i, $i \geq 1$, are flat, and

(c) $d_f(c, F_i) = r$, for all $i \geq 1$.

By the definition, the center of the circumscribed ball is a center of the set S. Here is a nontrivial set S circumscribing a ball in a generalized sense:

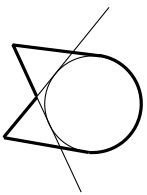

3. Generalization of the volume-area relationship

We now state the key lemma that is in fact a direct consequence of (5).

Lemma 1. *Let S and B be* any *measurable sets, fix $c \in \mathbb{R}^n$ and let $d \geq 1$ be such that $H^d(B) \in (0, \infty)$ and $H^{d-1}(S) \in (0, \infty)$. Set $S_r = f_{c,r}(S)$ and $B_r = f_{c,r}(B)$. Then*

$$\frac{\mathrm{d}}{\mathrm{d}h} H^d(B_r) = H^{d-1}(S_r),$$

where

$$h = d \frac{H^d(B)}{H^{d-1}(S)} r.$$

Also

$$H^d(B_r) = \frac{H^d(B)}{H^{d-1}(S)} H^{d-1}(S_r) r. \tag{7}$$

Proof.

$$\begin{aligned} \frac{\mathrm{d}}{\mathrm{d}h} H^d(B_r) &= \frac{\mathrm{d}}{\mathrm{d}r} H^d(B_r) \cdot \frac{\mathrm{d}r}{\mathrm{d}h} = \frac{\mathrm{d}}{\mathrm{d}r} \left(r^d H^d(B)\right) \cdot \left(d \frac{H^d(B)}{H^{d-1}(S)}\right)^{-1} \\ &= r^{d-1} H^{d-1}(S) = H^{d-1}(S_r). \end{aligned}$$

Equation (7) follows directly from (5). □

It follows from Lemma 1 that there is always a relationship in the spirit of (3) between any pairs of families $\{S_r\}, \{B_r\}$ that are being "inflated" together (but otherwise may have nothing in common). In particular, S does not have to be a boundary of B in any sense, B does not have to be convex or of any particular shape, and the center of inflation c can be anywhere. However, the price for such general assumptions is the need to differentiate with respect to h, the multiple of the inflation factor r, not with respect to r itself.

The parameter $n(\lambda_n(C)/(\lambda_{n-1})(\partial C))$ for convex polytopes in $\mathbb{R}^n$ was studied by Fjelstad and Ginchev [2003]. They called h the *harmonic parameter* of C and showed that it is a weighted average of distances from a central point to the faces (the weight being proportional to the size of the face), and for some objects like boxes, it is the harmonic mean of distances from a central point to the faces of the object, thus providing certain geometrical intuition when Lemma 1 is applied to B and $S = \partial B$.

The next theorem shows that, for reasonable shapes, there is always an appropriate representative of the shape that makes the parameter h to be exactly r, that is, (3) holds for that shape.

Theorem 2. *Let $\mathfrak{S}$ be a shape, fix $d \geq 1$, $c \in R^n$, and let ∂_c be a generalized boundary such that, for some $B \in \mathfrak{S}$,*

(i) $H^d(B) \in (0, \infty)$, *and*

(ii) $H^{d-1}(\partial_c B) \in (0, \infty)$.

Then there is a $B_1 \in \mathfrak{S}$ such that

$$\frac{\mathrm{d}}{\mathrm{d}r} H^d\big(f_{c,r}(B_1)\big) = H^{d-1}\big(f_{c,r}(\partial_c B_1)\big).$$

Proof. By Lemma 1 we need to find $B_1 \in \mathfrak{S}$ such that $h = r$, that is,

$$\frac{H^{d-1}(\partial_c B_1)}{H^d(B_1)} = d. \tag{8}$$

For that, by (7), it is enough to take

$$B_1 = f_{c,\alpha}(B), \quad \text{where } \alpha = \frac{H^{d-1}(\partial_c B)}{d\,H^d(B)}. \qquad \square$$

The statements of Theorem 2 may seem too abstract. However, in general, we cannot do any better, since a shape is a purely geometrical object. For example, without our measuring the distance, all balls in $\mathbb{R}^3$ are alike. If we can measure a distance, we can pick a ball and say this is the ball with radius 1. If we pick the wrong ball, say with radius $\varrho \neq 1$, its r-inflation would have volume $\frac{4}{3}\pi(\varrho r)^3$ and surface area $4\pi(\varrho r)^2$ — losing the relationship (3). Hence choosing the right representative for balls is equivalent to choosing the length unit.

We can pick the proper representative for cubes as well. Picking the cube with side length 1 is not good, since its r-inflation has volume $V = r^3$ and surface area $S = 6r^2$, that is, $\mathrm{d}V/\mathrm{d}r \neq S$. For cubes the right representative is a cube with side length 2, because then its r inflation has volume $V = 8r^3$ and surface area $S = 24r^2$, thus recovering (3). It was observed by Emert and Nelson [1997] that this right cube circumscribes the ball of radius 1 (which we already know is a special ball).

As another example, consider a torus — which is not a star-shaped set — with radii R and r (where r is a radius of the tube and R is a distance from a center of the tube to the center of the torus). Note that the shape is determined by the fraction R/r. The volume of such a torus is $V = 2\pi^2 Rr^2$ and the surface area is $A = 4\pi^2 Rr$. The right representative for a torus shape is a torus T_1 that satisfies $A/V = 3$, that is, the one that is inflated to have $r = 2/3$. Observe that there is apparently nothing significant about that particular torus. However, in order to know which representative to pick, we had to know how to calculate the volume and surface area of a torus in general. In the next section, we will show how to avoid this problem for certain star-shaped sets.

4. Star-shaped sets

The following lemma is an easy consequence of the definition of a star-shaped set.

Lemma 3. *A closed set S is star-shaped if and only if there is a point $c \in S$ such that*

$$S = \bigcup_{\alpha\in[0,1]} f_{c,\alpha}(\partial_c^* S). \tag{9}$$

The next theorem shows how to pick a representative S_1, whose existence is guaranteed by Theorem 2, from among certain star-shaped sets.

Theorem 4. *Let $d \geq 1$ and S_1 be a closed star-shaped set that circumscribes a ball of radius 1 centered at c in a generalized sense. Then*

$$H^d(S_1) = \frac{1}{d} H^{d-1}(\partial_c^* S_1).$$

In particular, if $H^d(S_1) \in (0, \infty)$, then

$$\frac{\mathrm{d}}{\mathrm{d}r} H^d\big(f_{c,r}(S_1)\big) = H^{d-1}\big(f_{c,r}(\partial_c^* S_1)\big).$$

Proof. Let F_i, $i \geq 0$, be the decomposition of $\partial_c^* S$ that witnesses that S circumscribes a ball of radius 1 centered at c in a generalized sense. Set

$$C_i = \bigcup_{\alpha\in[0,1]} f_{c,\alpha}(F_i), \quad i \geq 0.$$

Namely, C_i is the cone corresponding to the face F_i. By definition of F_i and ∂_c^*, $C_i \cap C_j = \varnothing$ for all $i \neq j$, and by (9),

$$S_1 = \bigcup_{i=0}^{\infty} C_i. \tag{10}$$

Note that C_i for $i \geq 0$ is a star-shaped set and c is its center. Moreover, $\partial_c^* C_i = F_i$. Thus

$$\begin{aligned} H^d(C_i) &= (\lambda_1 \times H^{d-1})(C_i) = \int_0^1 H^{d-1}\big(f_{c,\varrho}(\partial_c^* C_i)\big)\,\mathrm{d}\varrho \\ &= H^{d-1}(\partial_c^* C_i) \int_0^1 \varrho^{d-1}\,\mathrm{d}\varrho = \frac{1}{d} H^{d-1}(\partial_c^* C_i). \end{aligned}$$

The first part of the theorem then follows from (10). The second part is a consequence of Lemma 1. □

Corollary 5 [Emert and Nelson 1997, Theorem 1 and 2]. *If P_r is any regular n-dimensional polytope with the inner radius r or more generally a polytope that circumscribes a ball of radius r, then*

$$\frac{\mathrm{d}}{\mathrm{d}r}\lambda_n(P_r) = \lambda_{n-1}(\partial P_r).$$

Corollary 6. *If S_r is any closed star-shaped n-dimensional polytope that circumscribes a ball of radius r in a generalized sense, then*

$$\frac{\mathrm{d}}{\mathrm{d}r}\lambda_n(S_r) = \lambda_{n-1}(\partial S_r).$$

5. Discussion

Equation (3) is in principle an integral relationship

$$\lambda_n(P_r) = \int_0^r \lambda_{n-1}(\partial P_\varrho)\,\mathrm{d}\varrho,$$

which implicitly assumes

$$P_r = \bigcup_{\varrho=0}^{r} \partial P_\varrho. \tag{11}$$

By Lemma 3, this implies that P_r is star-shaped.

Moreover, if a star-shaped set P does not circumscribe any ball in the generalized sense, then for any center c of P, the faces of $\partial_c^* P$ have different distances from c. In other words, as the set P is inflated from a center c, the volume of corresponding cones grows by a different rate (this was observed in [Emert and

Nelson 1997, p. 368] and also in [Fjelstad and Ginchev 2003]). Consequently, one needs the faces to be equidistant to the center.

Therefore, we argue that Theorem 4 generalizes Equation (3) as much as possible while still keeping the geometrical intuition that provides a natural interpretation of the parameter r. Theorem 2 is much more general, but without any specific intuition behind it.

References

[Abramowitz and Stegun 1972] M. Abramowitz and I. A. Stegun (editors), *Handbook of mathematical functions, with formulas, graphs, and mathematical tables*, Dover, New York, 1972. MR 34 #8606 Zbl 0543.33001

[Coxeter 1963] H. S. M. Coxeter, *Regular polytopes*, 2nd ed., Macmillan, New York, 1963. MR 27 #1856 Zbl 0118.35902

[Emert and Nelson 1997] J. Emert and R. Nelson, "Volume and surface area for polyhedra and polytopes", *Math. Mag.* **70**:5 (1997), 365–371. MR 99a:52007 Zbl 0905.52002

[Fabian et al. 2001] M. Fabian, P. Habala, P. Hájek, V. Montesinos Santalucía, J. Pelant, and V. Zizler, *Functional analysis and infinite-dimensional geometry*, CMS Books Math./Ouvrages Math. SMC **8**, Springer, New York, 2001. MR 2002f:46001 Zbl 0981.46001

[Federer 1969] H. Federer, *Geometric measure theory*, Grundlehren Math. Wiss. **153**, Springer, New York, 1969. MR 41 #1976 Zbl 0176.00801

[Fjelstad and Ginchev 2003] P. Fjelstad and I. Ginchev, "Volume, surface area, and the harmonic mean", *Math. Mag.* **76**:2 (2003), 126–129.

[Kendall 1961] M. G. Kendall, *A course in the geometry of n dimensions*, Griffin's Stat. Monogr. Courses **8**, Hafner, New York, 1961. MR 25 #476 Zbl 0103.12002

[Morgan 2000] F. Morgan, *Geometric measure theory: a beginner's guide*, 3rd ed., Academic Press, San Diego, CA, 2000. MR 2001j:49001 Zbl 0974.49025

Received: 2008-12-30 Accepted: 2010-01-07

jnkrenic@uncg.edu *Department of Physics, The University of North Carolina at Greensboro, Greensboro, NC 27403, United States*

rychtar@uncg.edu *Department of Mathematics and Statistics, The University of North Carolina at Greensboro, Greensboro, NC 27403, United States*

Weakly viewing lattice points

Neil R. Nicholson and R. Christopher Sharp

(Communicated by Gaven J. Martin)

A specific rectangular array of lattice points is investigated. We say that the array is weakly visible from a lattice point not in the array if no point in the array lies on the line connecting the external point to any other point in the array. A lower bound is found for the distance from a weakly viewing point to the array, and a point of minimal distance is determined for arrays of a specific size. A secondary type of visibility is also discussed, and a closest point viewing the array in this style is completely determined.

1. Introduction

Laison and Schick [2007] describe the situation of a photographer attempting to photograph every person in a rectangular formation, with all persons, including the photographer, standing on lattice points. The photos must be taken from a fixed position and each member of the formation must have a straight-line view of the photographer, unobstructed by all other persons in the rectangle. They prove that there are positions for the photographer to stand, but these may be quite a long way from the formation. How can we minimize this distance?

The problem is turned into one involving lattice points in the plane (the persons to be photographed forming the rectangle), and such an unobstructed view between two points is termed *weak visibility*. Utilizing a result from [Herzog and Stewart 1971], Laison and Schick proceed to investigate a more complicated question: assume the lattice points outside the formation also form obstructions. They term this situation being *externally visible*. In this paper we only consider the simpler question of weak visibility. We begin in Section 2 with the necessary terminology and preliminary results. In Section 3 we prove our main results. Section 4 considers a more specific type of visibility which we call *weak integer visibility*. Lastly, natural questions for future research are provided in Section 5.

MSC2000: 11H06.
Keywords: weak visibility, lattice point.

2. Definitions and basics

All points are assumed to be lattice points in the first quadrant. Let $\Delta_{r,s}$ be the $r \times s$ rectangle of points with its lower left corner placed at $(1, 1)$. Say $\Delta_{r,s}$ is *weakly visible* from a point P if no point in $\Delta_{r,s}$ lies on any line segment connecting P and any other point in $\Delta_{r,s}$. Laison and Schick immediately prove the following result.

Theorem 2.1 [Laison and Schick 2007]. *The points* $P_1 = (rs - s + r, s + 1)$ *and* $P_2 = (r + 1, rs - r + s)$ *weakly view* $\Delta_{r,s}$ $(r, s \in \mathbb{Z}^+)$.

It turns out that this point may be quite far from $\Delta_{r,s}$, with distance being measured to the point (r, s). In the next section, we will place a lower bound on this distance dependent upon only the greater dimension of $\Delta_{r,s}$.

Notice that if $s < r$, then the point P_1 (of Theorem 2.1) is of closer distance to $\Delta_{r,s}$ than P_2. If $r < s$, then P_2 is closer to $\Delta_{r,s}$. If $r = s$, then the points are equidistant from $\Delta_{r,s}$. Because of this we will assume $s \leq r$ for the remainder of the paper. The following lemma provides maximal and minimal values for certain calculations.

Lemma 2.2. *The lines of maximal* (*resp. minimal*) *positive slope passing through at least two points of* $\Delta_{r,s}$ *have slope* $s - 1$ (*resp.* $1/(r - 1)$).

Our last two definitions are the main reference tools for placing bounds on the visibility distance. Let $\mathrm{Adj}_{r,s}$, the *adjacency square to* $\Delta_{r,s}$, be the square of points whose corners are the points (r, s), $(r, r+s-1)$, $(2r-1, r+s-1)$, and $(2r-1, s)$. Define the *adjacency flag of slope* m, where $m = m_y/m_x$, by

$$\mathrm{Adj}_{r,s}^{F(m)} = \big\{(x, y) \;\big|\; mx - (m(r - m_x) - 1) \leq y \leq mx - (m(1 + m_x) - s)\big\}.$$

Intuitively, this is the union of all points between the extremal lines of slope m passing through at least two points of $\Delta_{r,s}$. See Figures 1 and 2.

3. Bounding visibility distance

To begin the search for a point of minimal distance weakly viewing $\Delta_{r,s}$, we look to adjacency flags. For certain values of m, every point in the adjacency flag can be disregarded.

Lemma 3.1. *Suppose that*

$$(1)\ \ m \leq s/2, m \in \mathbb{Z}^+ \qquad \text{or} \qquad (2)\ \ 2/r \leq m, 1/m \in \mathbb{Z}.$$

Then every point in $\mathrm{Adj}_{r,s}^{F(m)}$ *does not weakly view* $\Delta_{r,s}$.

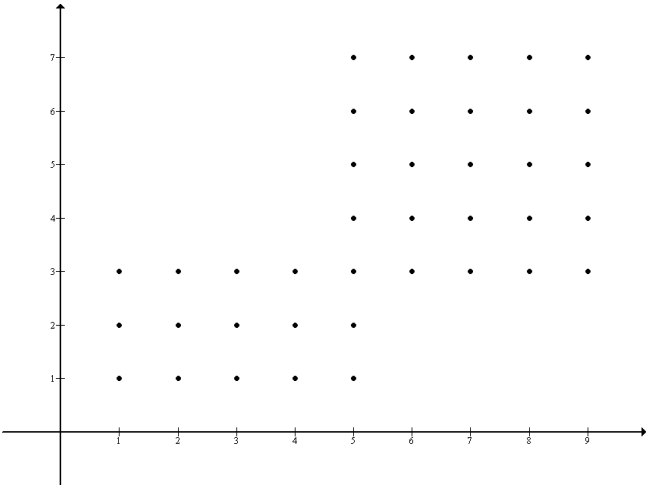

Figure 1. $\Delta_{5,3}$ and $\mathrm{Adj}_{5,3}$.

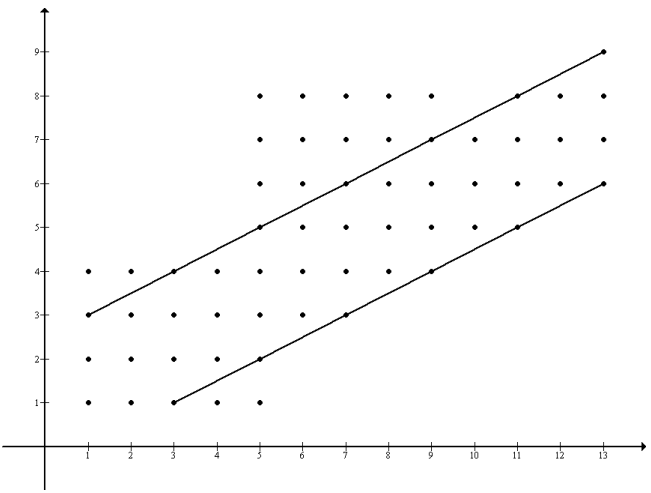

Figure 2. $\Delta_{5,4}$ with a portion of $\mathrm{Adj}_{5,4}^{F(1/2)}$.

Proof. We will prove the first case; the second is proven similarly. Suppose $m \in \mathbb{Z}^+$ and $m \leq s/2$. Take $(x_0, y_0) \in \mathrm{Adj}_{r,s}^{F(m)}$. Let L be the line

$$y - y_0 = m(x - x_0). \tag{1}$$

Let (a_0, b_0) be the point no in $\Delta_{r,s}$ on L closest to L. First, we claim that there is a point on L in $\Delta_{r,s}$. To prove this, we consider two possibilities:

Case 1: $s < b_0$. Since $(a_0, b_0) \notin \Delta_{r,s}$, then $2 \leq a_0$ and $b_0 \leq s + m$ by the choice of (a_0, b_0). Thus, since $m \in \mathbb{Z}^+$, $(a_0 - 1, b_0 - m) \in \Delta_{r,s}$.

Case 2: $b_0 \leq s$. Since $m \in \mathbb{Z}^+$, we must have $a_0 = r+1$. We need only show $1 \leq b_0 - m \leq s$. We know $b_0 - m \leq s$ and since $(a_0, b_0) \in \mathrm{Adj}_{r,s}^{F(m)}$, we have:

$$ma_0 - mr + m + 1 \leq b_o, \tag{2}$$

$$ma_0 - mr + 1 \leq b_0 - m, \tag{3}$$

$$m(a_0 - r) + 1 \leq b_0 - m, \tag{4}$$

$$1 \leq b_0 - m. \tag{5}$$

Line (5) of the derivation follows from $r < a_0$. Both cases are proven, showing that there is indeed a point on L in $\Delta_{r,s}$. To finish the proof, we show that if $(a, b) \in \Delta_{r,s} \cap \mathrm{Adj}_{r,s}^{F(m)}$, then either $(a+1, b+m)$ or $(a-1, b-m) \in \Delta_{r,s}$. There are three cases to consider: $a = 1$, $a = r$, and $1 < a < r$.

If $a = 1$, then $b \leq s - m$, giving $(a+1, b+m) \in \Delta_{r,s}$. If $a = r$, then $m \leq b$, yielding $(a-1, b-m) \in \Delta_{r,s}$. If $1 < a < r$ but $(a-1, b-m) \notin \Delta_{r,s}$, then

$$b - m \leq 0, \quad b \leq m, \quad b + m \leq s.$$

Thus, $(a+1, b+m) \in \Delta_{r,s}$. Together with the first claim this shows that there are two points in $\Delta_{r,s}$ on L. Hence, (x_0, y_0) does not weakly view $\Delta_{r,s}$. □

Though it may seem restricted in its usefulness, this lemma is the main tool in proving our main result, Theorem 3.2. To prove it, we need one additional definition. Notice that the flag $\mathrm{Adj}_{r,s}^{F(1)}$ partitions $\mathrm{Adj}_{r,s}$ into two regions: those points that lie in $\mathrm{Adj}_{r,s}^{F(1)}$ and those that do not. We will refer to those points of $\mathrm{Adj}_{r,s}$ not in $\mathrm{Adj}_{r,s}^{F(1)}$ as the *lower triangle of* $\mathrm{Adj}_{r,s}$, denoted $\mathrm{Adj}_{r,s}^{LT}$. In particular, it is the triangle of points whose vertices are $(s+r, s)$, $(2r-1, s)$, and $(2r-1, r)$.

Theorem 3.2. *For $r, s > 1$, no point in $\mathrm{Adj}_{r,s}$ weakly views $\Delta_{r,s}$.*

Proof. First note that no point on $y = s$ weakly views $\Delta_{r,s}$. Via the following claims we will show the remainder of $\mathrm{Adj}_{r,s}^{LT}$ is contained in the union of adjacency flags satisfying the hypotheses of Lemma 3.1 (in the case of $s = 2$ we will need one additional observation).

Claim 1. *The upper edge of $\mathrm{Adj}_{r,s}^{LT}$ is fully contained in $\mathrm{Adj}_{r,s}^{1/2}$.*

The upper and lower boundaries of $\mathrm{Adj}_{r,s}^{1/2}$ are, respectively,

$$y = \tfrac{1}{2}x - \tfrac{3}{2} + s \tag{6}$$

and

$$y = \tfrac{1}{2}x - \tfrac{1}{2}r. \tag{7}$$

Line (6) intersects $x = 2r - 1$ at $(2r-1, r+s-2)$. Thus, the upper corner of $\mathrm{Adj}_{r,s}^{LT}$ (the point $(2r-1, r)$) lies within $\mathrm{Adj}_{r,s}^{F(1/2)}$. The line

$$y = x - r + 1 \tag{8}$$

forms the upper boundary of $\mathrm{Adj}_{r,s}^{LT}$ and it intersects (7) at $x = r-2$, which is to the left of $(r+s, s+1)$. Therefore Claim 1 holds.

Claim 2. *The lower edge of* $\mathrm{Adj}_{r,s}^{LT}$ *is fully contained in* $\mathrm{Adj}_{r,s}^{F(2/r)}$ $(s \geq 3)$.

As in Claim 1, the segment connecting

$$(s+r, s+1) \quad \text{and} \quad (2r-1, s+1)$$

(the lower edge of $\mathrm{Adj}_{r,s}^{LT}$ satisfying $y > s$) lies on or between the lines forming the boundary of $\mathrm{Adj}_{r,s}^{F(2/r)}$. The details are left to the reader.

Claim 3. $\mathrm{Adj}_{r,s}^{LT} \subseteq \bigcup_m \mathrm{Adj}_{r,s}^{F(1/m)} (2 \leq m \leq r/2)$.

Due to the previous two claims, it is necessary only to consider

$$\mathrm{Adj}_{r,s}^{F(1/n)} \cap \mathrm{Adj}_{r,s}^{F(1/(n+1))}.$$

The upper boundaries of these flags intersect at $(1, s-1)$ while the lower boundaries intersect at $(r, 2)$. We need only show the intersection of the lower boundary of $\mathrm{Adj}_{r,s}^{F(1/n)}$ and the upper boundary of $\mathrm{Adj}_{r,s}^{F(1/(n+1))}$ occurs at or to the right of $x = 2r-1$, the right edge of $\mathrm{Adj}_{r,s}^{LT}$. This intersection occurs at

$$x = (n+1)r - 3n(n+1) - n + sn(n+1). \tag{9}$$

For $s = 3$,

$$2r-1 < \tfrac{5}{2}r+1 \leq 3r-n \leq (n+1)r-n = (s-3)n(n+1)-n+r(n+1),$$

while for $s \geq 4$, both

$$-1 < (s-3)n(n+1-n) \quad \text{and} \quad 2r < (n+1)r. \tag{10}$$

For $s = 2$, the lower edge of $\mathrm{Adj}_{r,s}^{F(2/r)}$ intersects $x = 2r-1$ at $y = 4$, leaving numerous points of $\mathrm{Adj}_{r,s}^{LT}$ (those with $y = 3$) unaccounted for in the above claims. However, consider the points $(x, 3)$ $(r \leq x \leq 2r-1)$. Take the line through $(x, 3)$ and $(r, 2)$. This line also passes through $(2r-x, 1)$, which lies in $\Delta_{r,s}$. Moreover, the overlapping flags of Claim 3 contain all (x, y) of $\mathrm{Adj}_{r,s}^{LT}$ when $y \geq 4$.

In all cases, we have shown that Claim 3 holds; that is,

$$\mathrm{Adj}_{r,s}^{LT} \subseteq \bigcup_m \mathrm{Adj}_{r,s}^{F(1/m)} (2 \leq m \leq r/2).$$

Since $r \geq s$, we know

$$\mathrm{Adj}_{r,s} - (\mathrm{Adj}_{r,s}^{LT} \cup (2r-1, s)) \subseteq \mathrm{Adj}_{r,s}^{F(1)}. \tag{11}$$

Because $(2r-1, s)$ lies on $x = 2r-1$ and $s \geq 2$, the result holds. □

Considering that every point in the adjacency square does not weakly view $\Delta_{r,s}$, we place a lower bound on the distance any point weakly viewing $\Delta_{r,s}$ must be from our $\Delta_{r,s}$:

Corollary 3.3. *If a point P weakly views $\Delta_{r,s}$, then P is at least $\sqrt{r^2+1}$ units away from $\Delta_{r,s}$.*

Proof. The closest possible P would be $(2r, s+1)$, which is of distance $\sqrt{r^2+1}$ from $\Delta_{r,s}$. □

We conclude our discussion on weak visibility with a complete determination of the specific case $s = 2$. This result is an improvement upon the initial point P_1 of in Theorem 2.1.

Corollary 3.4. *A point of minimal distance from $\Delta_{r,2}$ weakly viewing $\Delta_{r,2}$ is $(2r, 3)$, for $r \geq 2$.*

Proof. The point $P = (2r, 3)$ lies below the line of minimal slope (from Lemma 2.2) passing through at least two points of $\Delta_{r,s}$ and P realizes the lower bound of Corollary 3.3. □

4. Weak integer visibility

Lemma 3.1 induces a different though significantly weaker version of viewing $\Delta_{r,s}$. Let $m \in \mathbb{Z}$. Say a point P *weakly integer views* $\Delta_{r,s}$ if no line of slope m or $1/m$ passes through P and two or more points of $\Delta_{r,s}$. The original question of weak visibility can now be posed in terms of weak integer visibility and its solution is completely determined. We begin by considering adjacency flags of integral (resp. integer reciprocal) slopes. Lemma 4.1 is a generalization of Claim 3 in the proof of Theorem 3.2. Its computational proof is left to the reader.

Lemma 4.1. *Let $n \in \mathbb{Z}^+$.*

(1) *The upper boundary of $\mathrm{Adj}_{r,s}^{F(n)}$ and the lower boundary of $\mathrm{Adj}_{r,s}^{F(n+1)}$ intersect at $((r-3)n + r + s - 2, (r-3)n^2 + (r+s-4)n + s)$.*

(2) *The lower boundary of $\mathrm{Adj}_{r,s}^{F(1/n)}$ and the upper boundary of $\mathrm{Adj}_{r,s}^{F(1/(n+1))}$ intersect at $((s-3)n^2 + (s+r-4)n + r, (s-3)n + s + r - 2)$.*

Each pair of adjacency flags creates a region of lattice points that weakly integer views $\Delta_{r,s}$: all points that are both below the higher sloped flag and above the lower sloped flag. Within each region there is a point closest to $\Delta_{r,s}$ weakly integer viewing $\Delta_{r,s}$, as described below. By comparing these points, we can find the point of minimal distance weakly integer viewing $\Delta_{r,s}$.

Notice where Lemma 4.1 places the intersection of flags of slopes n and $n+1$, and of those of slopes $1/n$ and $1/(n+1)$. For fixed values of r and s, the coordinate

functions of the intersection point are strictly increasing with respect to n. Within these regions of points weakly integer viewing $\Delta_{r,s}$ there is a point closest to $\Delta_{r,s}$.

Lemma 4.2. *Let $n \in \mathbb{Z}$.*

(1) *The point of minimal distance to $\Delta_{r,s}$ between the upper boundary of $\mathrm{Adj}_{r,s}^{F(n)}$ and the lower boundary of $\mathrm{Adj}_{r,s}^{F(n+1)}$ is*

$$\big((r-3)n+r+s,\,(r-3)n^2+(r+s-2)n+s+1\big). \tag{12}$$

(2) *The point of minimal distance to $\Delta_{r,s}$ between the lower boundary of $\mathrm{Adj}_{r,s}^{F(1/n)}$ and the upper boundary of $\mathrm{Adj}_{r,s}^{F(1/(n+1))}$ is*

$$\big((s-3)n^2+(s+r-2)n+r,\,(s-3)n+s+r\big). \tag{13}$$

Proof. Suppose two lines L_1 and L_2 of positive integral slopes n and $n+1$, respectively, intersect at (a,b). In the positive direction, the next lattice points to lie on L_1 and L_2 are $(a+1,b+n)$ and $(a+1,b+n+1)$. The triangle created by these two points and (a,b) contains no lattice points on its interior or its boundary (other than its vertices). Similarly, the quadrilateral whose vertices are $(a+1,b+n)$, $(a+1,b+n+1)$, $(a+2,b+2n)$, and $(a+2,b+2n+2)$ contains no lattice points on its interior. However, there is a single nonvertex lattice point on its exterior: $(a+2,b+2n+1)$.

The second case follows mutatis mutandis. □

With regards to the comments preceding Lemma 4.2, to prove the following theorem we need only consider the two pairs of flags of slopes 1 and 2 and slopes 1 and $1/2$.

Theorem 4.3. *The point of minimal distance weakly integer viewing $\Delta_{r,s}$ is*

$$(2(r+s)-4,\,r+2s-3).$$

Proof. Consider the two points weakly integer viewing $\Delta_{r,s}$ in the regions formed by the pair $\mathrm{Adj}_{r,s}^{F(1)}$ and $\mathrm{Adj}_{r,s}^{F(2)}$ and by the pair $\mathrm{Adj}_{r,s}^{F(1)}$ and $\mathrm{Adj}_{r,s}^{F(1/2)}$. We assume $s<r$. Because of this, the point of Lemma 4.2 falling between the flags of slope 1 and $1/2$ is nearer to $\Delta_{r,s}$. Moreover, this point is closer to $\Delta_{r,s}$ than the nearest point found outside the boundaries of considered flags, the point of Theorem 2.1: $(rs-s+r,\,s+1)$. □

5. Further questions

The foremost natural question is still that posed in [Laison and Schick 2007]: is there a formula dependent only upon r and s giving the point closest to $\Delta_{r,s}$ weakly viewing $\Delta_{r,s}$? If not, how strong can the bounds be made? The flags mentioned can be broken into two types: integral (or reciprocal of) and fractional slopes. We

did not discuss fractional sloped flags at all, but a deeper discussion of them may lead to more precise answers.

In terms of the original question, what if the formation is not rectangular? What can be said about triangular, pentagonal, or other simple geometric shapes? Another way of making the situation more realistic is by considering each lattice point to have some sort of weight attached to it.

Finally, following Laison and Schick's thoughts, what happens when we attempt to weakly view similar structures in higher dimensions? The problem becomes much more realistic by attaching weight functions corresponding to persons' heights to lattice points on the xy-plane in $\mathbb{R}^3$.

References

[Herzog and Stewart 1971] F. Herzog and B. M. Stewart, "Patterns of visible and nonvisible lattice points", *Amer. Math. Monthly* **78** (1971), 487–496. MR 44 #1630 Zbl 0217.03501

[Laison and Schick 2007] J. D. Laison and M. Schick, "Seeing dots: visibility of lattice points", *Math. Mag.* **80**:4 (2007), 274–282. MR 2008j:11079

Received: 2009-03-12 Accepted: 2010-03-08

nicholsonn@william.jewell.edu *William Jewell College, 500 College Hill, Box 1107, Liberty, MO 64068, United States*

csharp@ku.edu *Department of Mathematics, University of Kansas, 405 Snow Hall, 1460 Jayhawk Boulevard, Lawrence, KS 66045, United States*

Lights Out on finite graphs

Stephanie Edwards, Victoria Elandt, Nicholas James,
Kathryn Johnson, Zachary Mitchell and Darin Stephenson

(Communicated by Ron Gould)

Lights Out is a one-player game played on a finite graph. In the standard game the vertices can be either on or off; pressing a vertex toggles its state and that of all adjacent vertices. The goal of the game is to turn off all of the lights. We study an extension of the game in which the state of a vertex may be one of a finite number of colors. We determine which graphs in certain families (spider graphs and generalized theta graphs) are winnable for every initial coloring. We also provide a construction that gives every always-winnable tree for any prime power number of colors.

1. Introduction

The Lights Out game was popularized as a hand-held electronic puzzle produced by Tiger Electronics in 1995. The puzzle consists of a 5×5 square grid of buttons, each of which can be either on or off. A move consists of pressing one of the buttons, which changes the state of that button and all vertical and horizontal neighbors. Given an initial configuration in which some subset of the lights are on, the goal of the solver is to turn off all the lights. An initial configuration of lights will be called *winnable* if the puzzle can be solved when starting from that configuration.

The mathematical study of this puzzle and its generalizations has produced interesting results in graph theory, some of which predate the electronic version of the game. The puzzle on 5×5 grids was studied by Anderson and Feil [1998], who used linear algebra over $\mathbb{Z}_2$ to classify winnable configurations. The analysis on $n \times m$ grids was done using Fibonacci polynomials in [Goldwasser and Klostermeyer 1997; Goldwasser et al. 1997; 2002]. Earlier, Sutner [1989] had shown that the winnability of configurations in Lights Out is also equivalent to a question on finite cellular automata.

MSC2000: 05C15, 05C50, 05C78, 91A43.
Keywords: Lights Out, parity domination, finite graphs.
The authors thank Hope College and the NSF (REU grant #0645887) for funding and facilities.

The puzzle has a natural generalization to any finite graph, in which each vertex of the graph starts as either on or off, and pressing a vertex toggles that vertex and all adjacent vertices. Amin and Slater [1996] have studied this generalization for some classes of finite graphs under the equivalent notion of parity domination theory. In particular, they classify paths, 'spider' graphs (i.e., generalized stars), and 'caterpillar' graphs for which every initial configuration is winnable — in their language, *all parity realizable* graphs — and they give a construction which produces all trees that are winnable from every initial configuration.

Giffen and Parker [2009] have further generalized the puzzle to the setting in which each vertex on the finite graph has k states, which are denoted by the elements of $\mathbb{Z}_k$. The state $0 \in \mathbb{Z}_k$ is considered off. Pressing a vertex increments that vertex and all adjacent vertices by 1 (mod k). A graph G is *always winnable* (AW) over $\mathbb{Z}_k$ if every initial configuration is winnable with the above assumptions. Giffen and Parker classify winnable configurations on paths and cycles, and also determine which paths, cycles and caterpillar graphs are AW over $\mathbb{Z}_k$. Moreover, they develop a notion of domination theory for finite graphs that is equivalent to the multicolored Lights Out puzzle.

This paper generalizes both the results in [Amin and Slater 1996; Giffen and Parker 2009] by studying the winnability of Lights Out over $\mathbb{Z}_k$ for spider graphs, (generalized) theta graphs, and trees. We establish our basic notation and prove some helpful technical results in Section 2. In Section 3, we study the winnability of spider graphs and determine which spider graphs are AW over $\mathbb{Z}_k$. We prove similar results for generalized theta graphs in Section 4. In Section 5, we generalize the construction of Amin and Slater to produce all AW trees over $\mathbb{Z}_{p^e}$, where p is prime and e is a positive integer.

2. Notation and basic results

The term *graph* will designate a finite multigraph (without loops). Given a graph G, we denote the vertex set by $V(G)$ and the edge set by $E(G)$. An edge will typically be denoted by the pair of incident vertices. Given an enumeration

$$V(G) = \{v_1, \ldots, v_n\}$$

of the vertices of G, we define the *neighborhood matrix* of G to be

$$N(G) = \mathrm{adj}(G) + I_n,$$

where $\mathrm{adj}(G)$ is the usual adjacency matrix of G and I_n is the $n \times n$ identity matrix. A *coloring* of the vertices will correspond to a column vector $\vec{b} \in \mathbb{Z}_k^n$ where b_i is the color of v_i. The act of 'pressing vertex v_i' adds the ith column of $N(G)$ to $\vec{b}$, with addition taking place in $\mathbb{Z}_k^n$.

Remark 2.1. We have allowed a graph G to have multiple edges, even though most of the graphs considered in this paper do not have multiple edges. This is due to the fact that the reduction described in Proposition 2.7 may result in multiple edges when used on generalized theta graphs in Section 4. If there are m edges between vertices v and w, then pressing v will increment the color on v by 1 and the color on w by m.

An initial coloring $\vec{b} \in \mathbb{Z}_k^n$ is called *winnable* if there exists a sequence of presses that transforms $\vec{b}$ to $\vec{0}$. As shown for two colors in Anderson and Feil [1998], $\vec{b}$ is winnable if and only if the equation

$$N(G)\vec{x} = -\vec{b}$$

has a solution vector $\vec{x} \in \mathbb{Z}_k^n$. In this case, the solution vector $\vec{x}$ is called the *winning strategy* for $\vec{b}$ and gives the vertices that should be pressed, and how many times, in order to convert $\vec{b}$ to $\vec{0}$. Thus, an initial coloring $\vec{b}$ is winnable if and only if $-\vec{b}$ (and hence $\vec{b}$) is in the column space of $N(G)$ over $\mathbb{Z}_k$. A graph G will be called *always winnable* (AW) over $\mathbb{Z}_k$ if every initial coloring $\vec{b} \in \mathbb{Z}_k^n$ can be won (i.e., if the column space of $N(G)$ is equal to $\mathbb{Z}_k^n$).

We use $d(G)$ to denote $\det(N(G))$, computed over $\mathbb{Z}$, since this number occurs often. We adopt the convention that the determinant of the 'empty' matrix is 1. Thus, if G is the graph with no vertices and no edges, $d(G) = 1$ by convention. If G_1 and G_2 are the connected components of G, then $N(G)$ is block-diagonal, and $d(G) = d(G_1)d(G_2)$.

Proposition 2.2. *For any graph G and integer $k \geq 2$, the following are equivalent.*

(1) *G is AW over $\mathbb{Z}_k$.*

(2) *The column space of $N(G)$ is $\mathbb{Z}_k^n$.*

(3) *The null space of $N(G)$ is $\{\vec{0}\}$.*

(4) *$d(G)$ is relatively prime to k.*

Proof. When k is prime, this is immediate from the basic theory of vector spaces over fields. the general case involves the relationship between determinants and free modules over a commutative ring; see [Bourbaki 1974, III.8.2, Theorem 1]. □

The following corollary is a consequence of the equivalence of (1) and (4) in the preceding proposition.

Corollary 2.3. *Let G be any graph.*

(1) *For any integer $k \geq 2$, G is AW over $\mathbb{Z}_k$ if and only if G is AW over $\mathbb{Z}_p$ for every prime factor p of k.*

(2) *For any prime number p and any positive integer e, G is AW over $\mathbb{Z}_{p^e}$ if and only if G is AW over $\mathbb{Z}_p$.*

Remark 2.4. It is also immediate that a graph is AW if and only if each of its connected components is AW.

We now give some useful technical results that involve winnability of colorings on related graphs. Given a graph G and a subset $S \subset V(G)$, we define $G - S$ to be the graph obtained by deleting the vertices in S from G, along with any edges incident with vertices in S.

Proposition 2.5. *Suppose a graph G has a set of distinct vertices*

$$\{v_{n-3}, v_{n-2}, v_{n-1}, v_n\}$$

with edges

$$\{v_{n-3}v_{n-2}, v_{n-2}v_{n-1}, v_{n-1}v_n\},$$

where $\deg v_{n-2} = \deg v_{n-1} = 2$ *and* $\deg v_n = 1$. (*Note that v_{n-3} can have any degree.*) *Let* $\widetilde{G} = G - \{v_{n-2}, v_{n-1}, v_n\}$.

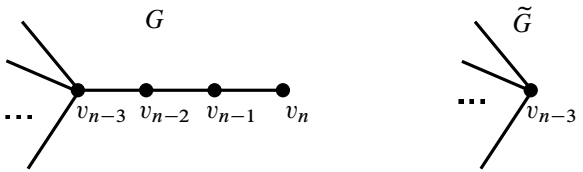

(1) *The following are equivalent*:
   (a) *The initial coloring* $\vec{b} = \langle b_1, b_2, \ldots, b_{n-3}\rangle^T \in \mathbb{Z}_k^{n-3}$ *is winnable on* $\widetilde{G}$.
   (b) *The initial coloring*

$$\vec{b'} = \langle b_1, b_2, \ldots, b_{n-3} + c_1, c_1 + c_2, c_1 + c_2 + c_3, c_2 + c_3\rangle^T \in \mathbb{Z}_k^n$$

   is winnable on G for all choices of $c_1, c_2, c_3 \in \mathbb{Z}_k$.
   (c) *The initial coloring* $\vec{b'} = \langle b_1, b_2, \ldots, b_{n-3}, 0, 0, 0\rangle^T \in \mathbb{Z}_k^n$ *is winnable on G.*

(2) *G is AW over $\mathbb{Z}_k$ if and only if $\widetilde{G}$ is AW over $\mathbb{Z}_k$.*

Proof. Let J be the $(n-3) \times 3$ matrix such that $j_{(n-3),1} = 1$ and all other entries are 0. Then

$$N(G) = \left(\begin{array}{c|ccc} N(\widetilde{G}) & & J & \\ \hline & 1 & 1 & 0 \\ J^T & 1 & 1 & 1 \\ & 0 & 1 & 1 \end{array}\right).$$

(a) $\Rightarrow$ (b) Suppose $\vec{x} = \langle x_1, \ldots, x_{n-3}\rangle^T$ is a winning strategy for $\vec{b} \in \mathbb{Z}_k^{n-3}$ on $\widetilde{G}$. For any $c_1, c_2, c_3 \in \mathbb{Z}_k$, let

$$\vec{x}' = \langle x_1, \ldots, x_{n-3}, -c_1, -c_2 - x_{n-3}, -c_3 + x_{n-3}\rangle^T,$$
$$\vec{b}' = \langle b_1, b_2, \ldots, b_{n-3} + c_1, c_1 + c_2, c_1 + c_2 + c_3, c_2 + c_3\rangle^T.$$

Then $N(G)\vec{x}' = -\vec{b}'$, showing that $\vec{x}'$ is a winning strategy for $\vec{b}'$ on G.

(b) $\Rightarrow$ (c) Immediate.

(c) $\Rightarrow$ (a) For a given vector $\vec{b} \in \mathbb{Z}_k^{n-3}$, suppose that

$$\vec{b}' = \langle b_1, b_2, \ldots, b_{n-3}, 0, 0, 0\rangle^T$$

can be won on G with winning strategy $\vec{y} = \langle y_1, \ldots, y_n\rangle^T$. The last two entries of $N(G)\vec{y} = -\vec{b}'$ imply that $y_{n-2} + y_{n-1} + y_n = 0 \pmod k$ and $y_{n-1} + y_n = 0 \pmod k$. This implies that $y_{n-2} = 0 \pmod k$. This, combined with the fact that $N(G)\vec{y} = -\vec{b}'$, implies that

$$N(\widetilde{G}) \begin{pmatrix} y_1 \\ \vdots \\ y_{n-3} \end{pmatrix} = - \begin{pmatrix} b_1 \\ \vdots \\ b_{n-3} \end{pmatrix}.$$

Thus, $\vec{b}$ is winnable on $\widetilde{G}$. □

Corollary 2.6. *We retain the hypotheses and notation of Proposition 2.5. An initial coloring $\vec{a} = \langle a_1, a_2, \ldots, a_n\rangle^T \in \mathbb{Z}_k^n$ is winnable on G if and only if the initial coloring*

$$\vec{a}' = \langle a_1, a_2, \ldots, a_{n-4}, a_{n-3} - a_{n-1} + a_n\rangle^T \in \mathbb{Z}_k^{n-3}$$

is winnable on $\widetilde{G}$.

Proposition 2.7. *Suppose a graph G has a set of distinct vertices*

$$\{v_{n-4}, v_{n-3}, v_{n-2}, v_{n-1}, v_n\}$$

with edges $\{v_{n-3}v_{n-2}, v_{n-2}v_{n-1}, v_{n-1}v_n, v_nv_{n-4}\}$, where $\deg v_{n-2} = \deg v_{n-1} = \deg v_n = 2$. (Note that v_{n-3} and v_{n-4} can have any degree.) *Let $\widehat{G}$ be the union of $G - \{v_{n-2}, v_{n-1}, v_n\}$ with a new edge $v_{n-3}v_{n-4}$.*

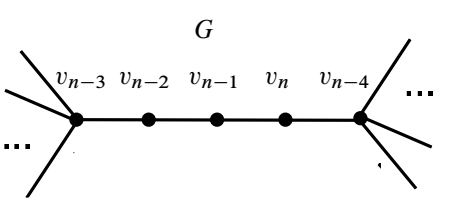

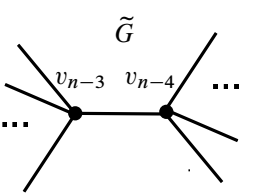

(1) *The following are equivalent*:

(a) *The initial coloring*

$$\vec{b} = \langle b_1, b_2, \ldots, b_{n-4}, b_{n-3} \rangle^T \in \mathbb{Z}_k^{n-3}$$

is winnable on $\widehat{G}$.

(b) *The initial coloring*

$$\vec{b}' = \langle b_1, b_2, \ldots, b_{n-4} + c_3, b_{n-3} + c_1, c_1 + c_2, c_1 + c_2 + c_3, c_2 + c_3 \rangle^T \in \mathbb{Z}_k^n$$

is winnable on G *for all choices of* $c_1, c_2, c_3 \in \mathbb{Z}_k$.

(c) *The initial coloring*

$$\vec{b}' = \langle b_1, b_2, \ldots, b_{n-4}, b_{n-3}, 0, 0, 0 \rangle^T \in \mathbb{Z}_k^n$$

is winnable on G.

(2) G *is AW over* $\mathbb{Z}_k$ *if and only if* $\widehat{G}$ *is AW over* $\mathbb{Z}_k$.

Proof. We proceed as in the proof of Proposition 2.5.

(a) $\Rightarrow$ (b): If $\vec{x} = \langle x_1, \ldots, x_{n-3} \rangle^T$ is a winning strategy for $\vec{b} \in \mathbb{Z}_k^{n-3}$ on $\widehat{G}$, then, for any $c_1, c_2, c_3 \in \mathbb{Z}_k$, the vector

$$\vec{x}' = \langle x_1, \ldots x_{n-4}, x_{n-3}, -c_1 + x_{n-4}, -c_2 - x_{n-3} - x_{n-4}, -c_3 + x_{n-3} \rangle^T$$

is a winning strategy on G for

$$\vec{b}' = \langle b_1, b_2, \ldots, b_{n-4} + c_3, b_{n-3} + c_1, c_1 + c_2, c_1 + c_2 + c_3, c_2 + c_3 \rangle^T.$$

(b) $\Rightarrow$ (c): Immediate.

(c) $\Rightarrow$ (a): Given a winning strategy $\vec{y} \in \mathbb{Z}_k^n$ for

$$\vec{b}' = \langle b_1, b_2, \ldots, b_{n-3}, 0, 0, 0 \rangle^T$$

on G, the fact that $N(G)\vec{y} = -\vec{b}'$ shows that $y_{n-4} = y_{n-2} \pmod k$ and $y_{n-3} = y_n \pmod k$. This implies that

$$N(\widehat{G}) \begin{pmatrix} y_1 \\ \vdots \\ y_{n-3} \end{pmatrix} = - \begin{pmatrix} b_1 \\ \vdots \\ b_{n-3} \end{pmatrix}.$$

Thus, $\vec{b}$ is winnable on $\widehat{G}$. □

Corollary 2.8. *We retain the hypotheses and notation of Proposition 2.7. An initial coloring* $\vec{a} = \langle a_1, a_2, \ldots, a_n \rangle^T \in \mathbb{Z}_k^n$ *is winnable on* G *if and only if the initial coloring*

$$\vec{a}' = \langle a_1, a_2, \ldots, a_{n-5}, a_{n-4} - a_{n-1} + a_{n-2}, a_{n-3} - a_{n-1} + a_n \rangle^T \in \mathbb{Z}_k^{n-3}$$

is winnable on $\widehat{G}$.

For any matrix A, let A_{ij} represent the minor obtained by deleting the ith row and jth column from A. Again, we assume that the determinant of an 'empty' matrix, formed by taking a minor of a matrix with only one row or column, is 1.

Lemma 2.9. *Let M be an $m \times m$ matrix and N an $n \times n$ matrix. Let J be the $m \times n$ matrix such that $j_{m,1} = 1$ and all other entries of J are 0. Then*

$$\det \begin{pmatrix} M & J \\ J^T & N \end{pmatrix} = \det(M)\det(N) - \det M_{mm} \det N_{11}.$$

Proof. This follows from a standard proof by induction. □

Proposition 2.10. Let G_1 and G_2 be graphs, let v be a vertex of G_1, and let w be a vertex of G_2. Let $H = H(G_1, G_2, v, w)$ be the graph formed by connecting G_1 and G_2 with an edge vw. Then

$$d(H) = d(G_1)d(G_2) - d(G_1 - \{v\})d(G_2 - \{w\}).$$

Proof. Assume G_1 has m vertices, of which v is the last, and G_2 has n vertices, of which w is the first. The result follows immediately from Lemma 2.9, since

$$N(H) = \begin{pmatrix} N(G_1) & J \\ J^T & N(G_2) \end{pmatrix}$$

where J is as in the previous result, $N(G_1 - \{v\}) = N(G_1)_{mm}$ and $N(G_2 - \{w\}) = N(G_2)_{11}$. □

Corollary 2.11. Suppose $k = p^e$ for some prime p and positive integer e. Let G_1 and G_2 be graphs that are AW over $\mathbb{Z}_k$. Let $v \in V(G_1)$ and $w \in V(G_2)$, and suppose that $G_1 - \{v\}$ is not AW over $\mathbb{Z}_k$. Then the graph $H(G_1, G_2, v, w)$ constructed in the previous result is AW over $\mathbb{Z}_k$.

Proof. Since G_1 and G_2 are AW over $\mathbb{Z}_k$, we have $p \nmid d(G_1)$ and $p \nmid d(G_2)$. Since $G_1 - \{v\}$ is not AW over $\mathbb{Z}_k$, we have $p | d(G_1 - \{v_1\})$. Therefore,

$$p \nmid [d(G_1)d(G_2) - d(G_1 - \{v\})d(G_2 - \{w\})].$$ □

Proposition 2.12. Let G_i be any graphs for $1 \le i \le m$, and let $v_i \in V(G_i)$. Let $W = W(G_1, \ldots, G_m, v_1, \ldots, v_m)$ be the graph formed by all vertices and edges of the graphs G_i together with a new vertex w and edges $v_i w$ for $1 \le i \le m$. Then

$$d(W) = \prod_{j=1}^{m} d(G_j) - \sum_{i=1}^{m} \left(d(G_i - \{v_i\}) \prod_{j \ne i} d(G_j) \right).$$

Proof. This follows from Proposition 2.10 and induction. For the base case, attach the single vertex w to a graph G_1 by an edge wv_1. □

Corollary 2.13. Let $k = p^e$ for some prime number p and positive integer e, and suppose each G_i is AW over $\mathbb{Z}_k$. Then $W(G_1, \ldots, G_m, v_1, \ldots, v_m)$ is AW over $\mathbb{Z}_k$ if and only if

$$\sum_{i=1}^{m} d(G_i)^{-1} d(G_i - \{v_i\}) \neq 1 \pmod{p}.$$

Here, the inverse is taken mod p.

Proof. The graph W is AW over $\mathbb{Z}_k$ if and only if $d(W) \neq 0 \pmod{p}$. The result follows by applying Proposition 2.12 to expand $d(W) \neq 0 \pmod{p}$, then multiplying both sides of the resulting equation by $\prod_{j=1}^{m} d(G_j)^{-1}$. □

3. Spider graphs

In this section we study the winnability of spider graphs (also called *generalized stars*). Specifically, we define *reduced spider graph* and determine which initial colorings are winnable on reduced spiders. This is then used to determine which spider graphs are AW over $\mathbb{Z}_k$.

First we provide a formal definition of a spider graph.

Definition 3.1. Let $V(P_i) = \{v_{i,1}, v_{i,2}, \ldots, v_{i,n_i}\}$ be the vertices of a path with edges $E(P_i) = \{v_{i,j}v_{i,j+1} : 1 \leq j \leq n_i - 1\}$. A *spider graph* G is defined as the union of paths $P_1, \ldots, P_l$ for some $l > 2$ along with a new vertex v_0, with edges consisting of the original edges from each P_i together with edges $v_0 v_{i,1}$ for $1 \leq i \leq l$. We call the paths P_i the *legs* of the spider and leg i has *length* n_i. A *reduced spider graph* is a spider graph that has legs of lengths 1 and 2 only.

Notation 3.2. Throughout this section, we assume that a spider graph G has

- m legs of length 1 (mod 3), labeled $P_1, \ldots, P_m$,
- t legs of length 2 (mod 3), labeled $P_{m+1}, \ldots, P_{m+t}$, and
- $l - (m + t)$ legs of length 0 (mod 3), labeled $P_{m+t+1}, \ldots, P_l$.

For a reduced spider, we will have no legs of length 0 (mod 3), and in that case, $l = m + t$. An initial coloring $\vec{b}$ on a spider graph G is a vector $\mathbb{Z}_k^N$ (where $N = 1 + \sum_{i=1}^{l} n_i$) such that $b_{i,j}$ is the initial color of $v_{i,j}$ and b_0 is the initial color of v_0.

The next result shows which initial colorings are winnable on reduced spider graphs. Corollary 2.6 can then be used inductively to determine whether any given initial coloring of a general spider is winnable.

Theorem 3.3. *Let G be a reduced spider graph labeled as in Notation 3.2. Let $\vec{b} \in \mathbb{Z}_k^N$ be an initial coloring of G.*

(1) *If* $t = 0$ *then* $\vec{b}$ *is winnable on* G *if and only if* $\gcd(m-1, k)$ *divides*

$$-b_0 + \sum_{i=1}^{m} b_{i,1}.$$

(2) *If* $t \neq 0$ *then* $\vec{b}$ *is winnable on* G *if and only if* $b_{i,2} - b_{i,1} = b_{j,2} - b_{j,1}$ *for all* i *and* j *such that* $m+1 \leq i, j \leq m+t = l$.

Proof. Let G and $\vec{b}$ be as in the hypotheses of the theorem. In order to win, we must press each vertex some number of times. Suppose v_0 is pressed d_0 times and $v_{i,j}$ is pressed $d_{i,j}$ times. The effects of pressing these vertices are:

- the color of v_0 is changed by $d_0 + \sum_{i=1}^{m+t} d_{i,1}$;
- for $1 \leq i \leq m$, the color of $v_{i,1}$ is changed by $d_0 + d_{i,1}$;
- for $m+1 \leq i \leq m+t$, the color of $v_{i,1}$ is changed by $d_0 + d_{i,1} + d_{i,2}$;
- for $m+1 \leq i \leq m+t$, the color of $v_{i,2}$ is changed by $d_{i,1} + d_{i,2}$.

To win, we must change the color of every vertex to 0, which yields the following system of equations mod k. These equations are equivalent to the matrix equation $N(G)\vec{d} = -\vec{b}$.

$$b_0 + d_0 + \sum_{i=1}^{m+t} d_{i,1} = 0 \tag{3-1}$$

$$b_{i,1} + d_{i,1} + d_0 = 0 \quad \text{for } 1 \leq i \leq m \tag{3-2}$$

$$b_{i,1} + d_{i,1} + d_{i,2} + d_0 = 0 \quad \text{for } m+1 \leq i \leq m+t \tag{3-3}$$

$$b_{i,2} + d_{i,1} + d_{i,2} = 0 \quad \text{for } m+1 \leq i \leq m+t \tag{3-4}$$

Equation (3-4) allows us to reduce (3-3) to:

$$d_0 = b_{i,2} - b_{i,1} \quad \text{for } i = m+1, \ldots, m+t. \tag{3-5}$$

(1) Suppose $t = 0$. The initial coloring $\vec{b}$ is winnable on G if and only if Equations (3-1) and (3-2) are consistent. Rewriting (3-2) as $d_{i,1} = -d_0 - b_{i,1}$ and substituting into (3-1) shows that $\vec{b}$ is winnable if and only if

$$d_0(1-m) = -b_0 + \sum_{i=1}^{m} b_{i,1}$$

has a solution for d_0 mod k. This is true if and only if $\gcd(m-1, k)$ divides $-b_0 + \sum_{i=1}^{m} b_{i,1}$.

(2) Suppose $t \neq 0$. If an initial coloring $\vec{b}$ is winnable on G, Equation (3-5) gives $b_{i,2} - b_{i,1} = b_{j,2} - b_{j,1}$ for all $m+1 \leq i, j \leq m+t$.

Conversely, if $b_{i,2}-b_{i,1}=b_{j,2}-b_{j,1}$ for all $m+1\le i,\, j\le m+t$, the value of d_0 is determined by (3-5). The values of $d_{i,1}$ for $1\le i\le m$ are then determined by (3-2). Now, we may choose any integers $d_{i,1}$ for $m+1\le i\le m+t$ so that (3-1) holds, and this is possible since $t>0$. Finally, the values of $d_{i,2}$ for $m+1\le i\le m+t$ are determined (consistently) by (3-3) and (3-4). Therefore, the system has a solution vector $\vec{d}$. □

Theorem 3.4 (Characterization of AW spider graphs). *Let G be a spider graph* (see 3.2 for notation). *Then G is AW over $\mathbb{Z}_k$ if and only if either*

(1) $t=0$ *and* $\gcd(m-1,k)=1$, *or*

(2) $t=1$.

Proof. Consider a spider graph G. By Proposition 2.5, G is AW over $\mathbb{Z}_k$ if and only if $\widetilde{G}$ is AW over $\mathbb{Z}_k$, where $\widetilde{G}$ is the reduced spider graph with m legs of length 1 and t legs of length 2. We assume that $\widetilde{G}$ is also labeled as in 3.2.

Suppose that $t=0$ and $\gcd(m-1,k)=1$. Then by Theorem 3.3(1), every initial coloring on $\widetilde{G}$ is winnable over $\mathbb{Z}_k$. Conversely, suppose that $t=0$ and that $\gcd(m-1,k)\neq 1$. Then $\gcd(m-1,k)$ does not divide $-b_0+\sum_{i=1}^{m} b_{i,1}$ when $b_{1,1}=1$, $b_0=0$, and $b_{i,1}=0$ for $i=2,\dots m$. This gives an example of an initial coloring $\vec{b}$ which is not winnable on $\widetilde{G}$.

Suppose $t=1$. The condition in Theorem 3.3(2) is automatically satisfied for every initial coloring $\vec{b}$, and therefore $\widetilde{G}$ is AW over $\mathbb{Z}_k$.

Finally, suppose that $t>1$. In this case, there are clearly initial colorings on $\widetilde{G}$ that do not satisfy the condition in Theorem 3.3(2), showing that $\widetilde{G}$ is not AW. □

4. Generalized theta graphs

In this section we study the winnability of (generalized) theta graphs. We define a notion of *reduced* theta graph, and determine which initial colorings on reduced theta graphs are winnable. This information is then used to determine which theta graphs are AW over $\mathbb{Z}_k$.

Definition 4.1. Let $V(P_i)=\{v_{i,1},v_{i,2},\dots,v_{i,n_i}\}$ be the vertices of a path with edge set $E(P_i)=\{v_{i,j}v_{i,j+1}:1\le j\le n_i-1\}$. A (*generalized*) *theta graph* G is defined as the union of disjoint paths $P_1,\dots,P_l$ for some $l>2$ along with two new vertices v_0 and v_n, with edges given by

- the original edges from each P_i,
- edges $v_0v_{i,1}$ and $v_{i,n_i}v_n$ for $1\le i\le l$, and
- possibly one or more edges of the form v_0v_n (i.e., there may or may not be edges of the form v_0v_n).

We call the paths P_i, where $1 \le i \le l$, *paths* of the theta graph and path i has *length* n_i. We will refer to each of the edges v_0v_n as a *path of length* 0 in the theta graph. A *reduced theta graph* is a theta graph which only has paths of lengths 0, 1, and 2.

The winnability of generalized theta graphs modulo 2 has been studied in the literature. In [Amin and Slater 1992], the graphs we have called *generalized theta graphs* occur as a particular case of *series parallel graphs*, and a linear time algorithm is given for determining their winnability modulo 2.

Notation 4.2. Throughout this section, we assume that a theta graph G has

- m paths of length 1 (mod 3), labeled $P_1, \ldots, P_m$,
- t paths of length 2 (mod 3), labeled $P_{m+1}, \ldots, P_{m+t}$, and
- $l-(m+t)$ paths of length 0 (mod 3), labeled $P_{m+t+1}, \ldots, P_l$.

(Note: some of $P_{m+t+1}, \ldots, P_l$ could be 'empty paths' corresponding to edges v_0v_n.) An initial coloring $\vec{b}$ on a theta graph G is a vector $\mathbb{Z}_k^N$ (where $N = 2+\sum_{i=1}^{l} n_i$) such that $b_{i,j}$ is the initial color of $v_{i,j}$, b_0 is the initial color of v_0, and b_n is the color of v_n.

The next result shows which initial colorings are winnable on reduced theta graphs. Corollary 2.8 can then be used inductively to determine whether any given initial coloring of a general theta graph is winnable.

Theorem 4.3. *Let G be a reduced theta graph labeled as in Notation 4.2.*

(1) *If $t = 0$ then an initial coloring $\vec{b} \in \mathbb{Z}_k^N$ is winnable over $\mathbb{Z}_k$ if and only if the linear system*

$$\begin{cases} (1-m)d_0 + (l-2m)d_n = -b_0 + \sum_{i=1}^{m} b_{i,1}, \\ (l-2m)d_0 + (1-m)d_n = -b_n + \sum_{i=1}^{m} b_{i,1}, \end{cases}$$

has a solution for (d_0, d_n) mod k.

(2) *If $t \neq 0$ then an initial coloring $\vec{b} \in \mathbb{Z}_k^N$ is winnable over $\mathbb{Z}_k$ if and only if $b_{i,2}-b_{i,1} = b_{j,2}-b_{j,1}$ for all $m+1 \le i, j \le m+t$ and $\gcd(2-6m-3t+2l, k)$ divides*

$$-b_0 - b_n - (l-3m-t+1)(b_{m+1,1} - b_{m+1,2}) + \sum_{i=1}^{m} b_{i,1} + \sum_{i=1}^{m+t} b_{i,1}.$$

Proof. Let G and $\vec{b}$ be as in the hypotheses of the theorem. In order to win, we must press each vertex some number of times. Suppose v_0 is pressed d_0 times, v_n is pressed d_n times, and $v_{i,j}$ is pressed $d_{i,j}$ times. The effects of pressing these vertices are:

- the color of v_0 is changed by $d_0 + \sum_{i=1}^{m+t} d_{i,1} + (l-m-t)d_n$;
- for $1 \le i \le m$, the color of $v_{i,1}$ is changed by $d_0 + d_{i,1} + d_n$;
- for $m+1 \le i \le m+t$, the color of $v_{i,1}$ is changed by $d_0 + d_{i,1} + d_{i,2}$;
- for $m+1 \le i \le m+t$, the color of $v_{i,2}$ is changed by $d_{i,1} + d_{i,2} + d_n$;
- the color of v_n is changed by $d_n + \sum_{i=1}^{m} d_{i,1} + \sum_{i=m+1}^{m+t} d_{i,2} + (l-m-t)d_0$.

To win, we must change the color of every vertex to 0, which yields the following system of equations mod k. As before, these equations are equivalent to the matrix equation $N(G)\vec{d} = -\vec{b}$.

$$b_0 + d_0 + \sum_{i=1}^{m+t} d_{i,1} + (l-m-t)d_n = 0, \tag{4-1}$$

$$b_{i,1} + d_0 + d_{i,1} + d_n = 0 \quad \text{for } 1 \le i \le m, \tag{4-2}$$

$$b_{i,1} + d_0 + d_{i,1} + d_{i,2} = 0 \quad \text{for } m+1 \le i \le m+t, \tag{4-3}$$

$$b_{i,2} + d_{i,1} + d_{i,2} + d_n = 0 \quad \text{for } m+1 \le i \le m+t, \tag{4-4}$$

$$b_n + d_n + \sum_{i=1}^{m} d_{i,1} + \sum_{i=m+1}^{m+t} d_{i,2} + (l-m-t)d_0 = 0. \tag{4-5}$$

(1) Suppose $t = 0$. The system in the statement of part (1) arises from a straightforward substitution using (4-2) to eliminate $d_{i,1}$ from (4-1) and (4-5).

(2) Suppose $t \neq 0$ and the system given by (4-1) through (4-5) has a solution. Then (4-3) and (4-4) combine to show that $d_n - d_0 = b_{i,1} - b_{i,2}$ for $m+1 \le i \le m+t$, which in turn shows that $b_{i,1} - b_{i,2} = b_{j,1} - b_{j,2}$ for $m+1 \le i, j \le m+t$. Equations (4-2) and (4-3) can then be solved for $d_{i,1}$ for $1 \le i \le m+t$. Using the expressions for $d_{i,1}$ to eliminate all occurrences of $d_{i,1}$ from (4-1) and (4-5) and simplifying gives

$$b_0 + (1-3m-2t+l)d_0 + (l-2m-t)(b_{m+1,1} - b_{m+1,2}) - \sum_{i=1}^{m+t} b_{i,1} - \sum_{i=m+1}^{m+t} d_{i,2} = 0, \tag{4-6}$$

$$b_n + (1-3m-t+l)d_0 + (1-m)(b_{m+1,1} - b_{m+1,2}) - \sum_{i=1}^{m} b_{i,1} + \sum_{i=m+1}^{m+t} d_{i,2} = 0, \tag{4-7}$$

Adding (4-6) and (4-7), we find that

$$(2-6m-3t+2l)d_0 = -b_0 - b_n - (l-3m-t+1)(b_{m+1,1} - b_{m+1,2}) + \sum_{i=1}^{m} b_{i,1} + \sum_{i=1}^{m+t} b_{i,1}. \tag{4-8}$$

This implies that $\gcd(2-6m-3t+2l,k)$ divides the right-hand side of (4-8), as required.

Conversely, if $\gcd(2-6m-3t+2l,k)$ divides the right-hand side of (4-8) and $b_{i,1}-b_{i,2}=b_{j,1}-b_{j,2}$ for $m+1\le i,j\le m+t$, there exists d_0 such that (4-8) is satisfied. Since $t>0$, values of $d_{m+1,2},\dots,d_{m+t,2}$ can be chosen freely so that (4-6) is satisfied, and it follows that (4-7) is satisfied as well. Finally, values of $d_{i,1}$ can be determined for $1\le i\le m+t$ from (4-2), (4-3), and (4-4), with the last two equations being consistent since $b_{i,1}-b_{i,2}=b_{j,1}-b_{j,2}$ for $m+1\le i,j\le m+t$. □

Theorem 4.4 (Characterization of AW theta graphs). *Let G be a theta graph labeled as in Notation 4.2. Then G is AW over $\mathbb{Z}_k$ if and only if either*

(1) $t=0$ *and* $\gcd((l-2m)^2-(m-1)^2,k)=1$, *or*

(2) $t=1$ *and* $\gcd(-1-6m+2l,k)=1$.

Proof. Let G be a theta graph labeled as in Notation 4.2. By Proposition 2.7, G is AW over $\mathbb{Z}_k$ if and only if $\widehat{G}$ is AW over $\mathbb{Z}_k$, where $\widehat{G}$ is the reduced theta graph with m paths of length 1, t paths of length 2, and $l-m-t$ paths of length 0. We assume that $\widehat{G}$ is also labeled as in Notation 4.2.

If $t=0$, then by Theorem 4.3, $\widehat{G}$ is AW over $\mathbb{Z}_k$ if and only if

$$A\begin{pmatrix} d_0 \\ d_n \end{pmatrix}=\vec{y}$$

has a solution mod k for all $\vec{y}\in\mathbb{Z}_k^2$, where

$$A=\begin{pmatrix} 1-m & l-2m \\ l-2m & 1-m \end{pmatrix}.$$

This is true if and only if $\det A$ is a unit in $\mathbb{Z}_k$ [Bourbaki 1974, III.8.7, Proposition 13]. Finally, $\det A$ is a unit in $\mathbb{Z}_k$ if and only if $\gcd((l-2m)^2-(m-1)^2,k)=1$.

If $t=1$, then by Theorem 4.3, $\widehat{G}$ is AW over $\mathbb{Z}_k$ if and only if

$$\gcd(-1-6m+2l,k)=1.$$

Finally, if $t>1$, $\widehat{G}$ cannot be AW over $\mathbb{Z}_k$, since the condition

$$b_{i,1}-b_{i,2}=b_{j,1}-b_{j,2}$$

for $m+1\le i,j\le m+t$ will not be satisfied for all $\vec{b}$. □

5. Always winnable trees

In this section, we give a construction describing all AW trees over $\mathbb{Z}_p$ where p is prime. By Corollary 2.3(2), this construction also gives all AW trees over $\mathbb{Z}_{p^e}$ for positive integers e. We follow the outline of the process used in [Amin and

Slater 1996], although the transition to p colors requires some changes to the main argument. *From this point on, 'AW' will mean 'AW over $\mathbb{Z}_p$'.*

Definition 5.1. Let G_1 and G_2 be AW graphs, and let $v_i \in V(G_i)$ such that $G_1 - \{v_1\}$ is not AW. The process of forming the AW graph H defined in Proposition 2.10 is called a *type-1 operation*.

Definition 5.2. Let $G_1, \ldots, G_m$ be AW graphs, and let $v_i \in V(G_i)$ such that $G_i - \{v_i\}$ is AW for all i. If

$$\sum_{i=1}^{m} d(G_i)^{-1} d(G_i - \{v_i\}) \neq 1 \pmod{p}$$

then the process of forming the AW graph W as in Proposition 2.12 is called a *type-2 operation centered at w*.

The main theorem in this section characterizes AW trees.

Theorem 5.3. *A tree T is AW if and only if T can be formed by starting with copies of K_1 and using only type-1 and type-2 operations.*

Proof. Corollaries 2.11 and 2.13 show that if one begins with copies of a single vertex K_1 and applies a series of type-1 and type-2 operations, an AW tree will always result.

Conversely, let T be an AW tree. If T has diameter 0, then $T = K_1$. It is not possible for T to have diameter 1, since P_2 is not AW for any value of k. If T has diameter 2 (i.e., if T is an AW star with l leaves for some $l \geq 2$), then T can be formed from copies of K_1 using one type-2 operation. (The summation condition on the type-2 operation is true because T is AW. This implies that $l \neq 1 \pmod{p}$, as in [Giffen and Parker 2009, Corollary 4.6].)

Therefore, we assume T has diameter at least 3. Let $x \in V(T)$ such that $\deg x = l + 1$ and x is adjacent to l leaves, which we denote $v_1, v_2, \ldots, v_l$. Let w be the nonleaf vertex of T adjacent to x. Let T_x be the component of $T - \{wx\}$ containing x, and let T_w be the component of $T - \{wx\}$ containing w.

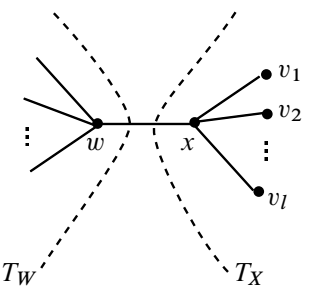

Suppose first that T_w is not AW, so that $p|d(T_w)$. Proposition 2.10 implies that

$$d(T) = d(T - \{v_1\}) - d(T - \{x, v_1\}) = d(T - \{v_1\}) - d(T_w).$$

The fact that $p|d(T_w)$ and $p \nmid d(T)$ implies that $p \nmid d(T - \{v_1\})$, showing that $T - \{v_1\}$ is AW. This shows that T can be formed via a type-1 operation in which edge xv_1 is added to join $T - \{v_1\}$ to $\{v_1\}$.

From now on, we will assume that T_w is AW. If $T_w - \{w\}$ is also AW, we may construct T via a type-2 operation centered at x. Thus, we may assume that T_w is AW while $T_w - \{w\}$ is not. Proposition 2.10 implies that

$$d(T) = d(T_x)d(T_w) - d(T_w - \{w\}).$$

Since $p|d(T_w - \{w\})$ and $p \nmid d(T)$, we see that $p \nmid d(T_x)$. Thus, T can be formed by a type-1 operation in which edge wx is added to join T_x to T_w. □

Example 5.4. We show the necessity of the type-2 operation for forming trees. Consider the following tree T over $\mathbb{Z}_3$.

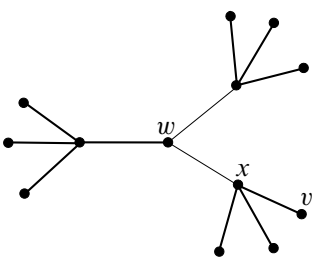

One can check that $d(T) = -20$, showing that T is AW over $\mathbb{Z}_3$. For any leaf v, the graph $T - \{v\}$ is not AW over $\mathbb{Z}_3$, since $d(T - \{v\}) = -12$. The two graphs T_w and T_x formed by deleting an edge wx incident with the center vertex w are both AW modulo 3. However, $T_w - \{w\}$ and $T_x - \{x\}$ are also AW. Thus, T cannot be formed from smaller trees using a type-1 operation. This tree can be formed via a type-2 operation centered at w.

Acknowledgment

The authors thank the referees for several suggestions leading to the improvement of this article.

References

[Amin and Slater 1992] A. T. Amin and P. J. Slater, "Neighborhood domination with parity restrictions in graphs", *Congr. Numer.* **91** (1992), 19–30. MR 93j:05141 Zbl 0798.68135

[Amin and Slater 1996] A. T. Amin and P. J. Slater, "All parity realizable trees", *J. Combin. Math. Combin. Comput.* **20** (1996), 53–63. MR 96i:05043 Zbl 0845.05029

[Anderson and Feil 1998] M. Anderson and T. Feil, "Turning lights out with linear algebra", *Math. Mag.* **71**:4 (1998), 300–303. MR 1573341

[Bourbaki 1974] N. Bourbaki, *Elements of mathematics. Algebra, I: Chapters 1-3*, Hermann, Paris, 1974. Reprinted by Springer, 1989. MR 50 #6689

[Giffen and Parker 2009] A. Giffen and D. Parker, "On generalizing the 'Lights Out' game and a generalization of parity domination", preprint, 2009, Available at http://faculty.gvsu.edu/parkerda/profstuff/papers/hyperlogpd.pdf.

[Goldwasser and Klostermeyer 1997] J. Goldwasser and W. Klostermeyer, "Maximization versions of "lights out" games in grids and graphs", pp. 99–111 in *Proceedings of the Twenty-eighth Southeastern International Conference on Combinatorics, Graph Theory and Computing* (Boca Raton, FL, 1997), vol. 126, 1997. MR 98j:05119

[Goldwasser et al. 1997] J. Goldwasser, W. Klostermeyer, and G. Trapp, "Characterizing switch-setting problems", *Linear and Multilinear Algebra* **43**:1-3 (1997), 121–135. MR 98k:15005 Zbl 0890.15004

[Goldwasser et al. 2002] J. Goldwasser, W. Klostermeyer, and H. Ware, "Fibonacci polynomials and parity domination in grid graphs", *Graphs Combin.* **18**:2 (2002), 271–283. MR 2003f:05089 Zbl 0999.05079

[Sutner 1989] K. Sutner, "Linear cellular automata and the Garden-of-Eden", *Math. Intelligencer* **11**:2 (1989), 49–53. MR 994964 Zbl 0770.68094

Received: 2009-04-13 Revised: 2009-12-21 Accepted: 2009-12-29

sedwards@hope.edu *Department of Mathematics, Hope College, Holland, MI 49423, United States*

victoria.l.elandt@uwsp.edu *Department of Mathematical Sciences, University of Wisconsin, Stevens Point, WI 54481-3897, United States*

nickjames8806@gmail.com *Department of Mathematics, University of Florida, Gainesville, FL 32611-8105, United States*

kathryn.johnson@hope.edu *Department of Mathematics, Hope College, Holland, MI 49423, United States*

zachary.mitchell@hope.edu *Department of Mathematics, Hope College, Holland, MI 49423, United States*

stephenson@hope.edu *Department of Mathematics, Hope College, Holland, MI 49423, United States*

Trace diagrams, signed graph colorings, and matrix minors

Steven Morse and Elisha Peterson

(Communicated by Kenneth S. Berenhaut)

Trace diagrams are structured graphs with edges labeled by matrices. Each diagram has an interpretation as a particular multilinear function. We provide a rigorous combinatorial definition of these diagrams using a notion of signed graph coloring, and prove that they may be efficiently represented in terms of matrix minors. Using this viewpoint, we provide new proofs of several standard determinant formulas and a new generalization of the Jacobi determinant theorem.

1. Introduction

Trace diagrams provide a graphical means of performing computations in multilinear algebra. The following example, which proves a vector identity, illustrates the power of the notation.

Example. For $\boldsymbol{u}, \boldsymbol{v}, \boldsymbol{w} \in \mathbb{C}^3$, diagrams for the cross product and inner product are

$\boldsymbol{u} \times \boldsymbol{v} =$  and $\boldsymbol{u} \cdot \boldsymbol{v} =$  .

By "bending" the diagrammatic identity

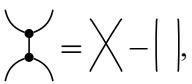
(1)

and attaching vectors, one obtains

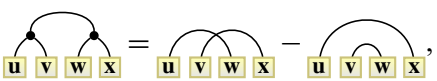

which is the vector identity

$$(\boldsymbol{u} \times \boldsymbol{v}) \cdot (\boldsymbol{w} \times \boldsymbol{x}) = (\boldsymbol{u} \cdot \boldsymbol{w})(\boldsymbol{v} \cdot \boldsymbol{x}) - (\boldsymbol{u} \cdot \boldsymbol{x})(\boldsymbol{v} \cdot \boldsymbol{w}).$$

MSC2000: primary 05C15, 15A69; secondary 57M07, 16W22.

Keywords: trace diagrams, graph coloring, matrix minors, multilinear algebra, planar algebra, tensor diagrams, determinant, cofactor.

We will later prove (1) and show that every step here can be mathematically rigorous.

In this paper, we define a set of combinatorial objects called *trace diagrams*. Each diagram translates to a well-defined multilinear function, provided it is *framed* (the framing specifies the domain and range of the function). We introduce the idea of *signed graph coloring* to describe this translation, and show that it preserves a tensorial structure. We prove two results regarding the relationship between multilinear algebra and trace diagrams. Under traditional notation, a multilinear function is characterized by its action on a basis of tensor products in the domain. Theorem 5.5 shows that trace diagram notation is more powerful than this standard notation for functions, since a single diagrammatic identity may simultaneously represent several different identities of multilinear functions. In the above example, the diagrammatic identity (1) is used to prove a vector identity; another vector identity arising from the same diagram is given in Section 5.

Our main results concern the "structural" properties of trace diagrams. In particular, we characterize their decomposition into *diagram minors*, which are closely related to matrix minors. Theorem 7.7 describes the condition under which this decomposition is possible, and Theorem 7.8 gives an upper bound for the number of matrix minors required in a formula for a trace diagram's function.

As an application, we use trace diagrams to provide new proofs of classical determinant identities. Cayley, Jacobi, and other 19th-century mathematicians described several methods for calculating determinants in general and for special classes of matrices [Muir 1882]. The calculations could often take pages to complete because of the complex notation and the need to keep track of indices. In contrast, we show that diagrammatic proofs of certain classic results come very quickly, once the theory has been suitably developed. One can easily generalize the diagrammatic identities by adding additional matrices, which is not as easy to do with the classical notation for matrices. Theorem 9.2, a novel generalization of a determinant theorem of Jacobi, is proven in this manner.

While the term *trace diagrams* is new, the idea of using diagrammatic notations for algebraic calculations has a rich history [Baez 1996; Bullock 1997; Cvitanović 2008; Lawton and Peterson 2009; Stedman 1990]. In the early 1950s, Roger Penrose invented a diagrammatic notation that streamlined calculations in multilinear algebra. In his context, indices became labels on edges between "spider-like" nodes, and tensor contraction meant gluing two edges together [Penrose 1971]. In knot theory, Kauffman [1991] generalized Penrose's diagrams and described their relation to knot polynomials. Przytycki and others placed Kauffman's work in the context of skein modules [Bullock et al. 1999; Przytycki 1991]. The concept of *planar algebras* [Jones 1999] unifies many of the concepts underlying diagrammatic manipulations. More recently, Kuperberg [1996] introduced spiders as a means

of studying representation theory. In mathematical physics, Levinson [Levinson 1956] pioneered the use of diagrams to study angular momentum. This approach proved to be extremely useful, with several textbooks written on the topic. Work on these notations and their broader impact on fundamental concepts in physics culminated in books by Stedman [1990] and Cvitanović [2008].

The name "trace diagrams" was first used in [Peterson 2006] and [Lawton and Peterson 2009], where diagrams were used to write down an additive basis for a certain ring of invariants. Special cases of trace diagrams have appeared before in the above works, but they are generally used only as a tool for algebraic calculation. This paper differs in emphasizing the diagrams themselves, their combinatorial construction, and their structural properties.

This paper is organized as follows. Section 2 provides a short review of multilinear algebra. In Section 3 we introduce the idea of *signed graph coloring*, which forms the basis for the translation between trace diagrams and multilinear algebra described rigorously in Sections 4 and 5. Section 6 describes the basic properties of trace diagrams, and Section 7 focuses on the fundamental relationship between matrix minors and trace diagram functions. New proofs of classical determinant results are derived in Section 8. Finally, in Section 9 we prove a new multilinear algebra identity using trace diagrams.

2. Multilinear algebra

This section reviews multilinear algebra and tensors. For further reference, a nice introductory treatment of tensors is given in Appendix B of [Fulton and Harris 1991].

Let V be a finite-dimensional vector space over a field $\mathbb{F}$. Informally, a *2-tensor* consists of finite sums of vector pairs $(\boldsymbol{u}, \boldsymbol{v}) \in V \times V$ modulo the relations

$$(\lambda \boldsymbol{u}, \boldsymbol{v}) = \lambda(\boldsymbol{u}, \boldsymbol{v}) = (\boldsymbol{u}, \lambda \boldsymbol{v})$$

for all $\lambda \in \mathbb{F}$. The resulting term is denoted $\boldsymbol{u} \otimes \boldsymbol{v}$. More generally, a *k-tensor* is an equivalence class of k-tuples of vectors, where k-tuples are equivalent if and only if they differ by the positioning of scalar constants. In other words, if $\prod_{i=1}^{k} \lambda_i = \prod_{i=1}^{k} \mu_i = \Lambda$ then

$$\lambda_1 \boldsymbol{u}_1 \otimes \cdots \otimes \lambda_k \boldsymbol{u}_k = \mu_1 \boldsymbol{u}_1 \otimes \cdots \otimes \mu_k \boldsymbol{u}_k = \Lambda \left(\boldsymbol{u}_1 \otimes \cdots \otimes \boldsymbol{u}_k \right).$$

Let $N = \{1, 2, \ldots, n\}$. In what follows, we assume that V has basis $\{\hat{\boldsymbol{e}}_1, \hat{\boldsymbol{e}}_2, \ldots, \hat{\boldsymbol{e}}_n\}$. The space of k-tensors $V^{\otimes k} \equiv V \otimes \cdots \otimes V$ is itself a vector space with n^k basis elements of the form

$$\hat{\boldsymbol{e}}_\alpha \equiv \hat{\boldsymbol{e}}_{\alpha_1} \otimes \hat{\boldsymbol{e}}_{\alpha_2} \otimes \cdots \otimes \hat{\boldsymbol{e}}_{\alpha_k};$$

one for each $\alpha = (\alpha_1, \alpha_2, \ldots, \alpha_k) \in N^k$. By convention $V^{\otimes 0} = \mathbb{F}$.

Let $\langle \cdot, \cdot \rangle$ be the inner product on V defined by $\langle \hat{\boldsymbol{e}}_i, \hat{\boldsymbol{e}}_j \rangle = \delta_{ij}$, where δ_{ij} is the Kronecker delta. This extends to an inner product on $V^{\otimes k}$ with

$$\langle \hat{\boldsymbol{e}}_\alpha, \hat{\boldsymbol{e}}_\beta \rangle = \delta_{\alpha_1\beta_1}\delta_{\alpha_2\beta_2}\cdots\delta_{\alpha_k\beta_k},$$

making $\{\hat{\boldsymbol{e}}_\alpha : \alpha \in N^k\}$ an orthonormal basis for $V^{\otimes k}$.

Given another vector space W over $\mathbb{F}$, a *multilinear function* $f : V^{\otimes k} \to W$ is one that is linear in each term, so that

$$f\left((\lambda \boldsymbol{u} + \mu \boldsymbol{v}) \otimes \boldsymbol{u}_2 \otimes \cdots \otimes \boldsymbol{u}_k\right) = \lambda f(\boldsymbol{u} \otimes \boldsymbol{u}_2 \otimes \cdots \otimes \boldsymbol{u}_k) + \mu f(\boldsymbol{v} \otimes \boldsymbol{u}_2 \otimes \cdots \otimes \boldsymbol{u}_k),$$

and a similar identity holds for each of the other $(k-1)$ terms.

Denote by $\mathrm{Fun}(V^{\otimes j}, V^{\otimes k})$ the space of *multilinear functions* from $V^{\otimes j}$ to $V^{\otimes k}$. There are two standard ways to combine these functions. First, given

$$f \in \mathrm{Fun}(V^{\otimes j}, V^{\otimes k}), \qquad g \in \mathrm{Fun}(V^{\otimes k}, V^{\otimes m}),$$

one may define a composition $g \circ f$. Second, given $f_1 \in \mathrm{Fun}(V^{\otimes j_1}, V^{\otimes k_1})$ and $f_2 \in \mathrm{Fun}(V^{\otimes j_2}, V^{\otimes k_2})$, then $f_1 \otimes f_2 \in \mathrm{Fun}(V^{\otimes (j_1+j_2)}, V^{\otimes (k_1+k_2)})$ is the multilinear function defined by letting f_1 operate on the first j_1 tensor components of $V^{\otimes (j_1+j_2)}$ and f_2 on the last j_2 components.

A multilinear function $f \in \mathrm{Fun}(V^{\otimes k}) \equiv \mathrm{Fun}(V^{\otimes k}, \mathbb{F})$ is commonly called a *multilinear form*. Also, functions $f : \mathbb{F} \to \mathbb{F}$ may be thought of as elements of $\mathbb{F}$. In particular, $\mathrm{Fun}(\mathbb{F}, \mathbb{F}) \cong \mathbb{F}$ via the isomorphism $f \mapsto f(1)$.

The space of tensors $V^{\otimes k}$ is isomorphic to the space of forms $\mathrm{Fun}(V^{\otimes k})$. Given $f \in \mathrm{Fun}(V^{\otimes k})$, the isomorphism maps

$$f \mapsto \sum_{\alpha \in N^k} f(\hat{\boldsymbol{e}}_\alpha)\hat{\boldsymbol{e}}_\alpha \in V^{\otimes k}. \tag{2}$$

This is the *duality* property of tensor algebra. Loosely speaking, multilinear functions do not distinguish between inputs and outputs; up to isomorphism all that matters is the total number of inputs and outputs.

One relevant example is the determinant, which can be written as a multilinear function $V^{\otimes k} \to \mathbb{F}$. In particular, if a $k \times k$ matrix is written in terms of its column vectors as $A = [\boldsymbol{a}_1\, \boldsymbol{a}_2\, \cdots\, \boldsymbol{a}_k]$, then the determinant maps the ordered k-tuple $\boldsymbol{a}_1 \otimes \cdots \otimes \boldsymbol{a}_k$ to $\det(A)$. This may be defined on the tensor product since a scalar multiplied on a single column may be factored outside the determinant. Determinants additionally are *antisymmetric*, since switching any two columns changes the sign of the determinant. Antisymmetric functions can also be considered as functions on an *exterior (wedge) product* of vector spaces, which we do not define here.

3. Signed graph coloring

This section introduces graph theoretic principles that will be used in defining trace diagram functions. Although the terminology of colorings is borrowed from graph theory, to our knowledge the notion of signed graph coloring is new, being first described in [Peterson 2006]. Some readers may wish to consult a graph theory text such as [West 2001] for further background on graph theory and edge-colorings, or an abstract algebra text such as [Fraleigh 1967] for further background on permutations.

Ciliated graphs and edge-colorings. A *graph* $G = (V, E)$ consists of a finite collection of *vertices* V and a finite collection of *edges* E. Throughout this paper, we permit an edge to be any one of the following:

(1) a 2-vertex set $\{v_1, v_2\} \subset V$, representing an (undirected) edge connecting vertices v_1 and v_2;

(2) a 1-vertex set $\{v\} \subset V$ called a *loop*, representing an edge connecting a vertex to itself; or

(3) the empty set $\{\} \subset V$, denoted $\bigcirc$, representing a trivial loop that does not connect any vertices.

In addition, we allow the collection of edges E to contain repeated elements of the same form.

Two vertices are *adjacent* if there is an edge connecting them; two edges are *adjacent* if they share a common vertex. An edge is *adjacent* to a vertex if it contains that vertex. Given a vertex v, the set of edges adjacent to v will be denoted $E(v)$. The *degree* $\deg(v)$ of a vertex v is the number of adjacent edges, where any loops at the vertex are counted twice. Vertices of degree 1 are commonly called *leaves*.

Definition 3.1. A *ciliated graph* $G = (V, E, \sigma_*)$ is a graph (V, E) together with an ordering $\sigma_v : \{1, 2, \ldots, \deg(v)\} \to E(v)$ of edges at each vertex $v \in V$.

By convention, when such graphs are drawn in the plane, the ordering is specified by enumerating edges in a counterclockwise fashion from a ciliation, as shown in Figure 1.

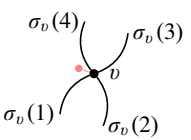

Figure 1. Proceeding counterclockwise from the ciliation at the vertex v, one obtains the edge ordering $\sigma_v(1)$, $\sigma_v(2)$, $\sigma_v(3)$, $\sigma_v(4)$.

Definition 3.2. Given the set $N = \{1, 2, \ldots, n\}$, an *n-edge-coloring* of a graph $G = (V, E)$ is a map $\kappa : E \to N$. The coloring is said to be *proper* if the graph does not contain any loops and no two adjacent edges have the same label; equivalently, for every vertex v the restriction $\kappa : E(v) \to N$ is one-to-one. When n is clear from context, we denote the set of all proper n-edge-colorings of a graph G by $\mathsf{col}(G)$.

Note that some graphs do not have proper n-edge-colorings for certain n. As a simple example, the graph  has no 2-edge-colorings.

Permutations and signatures of edge-colorings. Let S_n denote the set of permutations of $N = \{1, 2, \ldots, n\}$. We denote a specific permutation as follows: $\left(\begin{smallmatrix}1&2&3\\1&2&3\end{smallmatrix}\right)$ denotes the identity permutation, and $\left(\begin{smallmatrix}1&2&3\\3&2&1\end{smallmatrix}\right)$ denotes the permutation mapping $1 \mapsto 3$, $2 \mapsto 2$, and $3 \mapsto 1$. The *signature* of a permutation is $(-1)^k$, where k is the number of transpositions (or swaps) that must be made to return the permutation to the identity. For example, the permutation $\left(\begin{smallmatrix}1&2&3&4\\2&4&1&3\end{smallmatrix}\right)$ has signature -1, since it takes 3 transpositions to return it to the identity:

$$(2, 4, 1, 3) \rightsquigarrow (1, 4, 2, 3) \rightsquigarrow (1, 2, 4, 3) \rightsquigarrow (1, 2, 3, 4).$$

Proper edge-colorings induce permutations at the vertices of ciliated graphs. Given a proper n-edge-coloring κ and a degree-n vertex v, there is a well-defined permutation $\pi_\kappa(v) \in S_n$ defined by

$$\pi_\kappa(v) : i \mapsto \kappa(\sigma_v(i)).$$

In other words, 1 is taken to the label on the first edge adjacent to the vertex, 2 is taken to the label on the second edge, and so on. An example is shown in Figure 2.

Definition 3.3 [Peterson 2006]. Given a proper n-edge-coloring κ of a ciliated graph $G = (V, E, \sigma_*)$, the *signature* $\mathrm{sgn}_\kappa(G)$ is the product of permutation signatures on the degree-n vertices:

$$\mathrm{sgn}_\kappa(G) = \prod_{v \in V_n} \mathrm{sgn}(\pi_\kappa(v)),$$

where V_n is the set of degree-n vertices in V and $\mathrm{sgn}(\pi_\kappa(v))$ is the signature of the permutation $\pi_\kappa(v)$. If there are no degree-n vertices, the signature is $+1$.

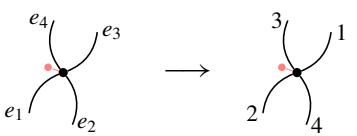

Figure 2. The proper edge-coloring at right induces the permutation $\left(\begin{smallmatrix}1&2&3&4\\2&4&1&3\end{smallmatrix}\right)$ on the ciliated vertex shown. The signature of the coloring is -1.

The *signed chromatic index* $\chi(G)$ is the sum of signatures over all proper edge-colorings:

$$\chi(G) = \sum_{\kappa \in \mathrm{col}(G)} \mathrm{sgn}_\kappa(G).$$

Example. For $n = 2$, the ciliated graph $G =$  has exactly two proper edge-colorings:

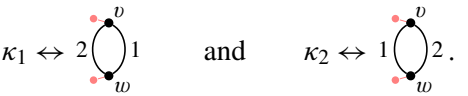

(3)

With the counterclockwise ordering, $\pi_{\kappa_1}(w) = \left(\begin{smallmatrix}1&2\\1&2\end{smallmatrix}\right)$ and $\pi_{\kappa_1}(v) = \left(\begin{smallmatrix}1&2\\2&1\end{smallmatrix}\right)$, so the signature of the first coloring is

$$\mathrm{sgn}_{\kappa_1}(G) = \mathrm{sgn}(\pi_{\kappa_1}(w))\ \mathrm{sgn}(\pi_{\kappa_1}(v)) = \mathrm{sgn}\left(\begin{smallmatrix}1&2\\1&2\end{smallmatrix}\right)\ \mathrm{sgn}\left(\begin{smallmatrix}1&2\\2&1\end{smallmatrix}\right) = -1.$$

In the second case, the permutations are $\left(\begin{smallmatrix}1&2\\2&1\end{smallmatrix}\right)$ at w and $\left(\begin{smallmatrix}1&2\\1&2\end{smallmatrix}\right)$ at v, so the signature is again -1. Therefore, the signed chromatic index of this ciliated graph is $\chi(G) = -2$.

Pre-edge-colorings.

Definition 3.4 [Peterson 2006]. A *pre-edge-coloring* of a graph $G = (E, V)$ is an edge-coloring $\check{\kappa} : \check{E} \to N$ of a subset $\check{E} \subset E$ of the edges of G. A *leaf-coloring* is a pre-edge-coloring of the edges adjacent to the degree-1 vertices.

Two pre-edge-colorings $\check{\kappa}_1 : \check{E}_1 \to N$ and $\check{\kappa}_2 : \check{E}_2 \to N$ are *compatible* if they agree on the intersection $\check{E}_1 \cap \check{E}_2$. In this case, the map $\check{\kappa}_1 \cup \check{\kappa}_2$ defined by $(\check{\kappa}_1 \cup \check{\kappa}_2)|_{\check{E}_i} = \check{\kappa}_i|_{\check{E}_i}$ is also a pre-edge-coloring.

If $\check{\kappa}_1 : \check{E}_1 \to N$ and $\check{\kappa}_2 : \check{E}_2 \to N$ are compatible and $\check{E}_1 \subset \check{E}_2$, we say that $\check{\kappa}_2$ *extends* $\check{\kappa}_1$ and write $\check{\kappa}_2 \succ \check{\kappa}_1$. We denote the (possibly empty) set of proper edge-colorings that extend $\check{\kappa}$ by

$$\mathrm{col}_{\check{\kappa}}(G) \equiv \{\kappa \in \mathrm{col}(G) : \kappa \succ \check{\kappa}\}.$$

The *signed chromatic subindex* of a pre-edge-coloring $\check{\kappa}$ is the sum of signatures of its proper extensions:

$$\chi_{\check{\kappa}}(G) = \sum_{\kappa \succ \check{\kappa}} \mathrm{sgn}_\kappa(G).$$

Example. For $n = 3$, the pre-edge-coloring $\check{\kappa} \leftrightarrow$  extends to exactly two proper edge-colorings:

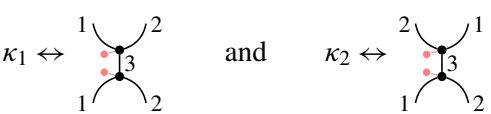

(4)

One computes the signed chromatic subindex by summing over the signature of each coloring. In the first case,

$$\operatorname{sgn}_{\kappa_1}(G) = \operatorname{sgn}\left(\begin{smallmatrix}1&2&3\\1&2&3\end{smallmatrix}\right)\ \operatorname{sgn}\left(\begin{smallmatrix}1&2&3\\3&2&1\end{smallmatrix}\right) = -1,$$

where the permutations are read in counterclockwise order from the vertex. In the second case, the permutations are $\left(\begin{smallmatrix}1&2&3\\1&2&3\end{smallmatrix}\right)$ and $\left(\begin{smallmatrix}1&2&3\\3&1&2\end{smallmatrix}\right)$, so

$$\operatorname{sgn}_{\kappa_2}(G) = \operatorname{sgn}\left(\begin{smallmatrix}1&2&3\\1&2&3\end{smallmatrix}\right)\ \operatorname{sgn}\left(\begin{smallmatrix}1&2&3\\3&1&2\end{smallmatrix}\right) = +1.$$

Summing the two signatures, the signed chromatic subindex is

$$\chi_{\breve{\kappa}}(G) = \operatorname{sgn}_{\kappa_1}(G) + \operatorname{sgn}_{\kappa_2}(G) = -1 + 1 = 0.$$

4. Trace diagrams

Penrose [1971] was probably the first to describe how tensor algebra may be performed diagrammatically. In his framework, edges in a graph represent elements of a vector space, and nodes represent multilinear functions. Trace diagrams are a generalization of Penrose's *tensor diagrams*, in which edges may be labeled by matrices and nodes represent the determinant.

The closest concept in traditional graph theory is a *voltage graph* (also called a *gain graph*), in which the edges of a graph are marked by group elements in an "orientable" way [Gross 1974]. Diagrams labeled by matrices also make frequent appearances in skein theory [Bullock 1997; Sikora 2001] and occasional appearances in the work of Stedman [1990] and Cvitanović [2008].

Definition. In the remainder of this paper, V will represent an n-dimensional vector space over a base field $\mathbb{F}$ (with $n \geq 2$), and $\{\hat{\boldsymbol{e}}_1, \hat{\boldsymbol{e}}_2, \ldots, \hat{\boldsymbol{e}}_n\}$ will represent an orthonormal basis for V.

Definition 4.1. An *n-trace diagram* is a ciliated graph $\mathcal{D} = (V_1 \sqcup V_2 \sqcup V_n, E, \sigma_*)$, where V_i is comprised of vertices of degree i, together with a labeling $A_{\mathcal{D}} : V_2 \to \operatorname{Fun}(V, V)$ of degree-2 vertices by linear transformations. If there are no degree-1 vertices, the diagram is said to be *closed*.

A *framed trace diagram* is a diagram together with a partition of the degree-1 vertices V_1 into two disjoint ordered collections: the *inputs* V_I and the *outputs* V_O.

Thus, trace diagrams contain vertices of degree 1, 2, or n only, and the degree-2 vertices represent matrices. An example is shown in Figure 3. Note that in the case $n = 2$, the vertices in V_2 and V_n have the same degree but are disjoint sets. By convention, framed trace diagrams are drawn with inputs at the bottom of the diagram and outputs at the top. Both are assumed to be ordered left to right.

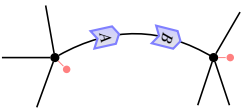

Figure 3. An unframed 4-trace diagram. Degree-n vertices are ciliated and degree-2 vertices are marked by matrices in an oriented manner.

As shown in Figure 3, we represent matrix markings at the degree-2 vertices as follows:

$$A \leftrightarrow$$ $$, \qquad A^{-1} \leftrightarrow$$  $$.$$

Note that when drawing the inverse of a matrix in a diagram, we use the shorthand $\bar{A}$ because the traditional notation A^{-1} is overly cumbersome.

The ordering at a degree-2 vertex v given by the ciliation is implicit in the orientation of the node. Precisely, the ciliation $\sigma : \{1, 2\} \to E(v)$ orders the adjacent edges as follows:

We refer to the first edge $\sigma_v(1)$ as the "incoming" edge and the second edge $\sigma_v(2)$ as the "outgoing" edge. In general,

since the nodes occur with opposite orientations.

Trace diagram colorings and their coefficients. Trace diagrams require a slightly different definition of edge-coloring:

Definition 4.2. A *coloring* of an n-trace diagram $\mathcal{D}$ is a map $\kappa : E \to N$. The coloring is *proper* if the labels at each n-vertex are distinct. The (possibly empty) space of all colorings of $\mathcal{D}$ is denoted $\mathsf{col}(\mathcal{D})$.

Note that in a proper coloring of a trace diagram, the edges adjoining a matrix may have the same label.

Definition 4.3. Given a coloring κ of a trace diagram $\mathcal{D}$ with matrix labeling $A_{\mathcal{D}} : V_2 \to \mathrm{Fun}(V, V)$, the *coefficient* $\psi_\kappa(\mathcal{D})$ of the coloring is defined to be

$$\psi_\kappa(\mathcal{D}) \equiv \prod_{v \in V_2} (A_{\mathcal{D}}(v))_{\sigma_v(2)\sigma_v(1)},$$

where $(A(v))_{\sigma_v(2)\sigma_v(1)} = \langle \hat{\boldsymbol{e}}_{\sigma_v(2)}, A(v)\hat{\boldsymbol{e}}_{\sigma_v(1)} \rangle$ represents the matrix entry in row $\sigma_v(2)$ and column $\sigma_v(1)$.

Example. In the simplest colored diagram with a matrix,

$$\psi\left(\begin{array}{c} i \\ \boxed{A} \\ j \end{array}\right) = (A)_{ij}. \tag{5}$$

Similarly,

$$\psi\left(\begin{array}{c} i \\ \boxed{A}\ j \\ \boxed{B} \\ k \end{array}\right) = (A)_{ij}(B)_{jk}.$$

Example. In the colored diagram 

, the coefficient is $(A)_{21}(A)_{12}$.

Trace diagram functions. Recall that $\{\hat{\boldsymbol{e}}_1, \ldots, \hat{\boldsymbol{e}}_n\}$ represents an orthonormal basis for the vector space V. In a framed trace diagram, a basis element $\hat{\boldsymbol{e}}_\alpha \in V^{\otimes|V_I|}$ is equivalent to a labeling of the input vertices by basis elements. This labeling induces a precoloring on the adjacent edges: if a vertex is labeled by $\hat{\boldsymbol{e}}_i$, then its adjacent edge is labeled by i. We denote this precoloring by α. Likewise, a basis element $\hat{\boldsymbol{e}}_\beta \in V^{\otimes|V_O|}$ induces a precoloring on edges adjacent to the output vertices, which we denote β. Since V_I and V_O comprise all degree-1 vertices in the diagram, if α and β exist (and are compatible) then $\alpha \cup \beta$ is a leaf-coloring of the diagram.

We now define the key concept relating trace diagrams and multilinear functions. Each diagram corresponds to a unique function, whose coefficients are the signed chromatic subindices of these leaf-colorings, weighted by coloring coefficients.

Definition 4.4. Given a trace diagram $\mathcal{D}$, the *weight* $\chi_\gamma(\mathcal{D})$ of a leaf-coloring γ is

$$\chi_\gamma(\mathcal{D}) = \sum_{\kappa \succ \gamma} \operatorname{sgn}_\kappa(\mathcal{D})\, \psi_\kappa(\mathcal{D}). \tag{6}$$

The *value* of a closed diagram $\mathcal{D}$ is

$$\chi(\mathcal{D}) = \sum_{\kappa \in \operatorname{col}(\mathcal{D})} \operatorname{sgn}_\kappa(\mathcal{D})\, \psi_\kappa(\mathcal{D}).$$

Definition 4.5. Given a framed trace diagram $\mathcal{D}$, the *trace diagram function* $f_{\mathcal{D}} : V^{\otimes|V_I|} \to V^{\otimes|V_O|}$ is the linear extension of the basis mappings

$$f_{\mathcal{D}} : \hat{\boldsymbol{e}}_\alpha \mapsto \sum_{\beta \in N^{|V_O|}} \chi_{\alpha\cup\beta}(\mathcal{D})\hat{\boldsymbol{e}}_\beta, \tag{7}$$

where $f_{\mathcal{D}} : \hat{\boldsymbol{e}}_\alpha \mapsto 0$ if $\hat{\boldsymbol{e}}_\alpha$ does not induce a precoloring or does not extend to any proper colorings.

Remark 4.6. If n is odd, trace diagrams may be drawn without ciliations, since $\operatorname{sgn}(\sigma)$ is invariant under cyclic reorderings:

$$\operatorname{sgn}\begin{pmatrix} 1 & \cdots & n-1 & n \\ a_1 & a_2 & \cdots & a_n \end{pmatrix} = \operatorname{sgn}\begin{pmatrix} 1 & \cdots & n-1 & n \\ a_2 & \cdots & a_n & a_1 \end{pmatrix}.$$

We will sometimes abuse notation by using the diagram $\mathcal{D}$ interchangeably with $f_{\mathcal{D}}$. When describing a diagram's function, we will sometimes mark the input vertices by vectors to indicate the input vectors. For example,

is used as shorthand for $f_{\wedge}(\boldsymbol{u} \otimes \boldsymbol{v})$. We also write formal linear sums of diagrams to indicate the corresponding sums of functions. See the next section for explicit details on why this is permissible.

Computations and examples. The next few examples show how to compute the value of a closed diagram. Later examples will demonstrate how trace diagram functions are computed.

Example. The "barbell" diagram ◯–◯ has no proper colorings, since in any coloring the same color meets a vertex twice. Therefore, the diagram's value is $\chi(\bigcirc\!\!-\!\!\bigcirc) = 0$.

Example. The simple loop ◯ (with no vertices) has n proper colorings, $\left\{\bigcirc^i\right\}$ for $i = 1, 2, \ldots, n$. Since there are no vertices, the weight of each coloring is $+1$. Hence, the value of the circle is $\chi(\bigcirc) = \sum_{i=1}^{n} 1 = n$.

The next example is the reason for the terminology "trace" diagram.

Example. The simplest closed trace diagram with a matrix is 

. There are n proper colorings of the form 

, for $i = 1, 2, \ldots, n$. The coefficient of the i-th coloring is $(A)_{ii} \equiv a_{ii}$, so the diagram's value is

$$\chi\left(\bigcirc\!\!\!\!\bigcirc^{A}\right) = a_{11} + \cdots + a_{nn} = \operatorname{tr}(A). \tag{8}$$

The propositions that follow will be used later in this paper, but they are also intended as examples illustrating how to compute trace diagram functions.

Proposition 4.7. *The function of the diagram*  *is the identity* $\boldsymbol{v} \mapsto \boldsymbol{v}$.

Proof. To compute $f_{|}(\hat{\boldsymbol{e}}_i)$, one considers the precoloring α in which the input edge has been labeled i. But this is also a full coloring, and since there are no vertices and no matrices, the weight of that coloring is $+1$. Hence, $\beta = \alpha = (i)$ is the only summand in (7) and $f_{|}(\hat{\boldsymbol{e}}_i) = \hat{\boldsymbol{e}}_i$. By linear extension, this means $f_{|}(\boldsymbol{v}) = \boldsymbol{v}$ for all $\boldsymbol{v} \in V$, so the diagram's function is the identity on V. □

Proposition 4.8. (i) $f_{\wedge^{A}} : \boldsymbol{v} \mapsto A\boldsymbol{v}$ *for any* $n \times n$ *matrix* A.

(ii) *Given* $n \times n$ *matrices* A *and* B, *the diagrams* 

and 

have the same function.

Proof. Recall that the coefficient of a coloring of  is $(A)_{ij}$, where i is the label at the top of the diagram and j is the label at the bottom of the diagram (5). Thus,

$$f_{\,\boxed{A}\,} : \hat{\boldsymbol{e}}_j \mapsto \sum_{i=1,\dots,n} \psi\left(\begin{array}{c} i \\ \boxed{A} \\ j \end{array} \right) = \sum_{i=1,\dots,n} (A)_{ij} \equiv A\hat{\boldsymbol{e}}_j .$$

By linear extension, $f_{\,\boxed{A}\,} : \boldsymbol{v} \mapsto A\boldsymbol{v}$, verifying the first result.

In the case of the diagram  , one reasons similarly to show that the diagram's function maps $\hat{\boldsymbol{e}}_k$ to

$$\sum_{i=1,\dots,n} \sum_{j=1,\dots,n} \psi\left(\begin{array}{c} i \\ \boxed{A} \\ j \\ \boxed{B} \\ k \end{array} \right) = \sum_{i=1,\dots,n} \sum_{j=1,\dots,n} (A)_{ij}(B)_{jk} \equiv AB\hat{\boldsymbol{e}}_k .$$

Thus, $\boldsymbol{v} \mapsto (AB)\boldsymbol{v}$, verifying the second result. □

We can now prove the diagrammatic identity (1) stated in the introduction.

Proposition 4.9. *As a statement about the functions underlying the corresponding* 3*-trace diagrams*,

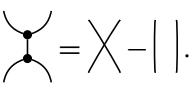

Proof. Proposition 4.7 implies that

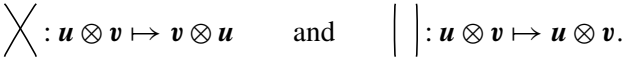

Now consider the function for the 3-diagram $\mathscr{D} =$  . The basis element $\hat{\boldsymbol{e}}_i \otimes \hat{\boldsymbol{e}}_i$, where $i \in \{1, 2, 3\}$, corresponds to $\alpha = (i, i)$ and induces the precoloring $\alpha \leftrightarrow$  , which does not extend to any proper colorings. Hence $f_{\mathscr{D}} : \hat{\boldsymbol{e}}_i \otimes \hat{\boldsymbol{e}}_i \mapsto 0$.

The basis element $\hat{\boldsymbol{e}}_i \otimes \hat{\boldsymbol{e}}_j$, where $i \neq j$, induces the precoloring $\alpha \leftrightarrow$  . The summation in (7) is nominally over 9 possibilities (the number of elements in $N \times N$), but we only need to consider the two full colorings that extend this precoloring. These are

$$\alpha \cup \beta_1 \leftrightarrow \begin{array}{c} i \quad j \\ \diagdown \; \diagup \\ k \\ \diagup \; \diagdown \\ i \quad j \end{array} \qquad \text{and} \qquad \alpha \cup \beta_2 \leftrightarrow \begin{array}{c} j \quad i \\ \diagup \; \diagdown \\ k \\ \diagdown \; \diagup \\ i \quad j \end{array} ,$$

where $k \in \{1, 2, 3\}$ is not equal to i or j. The signatures are $\operatorname{sgn}_{\alpha\cup\beta_1}(\mathscr{D}) = -1$ and $\operatorname{sgn}_{\alpha\cup\beta_2}(\mathscr{D}) = +1$. This statement was proven in detail for the case of $i = 1$ and $j = 2$ in (4); the other cases are proven similarly. Since there are no matrices in the diagram, the coefficients of the colorings are both 1, and the weights are equal to the signatures. Summing over $\hat{\boldsymbol{e}}_\beta$ gives

$$f_{\mathscr{D}} : \hat{\boldsymbol{e}}_i \otimes \hat{\boldsymbol{e}}_j \mapsto -\hat{\boldsymbol{e}}_i \otimes \hat{\boldsymbol{e}}_j + \hat{\boldsymbol{e}}_j \otimes \hat{\boldsymbol{e}}_i .$$

Combining this with the fact that $f_{\mathcal{D}} : \hat{\boldsymbol{e}}_i \otimes \hat{\boldsymbol{e}}_i \mapsto 0$ proves the general statement

$$f_{\mathcal{D}} : \boldsymbol{u} \otimes \boldsymbol{v} \mapsto \boldsymbol{v} \otimes \boldsymbol{u} - \boldsymbol{u} \otimes \boldsymbol{v},$$

which completes the proof. □

We close this section with the diagrams for the inner and cross products.

Proposition 4.10. *The inner product $\boldsymbol{u} \otimes \boldsymbol{v} \mapsto \boldsymbol{u} \cdot \boldsymbol{v}$ of n-dimensional vectors is represented by the n-trace diagram*  .

Proof. Since there is only one edge, $\hat{\boldsymbol{e}}_i \otimes \hat{\boldsymbol{e}}_j$ does not induce a coloring unless $i = j$. In this case, the weight of the coloring is 1. Therefore, $\hat{\boldsymbol{e}}_i \otimes \hat{\boldsymbol{e}}_j \mapsto 1$ if $i = j$, or 0 if $i \neq j$. By extension,  $= \boldsymbol{u} \cdot \boldsymbol{v}$. □

Proposition 4.11. *The cross product $\boldsymbol{u} \otimes \boldsymbol{v} \mapsto \boldsymbol{u} \times \boldsymbol{v}$ of 3-dimensional vectors is represented by the 3-diagram*  .

Proof. The input $\hat{\boldsymbol{e}}_i \otimes \hat{\boldsymbol{e}}_j$ corresponds to the precoloring  . If $i = j$, there is no proper coloring extending this precoloring, so the diagram's function maps $\hat{\boldsymbol{e}}_i \otimes \hat{\boldsymbol{e}}_i \mapsto 0$. Otherwise, the only proper coloring is  , where k is not equal to i or j. The signature of this coloring is $\left(\begin{smallmatrix}1&2&3\\ i&j&k\end{smallmatrix}\right)$. Thus, $\hat{\boldsymbol{e}}_i \otimes \hat{\boldsymbol{e}}_j \mapsto \operatorname{sgn}\left(\begin{smallmatrix}1&2&3\\ i&j&k\end{smallmatrix}\right)\hat{\boldsymbol{e}}_k$. It is straightforward to check that this extends to the standard cross product; for instance, $\hat{\boldsymbol{e}}_1 \otimes \hat{\boldsymbol{e}}_2 \mapsto \operatorname{sgn}\left(\begin{smallmatrix}1&2&3\\ 1&2&3\end{smallmatrix}\right)\hat{\boldsymbol{e}}_3 = \hat{\boldsymbol{e}}_3$. The other cases are similar. □

Transpose diagrams. Given a trace diagram $\mathcal{D}$, we define the *transpose diagram* $\mathcal{D}^*$ to be the trace diagram in which all orientations of matrix vertices in $\mathcal{D}$ have been reversed. The following result describes the relationship between the functions of $\mathcal{D}$ and $\mathcal{D}^*$.

Proposition 4.12 (Transpose diagrams). *Let $\mathcal{D}$ be a trace diagram and let $\mathcal{D}^T$ represent the same diagram in which all matrices have been replaced by their transpose. Then $f_{\mathcal{D}^*} = f_{\mathcal{D}^T}$.*

Proof. By (5),

$$\psi\left(\begin{array}{c} i \\ \downarrow \\ V \\ \downarrow \\ j \end{array}\right) = (A)_{ji} = (A^T)_{ij} = \psi\left(\begin{array}{c} i \\ \downarrow \\ A^T \\ \downarrow \\ j \end{array}\right).$$

Thus, the impact of transposing matrices on the underlying function is the same as that of reversing 2-vertex orientations. □

5. Multilinear functions and diagrammatic relations

Composition and tensor product diagrams. Given the base field $\mathbb{F}$, we let $\mathfrak{D}(I, O)$ denote the free $\mathbb{F}$-module over framed trace diagrams with $I = |V_I|$ inputs and $O = |V_O|$ outputs. There are two ways to combine elements of these spaces. Given $\mathscr{D}_1 \in \mathfrak{D}(I_1, O_1)$ and $\mathscr{D}_2 \in \mathfrak{D}(I_2, O_2)$ with $|O_1| = |I_2|$, one may form the *composition diagram* $\mathscr{D}_2 \circ \mathscr{D}_1$ by gluing the output strands of $\mathscr{D}_1$ to the input strands of $\mathscr{D}_2$. Since by convention inputs are drawn at the bottom of a diagram and outputs at the top, this composition involves drawing one diagram above another. Second, given arbitrary framed diagrams $\mathscr{D}_1 \in \mathfrak{D}(I_1, O_1)$ and $\mathscr{D}_2 \in \mathfrak{D}(I_2, O_2)$, we define the *tensor product diagram* $\mathscr{D}_1 \otimes \mathscr{D}_2 \in \mathfrak{D}(I_1 + I_2, O_1 + O_2)$ to be that obtained by placing $\mathscr{D}_2$ to the right of $\mathscr{D}_1$. See Figure 4 for depictions of these two diagram operations.

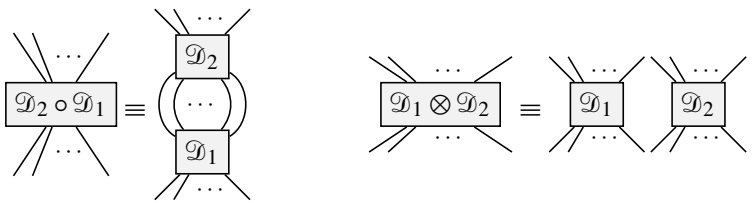

Figure 4. The composition of trace diagrams is formed by drawing one diagram above another (left). The tensor product of trace diagrams is found by drawing diagrams side by side (right).

Both of these structures are preserved under the mapping $\mathscr{D} \mapsto f_{\mathscr{D}}$. The proof is rather technical, but straightforward.

Theorem 5.1. *Let $\mathscr{D}_1 \in \mathfrak{D}(I_1, O_1)$ and $\mathscr{D}_2 \in \mathfrak{D}(I_2, O_2)$. The trace diagram function $f_{\mathscr{D}}$ satisfies (i) $f_{\mathscr{D}_1 \otimes \mathscr{D}_2} = f_{\mathscr{D}_1} \otimes f_{\mathscr{D}_2}$, and (ii) $f_{\mathscr{D}_2 \circ \mathscr{D}_1} = f_{\mathscr{D}_2} \circ f_{\mathscr{D}_1}$ (when the composition $\mathscr{D}_2 \circ \mathscr{D}_1$ is defined).*

Proof. To see that the tensorial structure is preserved, observe that

$$\begin{aligned} f_{\mathscr{D}_1 \otimes \mathscr{D}_2}(\hat{\boldsymbol{e}}_{\alpha_1} \otimes \hat{\boldsymbol{e}}_{\alpha_2}) &= \sum_{\beta_1, \beta_2 \in N^{|O_1|+|O_2|}} \chi_{\alpha_1 \cup \alpha_2 \cup \beta_1 \cup \beta_2}(\mathscr{D}_1 \otimes \mathscr{D}_2) \hat{\boldsymbol{e}}_{\beta_1} \otimes \hat{\boldsymbol{e}}_{\beta_2} \\ &= \sum_{\beta_1 \in N^{|O_1|}} \sum_{\beta_2 \in N^{|O_2|}} \chi_{\alpha_1 \cup \beta_1}(\mathscr{D}_1) \chi_{\alpha_2 \cup \beta_2}(\mathscr{D}_2) \hat{\boldsymbol{e}}_{\beta_1} \otimes \hat{\boldsymbol{e}}_{\beta_2} \\ &= \Bigg(\sum_{\beta_1 \in N^{|O_1|}} \chi_{\alpha_1 \cup \beta_1}(\mathscr{D}_1) \hat{\boldsymbol{e}}_{\beta_1} \Bigg) \otimes \Bigg(\sum_{\beta_2 \in N^{|O_2|}} \chi_{\alpha_2 \cup \beta_2}(\mathscr{D}_2) \hat{\boldsymbol{e}}_{\beta_2} \Bigg) \\ &= f_{\mathscr{D}_1} \otimes f_{\mathscr{D}_2}(\hat{\boldsymbol{e}}_{\alpha_1} \otimes \hat{\boldsymbol{e}}_{\alpha_2}). \end{aligned}$$

For composition, assume $\mathfrak{D}_2 \circ \mathfrak{D}_1$ is defined. Apply (7) twice to get

$$f_{\mathfrak{D}_2} \circ f_{\mathfrak{D}_1} : \hat{\boldsymbol{e}}_\alpha \mapsto \sum_{\gamma \in N^{|O_2|}} \left(\sum_{\beta \in N^{|O_1|}} \chi_{\alpha\cup\beta}(\mathfrak{D}_1)\chi_{\beta\cup\gamma}(\mathfrak{D}_2) \right) \hat{\boldsymbol{e}}_\gamma . \tag{9}$$

The following lemma simplifies the term in parentheses:

Lemma 5.2. $$\sum_{\beta \in N^{|O_1|}} \chi_{\alpha\cup\beta}(\mathfrak{D}_1)\chi_{\beta\cup\gamma}(\mathfrak{D}_2) = \chi_{\alpha\cup\gamma}(\mathfrak{D}_2 \circ \mathfrak{D}_1). \tag{10}$$

Proof. Recall that by definition $\chi_{\alpha\cup\gamma}(\mathfrak{D}_2 \circ \mathfrak{D}_1)$ is defined as a sum over all proper colorings κ of the composition diagram $\mathfrak{D}_2 \circ \mathfrak{D}_1$ that extend the precoloring $\alpha \cup \gamma$. A proper coloring κ induces proper colorings κ_1 of $\mathfrak{D}_1$ and κ_2 of $\mathfrak{D}_2$ that agree on the common edges. So we may write the right-hand side of (10) as

$$\begin{aligned}
\chi_{\alpha\cup\gamma}(\mathfrak{D}_2 \circ \mathfrak{D}_1) &= \sum_{\kappa \succ \alpha\cup\gamma} \operatorname{sgn}_\kappa(\mathfrak{D}_2 \circ \mathfrak{D}_1)\psi_\kappa(\mathfrak{D}_2 \circ \mathfrak{D}_1) \\
&= \sum_{\beta \in N^{|O_1|}} \sum_{\kappa \succ \alpha\cup\beta\cup\gamma} \operatorname{sgn}_\kappa(\mathfrak{D}_2 \circ \mathfrak{D}_1)\psi_\kappa(\mathfrak{D}_2 \circ \mathfrak{D}_1) \\
&= \sum_{\beta \in N^{|O_1|}} \sum_{\kappa_1 \succ \alpha\cup\beta} \sum_{\kappa_2 \succ \beta\cup\gamma} \operatorname{sgn}_{\kappa_1}(\mathfrak{D}_1)\operatorname{sgn}_{\kappa_2}(\mathfrak{D}_2)\psi_{\kappa_1}(\mathfrak{D}_1)\psi_{\kappa_2}(\mathfrak{D}_2) \\
&= \sum_{\beta \in N^{|O_1|}} \chi_{\alpha\cup\beta}(\mathfrak{D}_1)\chi_{\beta\cup\gamma}(\mathfrak{D}_2).
\end{aligned}$$

□

Returning to the proof of the theorem, since by definition

$$f_{\mathfrak{D}_2\circ\mathfrak{D}_1}(\hat{\boldsymbol{e}}_\alpha) = \sum_{\gamma \in N^{|O_2|}} \chi_{\alpha\cup\gamma}(\mathfrak{D}_2 \circ \mathfrak{D}_1)\hat{\boldsymbol{e}}_\gamma ,$$

it follows from the lemma and (9) that $f_{\mathfrak{D}_2} \circ f_{\mathfrak{D}_1} = f_{\mathfrak{D}_2\circ\mathfrak{D}_1}$. □

Intuitively, this result means that a trace diagram's function may be understood by breaking the diagram up into little pieces and gluing them back together. For example, the diagram in the introduction is decomposed as follows:

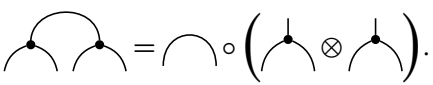

This is why the input $\boldsymbol{u} \otimes \boldsymbol{v} \otimes \boldsymbol{w} \otimes \boldsymbol{x}$ is mapped by the diagram to $(\boldsymbol{u} \times \boldsymbol{v}) \cdot (\boldsymbol{w} \times \boldsymbol{x})$.

Trace diagram relations.

Definition 5.3. A (*framed*) *trace diagram relation* is a summation $\sum_{\mathfrak{D}} c_{\mathfrak{D}}\mathfrak{D} \in \mathfrak{D}(I, O)$ of framed trace diagrams for which $\sum_{\mathfrak{D}} c_{\mathfrak{D}} f_{\mathfrak{D}} = 0$.

Under Theorem 5.1, one can apply trace diagram relations locally on small pieces of larger diagrams. This is exactly what was done in the introduction using the dot and cross product diagrams of Propositions 4.10 and 4.11.

Trace diagram relations also exist for *unframed* diagrams, provided the degree-1 vertices are ordered. Let $\mathfrak{D}(m)$ denote the free $\mathbb{F}$-module over tensor diagrams with m ordered degree-1 vertices. Recall that a framing is a partition of these vertices into a set of inputs and a set of outputs. This provides a mapping $\mathfrak{D}(m) \to \mathfrak{D}(I, O)$ defined whenever $I + O = m$, which we call a *framing*.

Definition 5.4. A (*general*) *trace diagram relation* is a summation $\sum_{\mathscr{D}} c_{\mathscr{D}} \mathscr{D} \in \mathfrak{D}(m)$ that restricts under some partition to a framed trace diagram relation.

Theorem 5.5. *Given a framing* $\mathfrak{D}(m) \to \mathfrak{D}(I, O)$, *every* (*general*) *trace diagram relation in* $\mathfrak{D}(m)$ *maps to a* (*framed*) *trace diagram relation in* $\mathfrak{D}(I, O)$.

Proof. By Definition 4.5, the weights of a function depend only on the leaf labels, and not on the partition or framing of the diagram. Since the weights are the same under different partitions, the relations do not depend on the framing. □

The fact that diagrammatic relations are *independent* of framing is very powerful. One may sometimes read off several identities of multilinear algebra from the same diagrammatic relation, as was done in the introduction with (1). Here is another identity of 3-dimensional vectors:

Example. Using an alternate framing of (1),

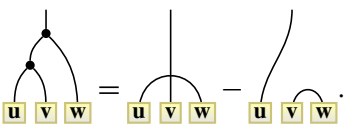

This proves the identity

$$(\boldsymbol{u} \times \boldsymbol{v}) \times \boldsymbol{w} = (\boldsymbol{u} \cdot \boldsymbol{w})\boldsymbol{v} - (\boldsymbol{v} \cdot \boldsymbol{w})\boldsymbol{u}.$$

It is even possible for certain diagrams to be decomposed in multiple ways, leading to algebraic identities.

Example. The single diagram

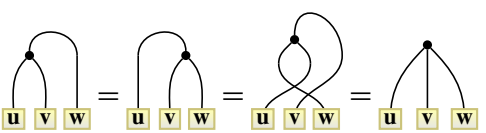

implies the vector identities

$$(\boldsymbol{u} \times \boldsymbol{v}) \cdot \boldsymbol{w} = \boldsymbol{u} \cdot (\boldsymbol{v} \times \boldsymbol{w}) = (\boldsymbol{w} \times \boldsymbol{u}) \cdot \boldsymbol{v} = \det[\boldsymbol{u}\ \boldsymbol{v}\ \boldsymbol{w}].$$

(The fact that  $= \det[\boldsymbol{u}\ \boldsymbol{v}\ \boldsymbol{w}]$ will be proven in the next section.)

6. Diagrammatic building blocks

This section builds a library of local diagrammatic relations that are needed to reason about general diagrams.

Notation 6.1. Let $N = \{1, 2, \ldots, n\}$. Given an ordered k-tuple $\alpha = (\alpha_1, \alpha_2, \ldots, \alpha_k) \in N^k$ consisting of distinct elements of N, let $\overleftarrow{\alpha}$ denote $(\alpha_k, \ldots, \alpha_2, \alpha_1)$. The switch between α and $\overleftarrow{\alpha}$ requires $\lfloor n/2 \rfloor$ transpositions, where $\lfloor n/2 \rfloor = n/2$ if n is even and $\lfloor n/2 \rfloor = (n-1)/2$ if n is odd, and so $\operatorname{sgn}(\overleftarrow{\alpha}) = (-1)^{\lfloor n/2 \rfloor} \operatorname{sgn}(\alpha)$.

Let S_α^c represent the set of permutations of $N \setminus \{\alpha_1, \alpha_2, \ldots, \alpha_k\}$. If $\beta = (\beta_1, \beta_2, \ldots, \beta_{n-k}) \in S_\alpha^c$, let $(\alpha\overleftarrow{\beta})$ denote the permutation

$$(\alpha\overleftarrow{\beta}) \equiv \begin{pmatrix} 1 & \cdots & k & k+1 & \cdots & n \\ \alpha_1 & \cdots & \alpha_k & \beta_{n-k} & \ldots & \beta_1 \end{pmatrix}.$$

Proposition 6.2. *If $\alpha \in N^k$ has no repeated elements, then*

$$: \hat{\boldsymbol{e}}_\alpha \longmapsto \sum_{\beta \in S_\alpha^c} \operatorname{sgn}(\alpha\overleftarrow{\beta})\hat{\boldsymbol{e}}_\beta.$$

If $\alpha \in N^k$ has any repeated elements, then the diagram maps $\hat{\boldsymbol{e}}_\alpha$ to 0.

Proof. By Definition 4.5, the image of $\hat{\boldsymbol{e}}_\alpha$ is automatically 0 if there are repeated elements, since the signature at the node is 0. Otherwise, the diagram maps $\hat{\boldsymbol{e}}_\alpha$ to

$$\sum_{\beta \in N^{n-k}} \chi_{\alpha\cup\beta}(\mathcal{D})\hat{\boldsymbol{e}}_\beta = \sum_{\beta \in N^{n-k}} \sum_{\kappa \succ \alpha\cup\beta} \operatorname{sgn}_\kappa(\mathcal{D})\hat{\boldsymbol{e}}_\beta = \sum_{\beta \in N^{n-k}} \operatorname{sgn}_{\alpha\cup\beta}(\mathcal{D})\hat{\boldsymbol{e}}_\beta.$$

Since there are no matrices in the diagram, the coefficient of the coloring is 1. Note that $\alpha \cup \beta$ is a coloring of all edges of the diagram. If β includes any of the same elements as α, the signature of the coloring is zero. Therefore, we may restrict to the summation in which $\beta \in S_\alpha^c$. In this situation, $\alpha \cup \beta$ is a proper coloring of the entire diagram, and the signature is then

$$\operatorname{sgn}_{\alpha\cup\beta}(\mathcal{D}) = \operatorname{sgn}(\alpha\overleftarrow{\beta}).$$

□

Some special cases of this result are particularly useful. When $k = n$, this proposition states that

$$: \hat{\boldsymbol{e}}_\alpha \longmapsto \operatorname{sgn}(\alpha) = \det(\hat{\boldsymbol{e}}_{\alpha_1} \cdots \hat{\boldsymbol{e}}_{\alpha_n}). \tag{11}$$

Therefore, by linear extension,

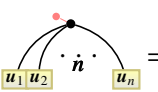

$$= \det(\boldsymbol{u}_1 \cdots \boldsymbol{u}_n). \tag{12}$$

When $k = 0$, Proposition 6.2 states that

$$: 1 \longmapsto \sum_{\beta \in S_n} \operatorname{sgn}(\overleftarrow{\beta})\hat{\boldsymbol{e}}_\beta = (-1)^{\lfloor n/2 \rfloor} \sum_{\beta \in S_n} \operatorname{sgn}(\beta)\hat{\boldsymbol{e}}_\beta. \tag{13}$$

The case $k = n-1$ provides a generalization of the three-dimensional cross product.

Proposition 6.3. *If $\alpha \in N^k$ has no repeated elements, then*

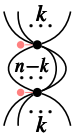

$$: \hat{\boldsymbol{e}}_\alpha \longmapsto (-1)^{\lfloor n/2 \rfloor}(n-k)! \sum_{\sigma \in S_\alpha} \operatorname{sgn}\left(\begin{smallmatrix}\alpha\\ \sigma\end{smallmatrix}\right)\hat{\boldsymbol{e}}_{\sigma(\alpha)},$$

where $\operatorname{sgn}\left(\begin{smallmatrix}\alpha\\ \sigma\end{smallmatrix}\right) = (-1)^t$ *when t transpositions are required to transform α into σ. If $\alpha \in N^k$ has any repeated elements, then the diagram maps $\hat{\boldsymbol{e}}_\alpha$ to 0.*

Proof. Applying Proposition 6.2 twice (and noting that if $\beta \in S_\alpha^c$ then $S_\beta^c = S_\alpha$), the image of $\hat{\boldsymbol{e}}_\alpha$ is

$$\sum_{\beta \in S_\alpha^c} \operatorname{sgn}(\alpha\overleftarrow{\beta}) \sum_{\sigma \in S_\alpha} \operatorname{sgn}(\beta\overleftarrow{\sigma})\hat{\boldsymbol{e}}_\sigma.$$

We claim that $\operatorname{sgn}(\alpha\overleftarrow{\beta}) \operatorname{sgn}(\beta\overleftarrow{\sigma}) = \operatorname{sgn}(\alpha\overleftarrow{\beta'}) \operatorname{sgn}(\beta'\overleftarrow{\sigma})$ for any $\beta, \beta' \in S_\alpha^c$. To see this, consider the process of transposing elements to change β into β'. If this process requires t transpositions, then $\operatorname{sgn}(\beta) = (-1)^t \operatorname{sgn}(\beta')$, which implies both $\operatorname{sgn}(\alpha\overleftarrow{\beta}) = (-1)^t \operatorname{sgn}(\alpha\overleftarrow{\beta'})$ and $\operatorname{sgn}(\beta\overleftarrow{\sigma}) = (-1)^t \operatorname{sgn}(\beta'\overleftarrow{\sigma})$. The claim follows.

Given this claim, every $\beta \in S_\alpha^c$ makes the same contribution to the sum, and the expression reduces to

$$(n-k)! \sum_{\sigma \in S_\alpha} \operatorname{sgn}(\alpha\overleftarrow{\beta}) \operatorname{sgn}(\beta\overleftarrow{\sigma})\hat{\boldsymbol{e}}_\sigma,$$

where β is an arbitrary element of S_α^c. The signature term simplifies as follows:

$$\begin{aligned}\operatorname{sgn}(\alpha\overleftarrow{\beta}) \operatorname{sgn}(\beta\overleftarrow{\sigma}) &= \operatorname{sgn}(\alpha\overleftarrow{\beta})(-1)^{\lfloor n/2 \rfloor} \operatorname{sgn}(\sigma\overleftarrow{\beta}) \\ &= (-1)^{\lfloor n/2 \rfloor} \operatorname{sgn}\left(\begin{smallmatrix}\alpha\\ \sigma\end{smallmatrix}\right) \operatorname{sgn}(\alpha\overleftarrow{\beta})^2 = (-1)^{\lfloor n/2 \rfloor} \operatorname{sgn}\left(\begin{smallmatrix}\alpha\\ \sigma\end{smallmatrix}\right). \quad \square\end{aligned}$$

The next result depends on the previous proof, and will be used repeatedly.

Lemma 6.4 (Cut-and-paste lemma). *If $\alpha \in N^k$ has no repeated elements, $\beta \in S_\alpha^c$, and A is any $n \times n$ matrix, then*

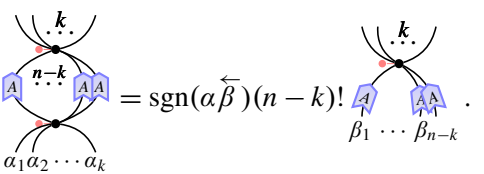

$$= \operatorname{sgn}(\alpha\overleftarrow{\beta})(n-k)! \quad . \tag{14}$$

If $\alpha \in N^k$ has repeated elements, then the diagram maps $\hat{\boldsymbol{e}}_\alpha$ to 0.

Proof. By Proposition 6.2, the left-hand side of (14) evaluates to

$$\sum_{\beta \in S_\alpha^c} \operatorname{sgn}(\alpha \overleftarrow{\beta}) \quad \beta_1 \cdots \beta_{n-k} \quad .$$

As in the proof of Proposition 6.3, the result is true because every choice of β contributes the same value to the summand. In this case, a transposition of elements of β corresponds to swapping two of the strands labeled by β_i in the diagram. But swapping two strands in the diagram leads to a change of signature at the node. In particular, if $\beta, \beta' \in S_\alpha^c$ are related by t transpositions, then $\operatorname{sgn}(\alpha \overleftarrow{\beta}) = (-1)^t \operatorname{sgn}(\alpha \overleftarrow{\beta'})$ and

$$= (-1)^t \quad .$$

Consequently, the summation may be replaced by the number of elements in S_α^c, which is $(n-k)!$. □

This result is called the "cut-and-paste lemma" because it allows nodes to be removed or added on to certain parts of a trace diagram. It will be used frequently in later sections.

The following result is vital to manipulating matrices within diagrams. Note that both statements in the theorem are *general* trace diagram relations.

Proposition 6.5 (Matrix action at nodes). *If A is any $n \times n$ matrix, then*

$$= \det(A) \quad . \tag{15}$$

If A is an invertible $n \times n$ matrix, and $\bar{A}$ *represents its inverse A^{-1}, then*

$$= \det(A) \quad . \tag{16}$$

Proof. Theorem 5.1 greatly simplifies this proof, since it allows one to compute a diagram's function by starting from an arbitrary input at the bottom, and working upward through the diagram. Let $\hat{\boldsymbol{e}}_\alpha \in N^n$ represent a basis input to (15) and let A_i denote the i-th column of A. Then

$$= \quad = \det(A_{\alpha_1} A_{\alpha_2} \cdots A_{\alpha_n}),$$

where the last step follows from (12). Observe that

$$\det(A_{\alpha_1}A_{\alpha_2}\cdots A_{\alpha_n}) = \operatorname{sgn}(\alpha)\det(A),$$

since the number of transpositions required to restore α to the identity permutation is the same number of column switches required to restore the matrix $(A_{\alpha_1}A_{\alpha_2}\cdots A_{\alpha_n})$ to the original matrix A. The proof is completed by noting that $\operatorname{sgn}(\alpha)\det(A)$ is the value of the right-hand side of (15) for the input $\hat{\boldsymbol{e}}_\alpha$.

The second statement (16) follows from the first, by insertion of an explicit copy of the identity matrix in the form of AA^{-1} on the top strands, and application of (15):

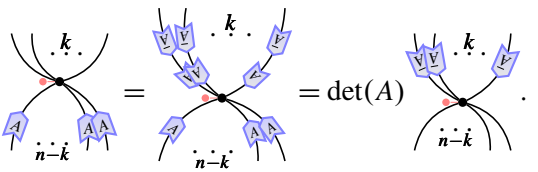

□

Example. One can use (15) to prove that $\det(AB) = \det(A)\det(B)$. Applying (15) directly gives

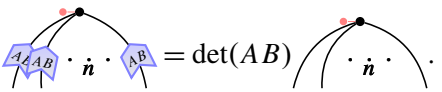

On the other hand, one may use the fact that  to write the same diagram as

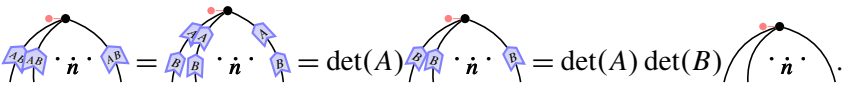

One can similarly apply Proposition 4.12 to the relation (15) to show that $\det(A^T) = \det(A)$.

Proposition 6.6 (Determinant diagram).

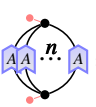

$$= (-1)^{\lfloor n/2 \rfloor} n! \det(A). \tag{17}$$

Proof. Proposition 6.5 gives the factor $\det(A)$, while Proposition 6.3 with $k = 0$ gives the factor $(-1)^{\lfloor n/2 \rfloor} n!$. □

7. Matrix minors

This section reveals the fundamental role of matrix minors in trace diagram functions. We begin with notation and a review of matrix minors. For a good classical treatment of matrix minors see [Lancaster and Tismenetsky 1985, Section 2.4].

Matrix minors and cofactors. Let A be an $n \times n$ matrix over a field $\mathbb{F}$ with

$$A = \begin{pmatrix} a_{11} & a_{12} & \cdots & a_{1n} \\ a_{21} & a_{22} & \cdots & a_{2n} \\ \vdots & \vdots & \ddots & \vdots \\ a_{n1} & a_{n2} & \cdots & a_{nn} \end{pmatrix}.$$

A *submatrix* of a matrix A is a smaller matrix formed by "crossing out" a number of rows and columns in A.

Let $N \equiv \{1, 2, \ldots, n\}$. Let $I = (I_1, \ldots, I_{k_1})$ and $J = (J_1, \ldots, J_{k_2})$ be ordered subsets of N in which $1 \le I_1 < \cdots < I_{k_1} \le n$ and similarly for J. Let $A_{I,J}$ denote the submatrix formed from the rows in I and the columns in J. The *complementary submatrix* $A^c_{I,J}$ is formed by crossing out the rows in I and the columns in J. For $n \ge 3$, the *interior* $\mathrm{int}(A)$ is the submatrix $A^c_{(1,n),(1,n)}$.

Example. Let $I = (1, 2)$ and $J = (3, 4)$. If

$$A = \begin{pmatrix} a & b & c & d \\ e & f & g & h \\ i & j & k & l \\ m & n & o & p \end{pmatrix},$$

then $A_{I,J} = \left(\begin{smallmatrix} c & d \\ g & h \end{smallmatrix}\right)$, $A^c_{I,J} = \left(\begin{smallmatrix} i & j \\ m & n \end{smallmatrix}\right)$, and $\mathrm{int}(A) = \left(\begin{smallmatrix} f & g \\ j & k \end{smallmatrix}\right)$.

Definition 7.1. If I and J have the same number of entries, the *minor* $[A_{I,J}]$ is the determinant of the submatrix $A_{I,J}$. The *complementary minor* $[A^c_{I,J}]$ is the determinant of the complementary submatrix $A^c_{I,J}$.

A direct formula for the $k \times k$ minor is

$$[A_{I,J}] = \sum_{\sigma \in S_k} \mathrm{sgn}(\sigma) a_{I_1, J_{\sigma(1)}} a_{I_2, J_{\sigma(2)}} \cdots a_{I_k, J_{\sigma(k)}}. \tag{18}$$

In the above example, $[A_{I,J}] = ch - gd$.

Definition 7.2. The (i, j)-*cofactor* of A is

$$C_{ij} \equiv (-1)^{i+j} [A^c_{i,j}].$$

The (I, J)-*cofactor* of A is

$$C_{I,J} = (-1)^{I_1 + \cdots + I_k + J_1 + \cdots + J_k} [A^c_{I,J}].$$

The *adjugate* (or *adjoint*) $\mathrm{adj}(A)$ of a square matrix is the matrix comprised of entries $(\mathrm{adj}(A))_{ij} \equiv C_{ji}$.

A student often sees cofactors first in the *cofactor expansion* formula useful for by-hand calculations of the determinant:

$$\det(A) = \sum_{j=1}^{n} a_{ij} C_{ij}, \tag{19}$$

where $i \in N$ is an arbitrary row. Adjugates are sometimes used to compute the matrix inverse since $A^{-1} = (1/\det(A))\operatorname{adj}(A)$ when A is invertible.

Diagrams for matrix minors.

Proposition 7.3. *Let A be an $n \times n$ matrix. Then*

$$[A_{I,J}] = \operatorname{sgn}(J^c \overleftarrow{J}) \quad = \operatorname{sgn}(I^c \overleftarrow{I}) \quad . \tag{20}$$

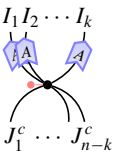

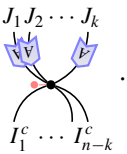

Proof. By Proposition 6.3 and the minor formula (18),

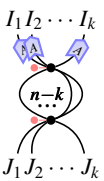

$$= (-1)^{\lfloor n/2 \rfloor}(n-k)! \sum_{\sigma \in S_k} \operatorname{sgn}(\sigma)$$

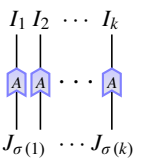

$$= (-1)^{\lfloor n/2 \rfloor}(n-k)![A_{I,J}].$$

Using the cut-and-paste lemma (14), the same diagram reduces to

$$(n-k)!\operatorname{sgn}(J\overleftarrow{J^c}) \quad = (n-k)!(-1)^{\lfloor n/2 \rfloor}\operatorname{sgn}(J^c \overleftarrow{J}) \quad .$$

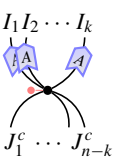

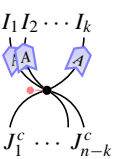

This verifies the first function. The second case is similar. □

The next section requires understanding the following diagrams for the cofactor and the adjugate:

Proposition 7.4. *Let A be an $n \times n$ matrix. Then*

$$C_{I,J} = \frac{(-1)^{\lfloor n/2 \rfloor}}{(n-k)!}$$

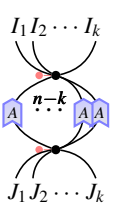

$$\text{and} \qquad \operatorname{adj}(A) = \frac{(-1)^{\lfloor n/2 \rfloor}}{(n-1)!}$$

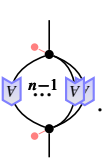

. (21)

Proof. By Proposition 7.3 and the cut-and-paste lemma (14) (and replacing I with I^c and J with J^c), the complementary minor is

$$[A^c_{I,J}] = \operatorname{sgn}(J\overleftarrow{J^c})$$ 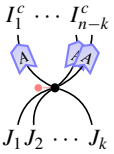 $$= \operatorname{sgn}(J\overleftarrow{J^c})\frac{\operatorname{sgn}(I^c\overleftarrow{I})}{(n-k)!}$$ 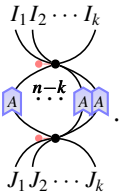 (22)

Matching this up with the cofactor $C_{I,J} = (-1)^{I_1+\cdots+I_k+J_1+\cdots+J_k}[A^c_{I,J}]$ requires a little bit of work with the signs.

Lemma 7.5. *Let $J = (J_1, \ldots, J_k)$ and $J^c = (J^c_1, \ldots, J^c_{n-k})$ be ordered increasing subsets of N whose union is N. Then*

$$\operatorname{sgn}(J^c\overleftarrow{J}) = (-1)^{nk+J_1+J_2+\cdots+J_k}.$$

Proof. Move the $\{J_i\}$ one at a time to their "proper" positions among the J^c. The ordering implies

$$(\ldots, J^c_{J_k-k+1}, \ldots, J^c_{n-k}, J_k, \ldots) = (\ldots, J_k+1, \ldots, n, J_k, \ldots),$$

so $n - J_k$ transpositions are required to return J_k to its proper place. Repeating this for each other J_i gives the identity after a total of $nk-(J_1+\cdots+J_k)$ transpositions. □

Thus $\operatorname{sgn}(J\overleftarrow{J^c})\operatorname{sgn}(I^c\overleftarrow{I}) = (-1)^{\lfloor n/2\rfloor}(-1)^{I_1+\cdots+I_k+J_1+\cdots+J_k}$, verifying the diagram for the general cofactor is as stated.

The adjugate diagram is the case $k = 1$ with matrix orientations reversed to handle the transpose. □

Decomposition of trace diagrams.

Definition 7.6. Given a matrix A, a *diagram A-minor* is an (unframed) diagram with a single n-vertex in which a subset of the edges may be labeled by A, in such a way that all matrix markings are compatibly oriented. In particular, the diagram may be written as ± 1 times a diagram of the form

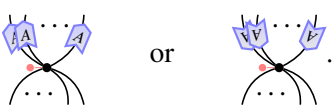

(The sign comes from the possible need to switch the order of edges at the n-vertex so that all edges with matrices are adjacent.)

By Proposition 7.3, a diagram A-minor evaluates to a matrix minor $\pm[A_{I,J}]$ when the ends of the strands are labeled by I and J. The next result states the conditions under which a trace diagram may be decomposed into diagram minors.

Theorem 7.7. *Let $\mathscr{D}$ be a trace diagram in which every matrix marking is adjacent to an n-vertex. Then $\mathscr{D} = C\mathscr{D}'$ for some $\mathscr{D}'$ that may be decomposed into diagram minors, where C is a constant that does not depend on any matrix entries.*

Proof. In this proof "equivalence" will mean equal up to a constant factor that does not depend on any matrix entries. The key step in the theorem is to use the cut-and-paste lemma to introduce additional n-vertices as necessary to separate matrices by node. For instance, the diagram

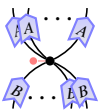

cannot be decomposed into minors. However, using the cut-and-paste lemma and Proposition 6.3, it is equivalent to

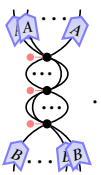

Proceeding in this manner, since every matrix is adjacent to an n-vertex, one may introduce enough vertices in $\mathscr{D}$ to obtain an equivalent diagram $\mathscr{D}'$ such that every n-vertex in $\mathscr{D}$ is adjacent to a unique matrix with consistent orientation. One may then cut around each n-vertex in a diagram, including the adjacent matrices, to decompose the diagram into diagram minors. □

It follows immediately from this theorem that any such diagram may be expressed as a polynomial function of matrix minors. This in itself is not surprising, since the entries of a matrix are technically minors. The power of the result is that the structure of trace diagrams allows one to accomplish this decomposition "efficiently" by giving an upper bound for the number of minors in the decomposition.

For the purposes of the next theorem, we say that a collection of matrix markings form a *compatible matrix collection* if (i) they have the same matrix label, (ii) they are adjacent to the same n-vertex, and (iii) they have the same orientation relative to the n-vertex. Given a trace diagram $\mathscr{D}$ in which every matrix is adjacent to an n-vertex, define the *compatible partition number* $N_{\mathscr{D}}$ of a trace diagram to be the minimum number of collections in a partition of all matrix markings in a diagram into compatible collections. For example,

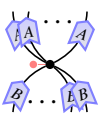

contains two compatible matrix collections, and the compatible partition number is 2.

Theorem 7.8. *Let $\mathscr{D}$ be a trace diagram in which every matrix marking is adjacent to a vertex, and let $N_{\mathscr{D}}$ be the compatible partition number of $\mathscr{D}$. Then, the trace diagram function $f_{\mathscr{D}}$ may be expressed as a summation over a product of $N_{\mathscr{D}}$ matrix minors.*

Proof. In the proof of Theorem 7.7, one may ensure that every compatible matrix collection remains adjacent to the same vertex. Thus, one may write $\mathscr{D} = C\mathscr{D}'$, where $\mathscr{D}'$ decomposes into $N_{\mathscr{D}}$ diagram minors (and possibly some additional n-vertices without matrix markings). Given this decomposition, both $\mathscr{D}$ and $\mathscr{D}'$ may be expressed as summations over a product of $N_{\mathscr{D}}$ matrix minors. □

While $N_{\mathscr{D}}$ provides an upper bound for the minimum number of minors, it is not necessarily sharp. For example, the diagram

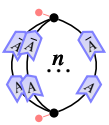

has a compatible partition number of 2, but evaluates to $(-1)^{\lfloor n/2 \rfloor} n!$.

8. Three short determinant proofs

There are several standard methods for computing the determinant. The *Leibniz rule* is the common definition using permutations. *Cofactor expansion* provides a recursive technique that lends itself well to by-hand calculations. *Laplace expansion* is similar but uses generalized cofactors. A lesser-known technique is *Dodgson condensation* [Dodgson 1866], which involves recursive computations using 2×2 determinants.

Diagrammatic techniques can unify these various approaches. Theorem 7.7 leads to a straightforward diagrammatic approach to finding determinant identities: decompose the diagram for the determinant into pieces containing at most one node, and express the result as a summation over matrix minors. This approach gives the cofactor and Laplace formulae.

Cofactor and laplace expansion.

Proposition 8.1 (Cofactor expansion). *For an $n \times n$ matrix A and $j \in \{1, 2, \ldots, n\}$,*

$$\det(A) = \sum_{i=1}^{n} a_{ij} C_{ij} = \sum_{i=1}^{n} a_{ji} C_{ji}. \tag{23}$$

Proof. Proposition 6.6 states that

$$= (-1)^{\lfloor \frac{n}{2} \rfloor} n! \det(A).$$

The diagram for the cofactor was found in Proposition 7.4. The main idea in the proof is that it is possible to label one strand of the diagram arbitrarily, a consequence of two applications of the cut-and-paste lemma (14):

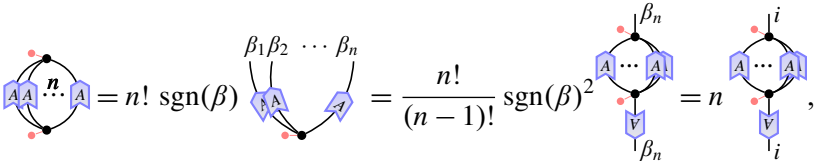

where $i = \beta_n$. This diagram may be evaluated by summing along an interior strand:

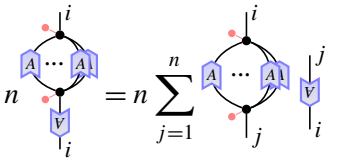

Canceling the common $(-1)^{\lfloor n/2 \rfloor} n!$ factor proves the first equality. The second equality follows by transposing the diagrams. □

This result is easily generalized by labeling several strands instead of just one (for a classical proof of this result, [Lancaster and Tismenetsky 1985, Theorem 1 in Section 2.4]).

Proposition 8.2 (Laplace expansion).

$$\det(A) = \sum_{1 \le J_1 < \cdots < J_k \le n} C_{I,J}[A_{I,J}] = \sum_{1 \le J_1 < \cdots < J_k \le n} C_{J,I}[A_{J,I}].$$

Proof. This proof is a variation of the one above, this time cutting open the diagram along k strands. First,

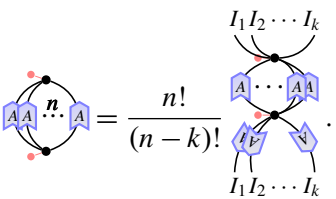

We now use the cut-and-paste lemma 6.4 to add an additional node at the bottom of the diagram, and then express the diagram as a summation over the interior labels

to obtain

$$\frac{n!}{(n-k)!\,k!}\operatorname{sgn}(I^c \overleftarrow{I})$$ 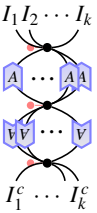 $$= \frac{n!\,k!}{(n-k)!\,k!}\operatorname{sgn}(I^c \overleftarrow{I}) \sum_{\substack{1\le J_1<\cdots \\ <J_k\le n}}$$ 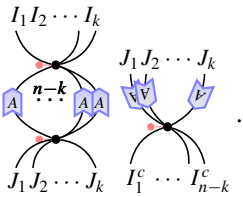

By Propositions 7.4 and 7.3, the first diagram here is $(-1)^{\lfloor n/2\rfloor}(n-k)!C_{I,J}$, and the second is $\operatorname{sgn}(I^c \overleftarrow{I})[A_{I,J}]$. Matching up terms, we have now proven that

$$\det(A) = \sum_{1\le J_1<\cdots<J_k\le n} C_{I,J}[A_{I,J}].$$

The second statement is proven similarly. □

A determinant theorem of Jacobi. We now turn to the Jacobi determinant theorem, first stated in [Jacobi 1841], which is used to derive Dodgson condensation [Rice and Torrence 2007]. In contrast with the previous proofs, we state first the diagrammatic theorem, and show Jacobi's result as a corollary. This proof was first given in [Morse 2008].

Proposition 8.3. *Let A be an invertible $n\times n$ matrix, and let I and J be ordered subsets of N. Then*

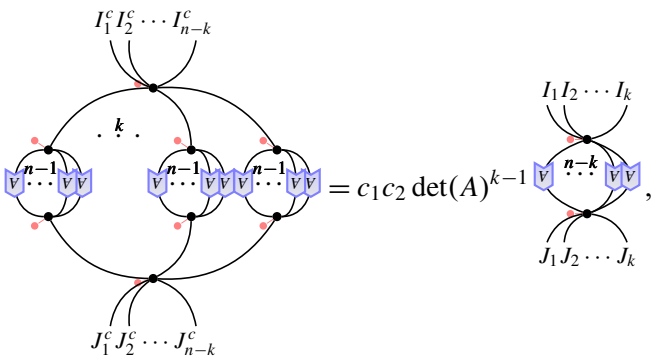 $$= c_1c_2\det(A)^{k-1}$$, (24)

where $c_1c_2 = \big((-1)^{\lfloor n/2\rfloor}(n-1)!\big)^k \operatorname{sgn}(J^c \overleftarrow{J})\operatorname{sgn}(I^c \overleftarrow{I})(k!/(n-k)!)$.

Proof. Use Proposition 6.5 to move each group of $n-1$ matrices in the left-hand diagram of (24) onto a single edge labeled by $\bar{A} = A^{-1}$, then use Proposition 6.3 with $k=1$ to eliminate the "bubbles" in the graph, as follows:

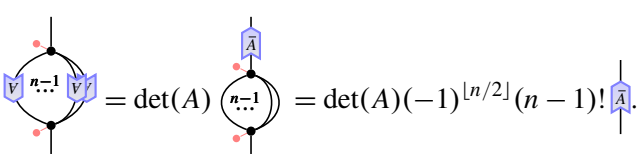

This reduces the diagram to

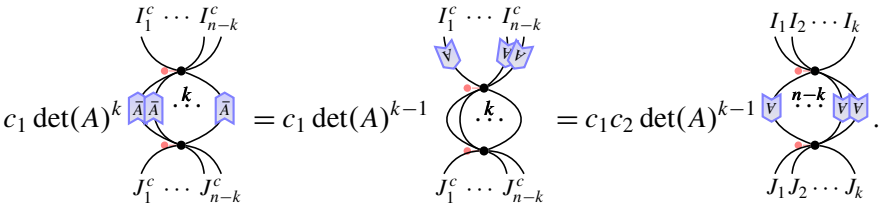

The second step is also a consequence of Proposition 6.5. The third step uses the cut-and-paste lemma (14) twice. The constants are $c_1 = \big((-1)^{\lfloor n/2 \rfloor}(n-1)!\big)^k$ and $c_2 = \operatorname{sgn}(J^c \overleftarrow{J})\operatorname{sgn}(I^c \overleftarrow{I})(k!/(n-k)!)$. □

Corollary 8.4 (Jacobi determinant theorem). *Let A be an $n \times n$ invertible matrix, and let $A_{I,J}$ be a $k \times k$ submatrix of A. Then*

$$[\operatorname{adj}(A)_{I,J}] = C_{J,I} \det(A)^{k-1}, \tag{25}$$

where $[\operatorname{adj}(A)_{I,J}]$ is the corresponding minor of the adjugate of A.

Proof. Rewrite (24) as $\mathscr{D}_1 = c_1 c_2 \det(A)^{k-1}\mathscr{D}_2$. By (21),

$$\mathscr{D}_2 = (-1)^{\lfloor n/2 \rfloor}(n-k)! C_{J,I} \equiv c_3 C_{J,I}. \tag{26}$$

To see the meaning of $\mathscr{D}_1$, consider the following restatement of (22):

$$[A_{I,J}] = \frac{\operatorname{sgn}(J^c \overleftarrow{J})\operatorname{sgn}(I \overleftarrow{I^c})}{k!}$$

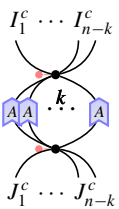

From this, one obtains a diagram for $[\operatorname{adj}(A)_{I,J}]$ by replacing each A with the adjugate diagram (21). The result is a multiple of $\mathscr{D}_1$:

$$[\operatorname{adj}(A)_{I,J}] = \frac{\operatorname{sgn}(J^c \overleftarrow{J})\operatorname{sgn}(I \overleftarrow{I^c})\left((-1)^{\lfloor n/2 \rfloor}\right)^k}{k!\,((n-1)!)^k}\mathscr{D} \equiv c_4 \mathscr{D}_1. \tag{27}$$

Combining (24), (26), and (27) gives

$$[\operatorname{adj}(A)_{I,J}] = c_4 \mathscr{D}_1 = c_1 c_2 c_4 \det(A)^{k-1}\mathscr{D}_2 = c_1 c_2 c_3 c_4 \det(A)^{k-1} C_{J,I}.$$

It is straightforward to check that $c_1 c_2 c_3 c_4 = 1$. □

The first proofs of this theorem took several pages to complete, and required careful attention to indices and matrix elements. A modern proof is given in [Rice and Torrence 2007] that also takes several pages, and relies on expressing the minor as the determinant of an $n \times n$ matrix derived from A. By contrast, the diagrammatic portion of the proof (Proposition 8.3) contains the essence of the result and was relatively easy. The more difficult part was showing that the diagrammatic relation corresponded to the correct algebraic statement.

Many identities in linear algebra are simply special cases of this theorem. For example, when $I = J = N$, then $[A^c_{I,J}] = 1$ trivially and so

$$\det(\mathrm{adj}(A)) = \det(A)^{n-1}.$$

Charles Dodgson's *condensation method* [1866] also depends on this result. The following example shows the condensation method at work on a 4×4 determinant.

$$\begin{vmatrix} -2 & -1 & -1 & -4 \\ -1 & -2 & -1 & -6 \\ -1 & -1 & 2 & 4 \\ 2 & 1 & -3 & -8 \end{vmatrix} \longrightarrow \begin{vmatrix} 3 & -1 & 2 \\ -1 & -5 & 8 \\ 1 & 1 & -4 \end{vmatrix} \longrightarrow \begin{vmatrix} 8 & -2 \\ -4 & 6 \end{vmatrix} \longrightarrow -8,$$

where -8 is the determinant of the original matrix. Each step involves taking 2×2 determinants, making the process easy to do by hand. However, the technique fails for some matrices since it involves division.

The method relies on the particular case $I = J = \{1, n\}$. Then $[A^c_{I,J}]$ is the determinant of the interior entries, and

$$[\mathrm{adj}(A)_{I,J}] = C_{11}C_{nn} - C_{1n}C_{n1},$$

where C_{ij} is the cofactor, so (25) becomes

$$\det(A) = \frac{C_{11}C_{nn} - C_{1n}C_{n1}}{\det(\mathrm{int}(A))}. \tag{28}$$

For 3×3 matrices, this is precisely Dodgson's method. Larger determinants are computed using several iterations of this formula.

9. Generalizations using trace diagrams

One of the advantages of using trace diagrams is the ease with which certain proofs are generalized. This is because, in contrast with traditional proofs, patterns in trace diagram proofs are more easily recognized. For example, the proof of Proposition 8.3 is readily generalized when $ik \leq n$ to the following:

Proposition 9.1. *Let A be an invertible $n \times n$ matrix, and let I and J be ordered subsets of N. Then*

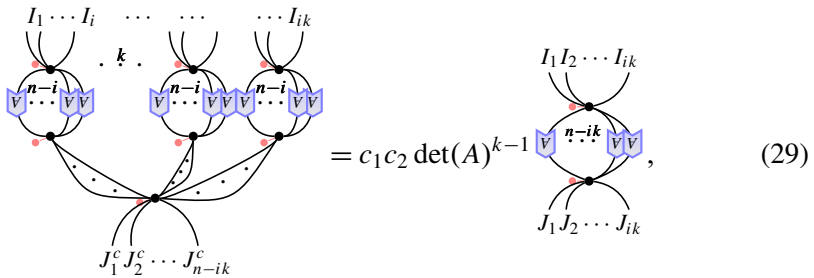

(29)

where $c_1 c_2 = \left((-1)^{\lfloor n/2 \rfloor}(n-i)!\right)^k (\operatorname{sgn}(J\overleftarrow{J^c})/(n-ik)!)$.

Proof. The proof is similar to that of Proposition 8.3. Begin by reducing the diagram at left by applying the following steps at each small collection of $n-i$ matrices in the diagram:

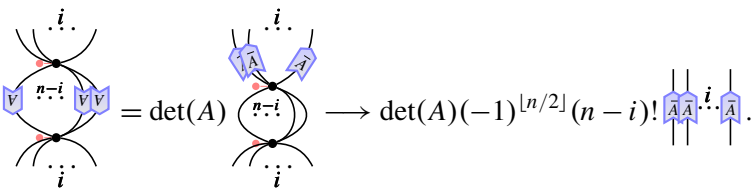

Note that the last step is only true in the context of the larger diagram, in which case it follows by two applications of the cut-and-paste lemma (14). After this step, the diagram reduces to

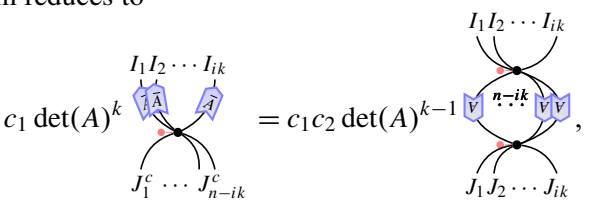

where $c_1 = \left((-1)^{\lfloor n/2 \rfloor}(n-i)!\right)^k$ and $c_2 = (\operatorname{sgn}(J\overleftarrow{J^c})/(n-ik)!)$. The details here are identical to those in the proof of Proposition 8.3. □

We will use this result to prove a generalization of the Jacobi determinant theorem, which concerns a more general notion of a matrix minor. We must first introduce some new concepts. Let V be an n-dimensional vector space. Given a multilinear transformation $\boldsymbol{A} : V^{\otimes i} \to V^{\otimes i}$, one can represent the value of the transformation by the coefficients

$$(\boldsymbol{A})_{\alpha,\beta} \equiv \langle \hat{\boldsymbol{e}}_\alpha, \boldsymbol{A}\hat{\boldsymbol{e}}_\beta \rangle,$$

where $\alpha, \beta \in N^i$. Diagrammatically, $\boldsymbol{A}$ is represented by an oriented node with i inputs and i outputs:

The *i-adjugate* of a matrix A $(0 \le i \le n)$ is the multilinear transformation $\mathrm{adj}_i(A) : V^{\otimes i} \to V^{\otimes i}$ whose coefficients are general cofactors:

$$\big(\mathrm{adj}_i(A)\big)_{I,J} = C_{J,I},$$

where I and J are ordered subsets of N with i elements. It follows from Proposition 7.4 that

$$\mathrm{adj}_i(A) = \frac{(-1)^{\lfloor n/2 \rfloor}}{(n-i)!}$$

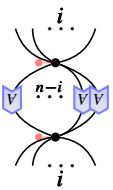

. (30)

We also need to generalize the idea of a matrix minor. Let $\boldsymbol{A}$ be a multilinear transformation, as defined above. Let a positive integer k be chosen for which $0 \le ik \le n$. Let $\boldsymbol{I} = (\boldsymbol{I}_1, \ldots, \boldsymbol{I}_k)$ consist of k i-tuples with $\boldsymbol{I}_j \equiv (I_{j,1}, \ldots, I_{j,i})$ and all elements of $\boldsymbol{I}$ distinct. Let the order of indices be chosen so that

$$1 \le I_{1,1} \le \cdots \le I_{1,i} \le \cdots \le I_{k,1} \le \cdots \le I_{k,i}.$$

Let $\boldsymbol{J}$ be similarly chosen. The *$\boldsymbol{I}, \boldsymbol{J}$-minor* of $\boldsymbol{A}$ is defined to be

$$[\boldsymbol{A}_{\boldsymbol{I},\boldsymbol{J}}] = \sum_{\sigma \in S_{ik}} \mathrm{sgn}(\sigma)(\boldsymbol{A})_{\boldsymbol{I}_1,\sigma(\boldsymbol{J}_1)}(\boldsymbol{A})_{\boldsymbol{I}_2,\sigma(\boldsymbol{J}_2)} \cdots (\boldsymbol{A})_{\boldsymbol{I}_k,\sigma(\boldsymbol{J}_k)}.$$

Generalizing Proposition 7.3 gives

$$[\boldsymbol{A}_{\boldsymbol{I},\boldsymbol{J}}] = \mathrm{sgn}(\boldsymbol{J}^c \overleftarrow{\boldsymbol{J}})$$

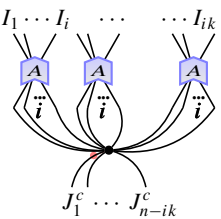

. (31)

We can now use the diagrammatic result (29) to generalize the Jacobi determinant theorem.

Theorem 9.2. *Let A be an $n \times n$ invertible matrix, and let $A_{\boldsymbol{I},\boldsymbol{J}}$ be an $ik \times ik$ submatrix of A. Then*

$$[\mathrm{adj}_i(A)_{\boldsymbol{I},\boldsymbol{J}}] = C_{\boldsymbol{J},\boldsymbol{I}} \det(A)^{k-1}. \tag{32}$$

Proof. Rewrite (29) as $\mathcal{D}_1 = c_1c_2\det(A)^{k-1}\mathcal{D}_2$. As in the proof of the Jacobi determinant theorem (Corollary 8.4), $\mathcal{D}_2 = (-1)^{\lfloor n/2\rfloor}(n-ik)!C_{\boldsymbol{J},\boldsymbol{I}} \equiv c_3 C_{\boldsymbol{J},\boldsymbol{I}}$. The diagram $\mathcal{D}_1$ is obtained by inserting k copies of the i-adjugate diagram (30) into the generalized minor diagram (31), and so

$$[\mathrm{adj}(A)_{\boldsymbol{I},\boldsymbol{J}}] = \left(\frac{(-1)^{\lfloor n/2\rfloor}}{(n-i)!}\right)^k \mathrm{sgn}(\boldsymbol{J}^c\overleftarrow{\boldsymbol{J}})\mathcal{D}_1 \equiv c_4\mathcal{D}_1.$$

Combining these results, one has $[\mathrm{adj}(A)_{\boldsymbol{I},\boldsymbol{J}}] \equiv c_1c_2c_3c_4\det(A)^{k-1}C_{\boldsymbol{J},\boldsymbol{I}}$, and it is straightforward to verify that $c_1c_2c_3c_4 = 1$. □

10. Final remarks

The main purpose of this paper has been to introduce the ideas of signed graph colorings and trace diagrams. A secondary purpose has been to provide a lexicon for their translation into linear algebra. The advantage in this approach to linear algebra lies in the ability to *generalize* results, as was done in Section 9.

There is much more to be said about trace diagrams. The case $n = 2$ was the starting point of the theory [Levinson 1956] and has been studied extensively, most notably providing the basis for spin networks [Carter et al. 1995; Kauffman 1991] and the Kauffman bracket skein module [Bullock et al. 1999]. In the general case, the coefficients of the characteristic equation of a matrix can be understood as the $n+1$ "simplest" closed trace diagrams [Peterson 2009].

The diagrammatic language also proves to be extremely useful in invariant theory. It allows for easy expression of the "linearization" of the characteristic equation [Peterson 2009], from which several classical results of invariant theory are derived [Drensky 2007]. Diagrams have already given new insights in the theory of character varieties and invariant theory [Bullock 1997; Lawton and Peterson 2009; Sikora 2001], and it is likely that more will follow.

Acknowledgments

The authors would like to thank the referee for many valuable comments and suggestions for improvements. We also thank Paul Falcone, Bill Goldman, Sean Lawton, and James Lee for valuable discussions and Amanda Beecher, Jennifer Peterson, and Brian Winkel for their comments on early drafts of this paper.

References

[Baez 1996] J. C. Baez, "Spin networks in gauge theory", *Adv. Math.* **117**:2 (1996), 253–272. MR 96j:58022 Zbl 0843.58012

[Bullock 1997] D. Bullock, "Rings of $\mathrm{SL}_2(\mathbf{C})$-characters and the Kauffman bracket skein module", *Comment. Math. Helv.* **72**:4 (1997), 521–542. MR 98k:57008 Zbl 0907.57010

[Bullock et al. 1999] D. Bullock, C. Frohman, and J. Kania-Bartoszyńska, "Understanding the Kauffman bracket skein module", *Journal of Knot Theory and its Ramifications* **8**:3 (1999), 265–277. MR 2000d:57012 Zbl 0932.57015

[Carter et al. 1995] J. S. Carter, D. E. Flath, and M. Saito, *The classical and quantum* $6j$*-symbols*, Mathematical Notes **43**, Princeton University Press, 1995. MR 97g:17008 Zbl 0851.17001

[Cvitanović 2008] P. Cvitanović, *Group theory*, Princeton University Press, Princeton, NJ, 2008. MR 2010b:22001 Zbl 1152.22001

[Dodgson 1866] C. L. Dodgson, "On condensation of determinants", *Proc. Royal Soc. London* **15** (1866), 150–155.

[Drensky 2007] V. Drensky, "Computing with matrix invariants", *Math. Balkanica* (*N.S.*) **21**:1-2 (2007), 141–172. MR 2008m:16045 Zbl 1161.16018

[Fraleigh 1967] J. B. Fraleigh, *A first course in abstract algebra*, Addison-Wesley, Reading, MA, 1967. MR 37 #1212 Zbl 0154.26303

[Fulton and Harris 1991] W. Fulton and J. Harris, *Representation theory*, Graduate Texts in Mathematics **129**, Springer, New York, 1991. MR 93a:20069 Zbl 0744.22001

[Gross 1974] J. L. Gross, "Voltage graphs", *Discrete Math.* **9** (1974), 239–246. MR 50 #153 Zbl 0286.05106

[Jacobi 1841] C. G. J. Jacobi, "De formatione et proprietatibus determinantium", *Journal für Reine und Angewandte Mathematik* **22** (1841), 285–318.

[Jones 1999] V. F. R. Jones, "Planar algebras I", preprint, 1999. arXiv math/9909027

[Kauffman 1991] L. H. Kauffman, *Knots and physics*, Series on Knots and Everything **1**, World Scientific, River Edge, NJ, 1991. MR 93b:57010 Zbl 0733.57004

[Kuperberg 1996] G. Kuperberg, "Spiders for rank 2 Lie algebras", *Comm. Math. Phys.* **180**:1 (1996), 109–151. MR 97f:17005 Zbl 0870.17005

[Lancaster and Tismenetsky 1985] P. Lancaster and M. Tismenetsky, *The theory of matrices*, 2nd ed., Academic Press, Orlando, FL, 1985. MR 87a:15001 Zbl 0558.15001

[Lawton and Peterson 2009] S. Lawton and E. Peterson, "Spin networks and $\mathrm{SL}(2,\mathbb{C})$-character varieties", pp. 685–730 in *Handbook of Teichmüller theory, Vol. II*, edited by A. Papadopoulos, IRMA Lect. Math. Theor. Phys. **13**, Eur. Math. Soc., Zürich, 2009. MR 2516745 Zbl 05560296

[Levinson 1956] I. B. Levinson, "Sum of Wigner coefficients and their graphical representation", *Proc. Physical-Technical Inst. Acad. Sci. Lithuanian SSR* **2** (1956), 17–30.

[Morse 2008] S. Morse, *Diagramming linear algebra: Some results and trivial proofs*, undergraduate thesis, United States Military Academy, 2008, Available at http://www.dean.usma.edu/departments/math/courses/ma498/archive/2008/SteveM% orseThesis.pdf.

[Muir 1882] T. Muir, *A Treatise on the Theory of Determinants*, Macmillan, 1882.

[Penrose 1971] R. Penrose, "Applications of negative dimensional tensors", pp. 221–244 in *Combinatorial Mathematics and its Applications* (Oxford, 1969), Academic Press, London, 1971. MR 43 #7372 Zbl 0216.43502

[Peterson 2006] E. Peterson, *Trace diagrams, representations, and low-dimensional topology*, Ph.D. thesis, University of Maryland, 2006, Available at http://www.dean.usma.edu/departments/math/people/peterson/research/thesis.p% df.

[Peterson 2009] E. Peterson, "On a diagrammatic proof of the Cayley–Hamilton theorem", preprint, 2009. arXiv 0907.2364

[Przytycki 1991] J. H. Przytycki, "Skein modules of 3-manifolds", *Bull. Polish Acad. Sci. Math.* **39**:1-2 (1991), 91–100. MR 94g:57011 Zbl 0762.57013

[Rice and Torrence 2007] A. Rice and E. Torrence, " 'Shutting up like a telescope': Lewis Carroll's 'curious' condensation method for evaluating determinants", *College Math. J.* **38**:2 (2007), 85–95. MR 2008d:15023

[Sikora 2001] A. S. Sikora, "SL_n-character varieties as spaces of graphs", *Trans. Amer. Math. Society* **353**:7 (2001), 2773–2804. MR 2003b:57004 Zbl 1046.57014

[Stedman 1990] G. E. Stedman, *Diagram techniques in group theory*, Cambridge University Press, 1990. MR 95a:81088 Zbl 0699.20013

[West 2001] D. B. West, *Introduction to graph theory*, 2nd ed., Prentice Hall, Upper Saddle River, NJ, 2001. MR 96i:05001 Zbl 1121.05304

Received: 2009-06-22 Revised: 2009-12-19 Accepted: 2009-12-27

stmorse@hotmail.com *United States Army, Fort Campbell, KY 42223, United States*

elisha.peterson@usma.edu *Department of Mathematical Sciences, United States Military Academy, West Point, NY 10996-1905, United States*

INVOLVE 3:1(2010)

Roundness properties of graphs

Matthew Horak, Eric LaRose, Jessica Moore,
Michael Rooney and Hannah Rosenthal

(Communicated by Scott Chapman)

The notion of the roundness of a metric space was introduced by Per Enflo as a tool to study geometric properties of Banach spaces. Recently, roundness and generalized roundness have been used in the context of group theory to investigate relationships between the geometry of a Cayley graph of a group and the algebraic properties of the group. In this paper, we study roundness properties of connected graphs in general. We explicitly calculate the roundness of members of two classes of graphs and we give results of computer calculations of the roundness of all connected graphs on 7, 8 and 9 vertices. We also show that no connected graph can have roundness between $\log_2 3$ and 2.

1. Introduction

The notions of metric roundness and generalized metric roundness were introduced by Per Enflo [1970a; 1970b] to investigate geometric questions in the theory of Banach spaces. Generalized roundness has also been used in group theory in connection with the coarse Baum–Connes and the Novikov conjectures [LaFont and Passidis 2006]. In the group-theoretic setting, a finitely generated group is viewed as a metric space by viewing elements of the group as vertices of the Cayley graph of the group with respect to a fixed finite generating set and taking the distance between two elements to be the number of edges in a shortest path between them in the Cayley graph.

Recently, more work has been done on the roundness and generalized roundness properties of finitely generated groups, for example in [Jaudon 2008; LaFont and Passidis 2006], relating algebraic properties of a group to the possible values that can be taken by the roundness or generalized roundness of its Cayley graphs with respect to different finite generating sets. However, very little work has been done regarding roundness properties of graphs in general, and a better understanding of

MSC2000: primary 05C99; secondary 46B20, 20F65.
Keywords: roundness, graph, metric invariant.
This work was partially supported by a CURM mini-grant funded by NSF grant DMS-063664.

the roundness of graphs may lead to deeper insight into the connection between the roundness of a Cayley graph and the algebraic properties of the corresponding group. In this paper, we begin to develop a theory of the roundness of general graphs, focusing on the possible values of the roundness of a finite connected graph. Since the roundness of an infinite connected graph is equal to the infimum of the roundnesses of its finite connected metrically embedded subgraphs, this is a first step in understanding roundness for infinite graphs.

This paper is organized as follows. In Section 2, we review the definition of roundness, state and prove several lemmas about roundness in the context of graph theory and work through two concrete examples. In Section 3, we investigate the roundness of the cyclic graphs C_n, finding the roundness of all of these graphs and proving that the roundness of C_n can be made arbitrarily close to 1 by taking values of n sufficiently large. In Section 4, we continue to investigate roundness by working through another class of graphs that we call *triangulated cycles*. We determine the roundness of triangulated cycles in this section and again prove that as the number of vertices in a triangulated cycle goes to infinity, its roundness goes to 1. Finally in Section 5, we summarize some computer-generated data on the distribution of roundness among all 7-, 8- and 9-vertex graphs and make some conjectures on the distribution of roundness based on these data. In this section, we also prove that no graph can have roundness between $\log_2 3$ and 2.

2. Definitions and preliminary lemmas

A *quadrilateral* in a metric space X is an ordered 4-tuple $Q = (A, B, C, D)$ of (not necessarily distinct) points $A, B, C, D \in X$. Informally, we envision Q as the vertices of a quadrilateral embedded in X, and even though there may be no paths in X between the vertices, we talk about the *sides* AB, BC, CD and DA and the *diagonals* AC and BD, as shown in Figure 1. Given four points, $A, B, C, D \in X$, we may form several different quadrilaterals depending on the order in which we take the points. We denote by $Q(A, B, C, D)$ the quadrilateral with sides AB, BC, CD and DA and diagonals AC and BD. If a quadrilateral has two or more of its vertices equal, we call it *degenerate*.

Definition 2.1 (Roundness). If $Q = Q(A, B, C, D)$ is a quadrilateral in the metric space (X, d), then the *roundness* of Q, $\rho(Q)$, is the supremum of all values q such that

$$d(A, C)^q + d(B, D)^q \leq d(A, B)^q + d(B, C)^q + d(C, D)^q + d(D, A)^q. \quad (1)$$

For a metric space X, the *roundness* of X is

$$\rho(X) = \inf\{\rho(Q(A, B, C, D)) \mid A, B, C, D \in X\}. \quad (2)$$

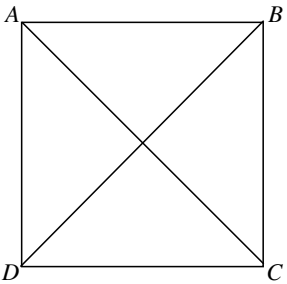

Figure 1. The quadrilateral $Q(A, B, C, D)$.

We remark that this definition of the roundness of a metric space is equivalent to another common formulation of metric roundness below.

Definition 2.2 (Equivalent definition of roundness). The *roundness* of the metric space (X, d) is the supremum of all values q such that for any four points $A, B, C, D \in X$,

$$d(A, C)^q + d(B, D)^q \leq d(A, B)^q + d(B, C)^q + d(C, D)^q + d(D, A)^q. \quad (3)$$

Note that by the triangle inequality, the roundness of any quadrilateral in a metric space is at least 1. This proves:

Lemma 2.3. *The roundness of any metric space X is greater than or equal to* 1.

Observation 2.4. Suppose that A, B, C, D are four distinct points in a metric space. By the symmetry of the inequalities in the definition of roundness, every quadrilateral on A, B, C, D has the same roundness as one of the three quadrilaterals, $Q(A, B, C, D)$, $Q(A, B, D, C)$ or $Q(A, C, B, D)$. Geometrically, this corresponds to the fact that rotating a quadrilateral or reflecting a quadrilateral along a diagonal or middle line preserves its sides and diagonals. Furthermore, at most one of these quadrilaterals can have finite roundness, because a quadrilateral of finite roundness must have its largest distance between vertices as a diagonal. This is true even in the case that the maximal distance between vertices is achieved by two or more pairs of vertices of the quadrilateral.

Throughout this paper we will make generous use of the following lemma that describes how the roundness of a quadrilateral changes if we change the lengths of its diagonals or sides.

Lemma 2.5. *Let Q_1 and Q_2 be quadrilaterals in the metric space X with the same side and diagonal lengths except for exactly one side or diagonal. Further suppose that if the quadrilaterals differ in a diagonal then the diagonal of Q_2 is strictly longer than the diagonal in Q_1 and if they differ in a side then the side in Q_2*

is strictly shorter than the side in Q_1. If $\rho(Q_1)$ is finite then so is $\rho(Q_2)$, and $\rho(Q_2) < \rho(Q_1)$.

Proof. Suppose that Q_1 has finite roundness $q_1 \geq 1$. Suppose that the lengths of the sides of Q_1 are w, x, y, z and the lengths of its diagonals are a, b. Then q_1 satisfies $a^{q_1} + b^{q_1} = w^{q_1} + x^{q_1} + {}^{q_1} + z^{q_1}$, and if $p > q_1$ then $a^p + b^p > w^p + x^p + y^p + z^p$.

Case 1. Q_1 and Q_2 differ on a diagonal. Let $a_2 > a$ be the length of the diagonal in Q_2 that differs from that of Q_1. Let p be a real number greater than or equal to q_1. Then, $a_2^p + b^p > a^p + b^p \geq w^p + x^p + y^p + z^p$. Therefore, $\rho(Q_2)$, which is the supremum of all values q such that $a_2^q + b^q \leq w^q + x^q + y^q + z^q$, is less than $q_1 = \rho(Q_1)$.

Case 2. Q_1 and Q_2 differ on a side. Let $w_2 < w$ be the length of the side in Q_2 that differs from that of Q_1. Let p be a real number greater than or equal to q_1. Then, $a^p + b^p \geq w^p + x^p + y^p + z^p > w_2^p + x^p + y^p + z^p$. Therefore, $\rho(Q_2)$, which is the supremum of all values q such that $a^q + b^q \leq w_2^q + x^q + y^q + z^q$, is less than $q_1 = \rho(Q_1)$. □

Roundness at it relates to graphs. In this paper, we are concerned with the roundness properties of metric spaces arising from connected graphs. Throughout, we let G denote a finite connected graph with vertex set V and edge set E. We view V as a metric space with the distance, $d(A, B)$, between vertices A and B given by the number of edges in a shortest edge path in G between A and B. We usually abuse notation by referring to G itself as a metric space, but when we do so we are always considering only the vertex set of G. Thus, $\rho(G)$ always denotes the roundness of the metric space consisting of only the vertex set of G. This is important, because if we were to view all of G as a metric space in the usual way by metrically identifying each edge with the unit interval, then any nonsimply connected graph would have roundness equal to 1, which follows from Lemma 2.6 from [LaFont and Passidis 2006]. Another reason this is important is that in the case G is a finite graph, there are only finitely many quadrilaterals in G. Therefore, the infimum of (1) in the definition of roundness is actually a minimum and the roundness of G is actually achieved by some minimum roundness quadrilateral in G.

Lemma 2.6. *Let X be a metric space. If X contains a metrically embedded circle, then $\rho(X) = 1$.*

Before proceeding with more preliminary lemmas related to graph roundness, we calculate roundness in two examples, the cyclic graph on 5 vertices, C_5, and a graph we call Graph Δ, shown in Figure 2. In the case of a finite graph G since there are only finitely many different quadrilaterals in G, the infimum in (2) is actually a minimum, and we may search for a specific quadrilateral that has

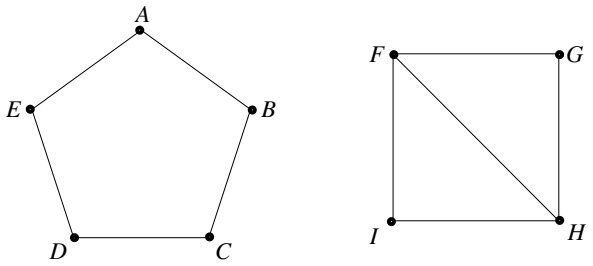

Figure 2. Graphs C_5 (left) and Δ (right).

minimal roundness among all quadrilaterals in G. The roundness of G is then the roundness of this minimal roundness quadrilateral.

Since C_5 and Δ are so small, we can find a minimal roundness quadrilateral by simply determining by hand the roundness of every possible quadrilateral in the graphs. Quadrilaterals $Q_1 = Q(A, B, C, D)$ in C_5 and $Q_2 = Q(F, G, H, I)$ in Δ turn out to be minimal roundness quadrilaterals in C_5 and Δ respectively. In Q_1 and Q_2, we have the distances shown in Figure 3. So, $\rho(Q_1)$ is the supremum over all p values such that

$$2^p + 2^p \leq 1^p + 1^p + 1^p + 2^p.$$

In this case, the supremum is found by solving the equation

$$2^p + 2^p = 1^p + 1^p + 1^p + 2^p$$

for $p = \log_2(3) \approx 1.58$. The roundness of Q_2 is the supremum over all p values such that

$$1^p + 2^p \leq 1^p + 1^p + 1^p + 1^p.$$

Again, the supremum is found by solving the equation

$$1^p + 2^p = 1^p + 1^p + 1^p + 1^p$$

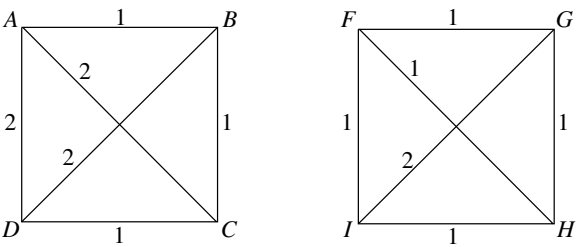

Figure 3. Quadrilaterals Q_1 and Q_2 with diagonal and side lengths indicated.

for $p = \log_2(3) \approx 1.58$. These examples illustrate that two different graphs can have the same roundness and that this roundness may even arise from "different" inequalities.

When calculating roundness of a particular graph G, one often starts by seeking an upper bound for $\rho(G)$ by finding a subgraph of G whose roundness is known or at least not too hard to determine. However, since the distance between vertices through a subgraph may be different than the distance through the whole graph, one must be careful to restrict attention to *metrically embedded subgraphs*, defined below and illustrated in Figure 4.

Definition 2.7. Let G_0 be a subgraph of the graph G. For vertices $A, B \in G$, denote by $d_G(A, B)$ the distance between A and B in G. If A and B happen to belong to G_0, denote by $d_{G_0}(A, B)$ the distance between A and B when viewed as vertices of the graph G_0. The subgraph G_0 is said to be *metrically embedded* in G if $d_{G_0}(A, B) = d_G(A, B)$ for every pair of vertices $A, B \in G_0$. In this case, G_0 is also said to be a *metric subgraph* of G.

The following lemma is easily verified, and it is useful in working through specific examples.

Lemma 2.8. *If G_0 is a metrically embedded subgraph of G, then $\rho(G) \leq \rho(G_0)$.*

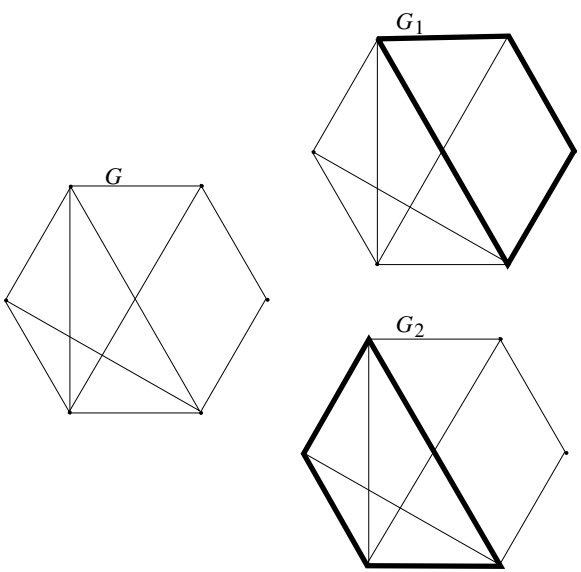

Figure 4. A metrically embedded subgraph, G_1, and a nonmetrically embedded subgraph, G_2 of the graph G.

An immediate application of Lemma 2.8 is that a graph containing a metrically embedded subgraph isomorphic with a cyclic graph with an even number of vertices, C_{2k}, has roundness equal to 1. This follows immediately from Lemma 2.8 and the fact that $\rho(C_{2k}) = 1$. We record this as,

Lemma 2.9. *If G contains a metrically embedded subgraph isomorphic with the cyclic graph C_{2k} for $k \geq 2$ then $\rho(G) = 1$.*

We end this subsection with two lemmas for which we provide short proofs. Together with Lemma 2.3, Lemma 2.10 implies that if a graph G has finite roundness, then $1 \leq \rho(G) \leq 2$. Additionally, Lemmas 2.10 and 2.11 imply that if a graph has finite roundness then its roundness is never given by a degenerate quadrilateral.

Lemma 2.10. *Let G be a finite connected graph. Then $\rho(G) = \infty$ or $\rho(G) \leq 2$.*

Proof. Let G be a finite connected graph such that $\rho(G) \neq \infty$. Since a complete graph has infinite roundness, G is not complete. Choose three vertices $A, B, C \in G$ such that $d(A, B) = d(B, C) = 1$ and $d(A, C) = 2$, which exist because G is not complete. We have $\rho(G) \leq \rho(Q(A, B, C, B)) = 2$. □

Lemma 2.11. *If Q is a quadrilateral in which two or more of the vertices are equal, then $\rho(Q) \geq 2$.*

Proof. If Q is comprised of one or two vertices, it follows immediately after writing down the inequalities that the roundness of Q satisfies that $\rho(Q) = \infty$, so we assume that Q is comprised of three distinct vertices, A, B, C as shown in Figure 5 with distances between vertices indicated. Since A, B and C are distinct, w, x and y are all nonzero. Again, it follows immediately after writing down the equation for roundness and taking into account the symmetries in Observation 2.4 that after possibly renaming the vertices of Q, the only quadrilateral that can possibly have finite roundness has the form $Q(A, B, C, B)$.

Case 1. $y \geq x + w$. In this case $\rho(Q)$ is the supremum of all values of q for which $(x + w)^q \leq 2w^q + 2x^q$. Since $(x + w)^2 \leq 2x^2 + 2w^2$, $\rho(Q) \geq 2$.

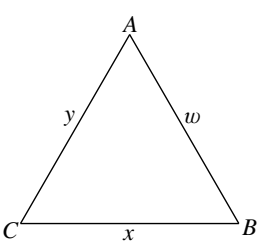

Figure 5. Degenerate quadrilateral of Lemma 2.11.

Case 2. $y < x + w$. In this case, $\rho(Q)$ is the supremum of all values q for which $y^q \leq 2w^q + 2x^q$. Note that if $y < w$ and $y < x$ then this inequality holds for all positive q, so $\rho(Q) = \infty$. So we now assume that $y \geq w$ and $y \geq x$. For $q = 2$, we have $y^2 < (w + x)^2 = w^2 + 2wx + x^2 \leq 2w^2 + 2x^2$. Therefore, $\rho(Q) > 2$. □

3. Roundness of cyclic graphs

As previously mentioned, in the cyclic graph with an even number of vertices C_{2n} it is not hard to find a quadrilateral whose roundness is equal to 1. Since 1 is the smallest possible value for the roundness of a metric space, this proves that $\rho(C_{2n}) = 1$. For odd cycles, C_{2n+1}, the situation is not as easy because $\rho(C_{2n+1}) \neq 1$ and proving that a candidate for a minimal roundness quadrilateral actually has minimal roundness among all quadrilaterals in C_{2n+1} is more involved. In this section we determine $\rho(C_{2n+1})$ by finding a minimal roundness quadrilateral in C_{2n+1}.

When we talk about the cyclic order of points in C_{2n+1}, we are always referring to the cyclic order given by C_{2n+1} or its reverse. We say that the quadrilateral $Q(A, B, C, D)$ in C_{2n+1} is *in cyclic order* if the vertices are encountered in the order A, B, C, D along a nonrepeating path in C_{2n+1} starting at A. Otherwise, $Q(A, B, C, D)$ is *out of cyclic order*. Depending on the particular way in which C_{2n+1} is represented geometrically by a drawing, the path may appear "clockwise" or "counterclockwise".

The natural guess for a minimal roundness quadrilateral in C_{2n+1} is one whose vertices are in cyclic order and as evenly spaced as possible. The fact that a quadrilateral of this form has roundness less than 2 proves that $\rho(C_{2n+1}) < 2$. We use this fact during the proof that this guess is in fact a minimal roundness quadrilateral in C_{2n+1}. In this section, we prove that quadrilaterals of this form are of minimal roundness in C_{2n+1}. Calculating the roundness of such a minimal roundness quadrilateral in C_{2n+1} gives the main theorem and corollary of this section.

Theorem 3.1. *Let n be an integer greater than or equal to 2.*

(1) *If $2n + 1$ has the form $4k + 1$ for an integer k, then $\rho(C_{2n+1})$ is the unique solution to the equation, $2(2k)^q = 3k^q + (k + 1)^q$.*

(2) *If $2n + 1$ has the form $4k - 1$ for an integer k, then $\rho(C_{2n+1})$ is the unique solution to the equation, $2(2k - 1)^q = 3k^q + (k - 1)^q$.*

Corollary 3.2. *Let C_k be the cyclic graph on k vertices. Then* $\lim_{k\to\infty} \rho(C_k) = 1$.

The first step in the proof of Theorem 3.1 is to prove that a minimal roundness quadrilateral in C_{2n+1} must have its vertices in the cyclic order given by C_{2n+1}. We do this by proving that for any quadrilateral Q' whose vertices are out of order, there is another (possibly out of order) quadrilateral Q'' such that $\rho(Q'') < \rho(Q')$.

The second step in the proof is to show that the vertices used in a minimal roundness quadrilateral must be such that the side lengths are as balanced as possible.

For the rest of the section, we consider a fixed cyclic graph C_{2n+1} and consider four points $A, B, C, D \in C_{2n+1}$ in cyclic order as shown in Figure 6. In this figure, w, x, y, z are the lengths of the paths clockwise around C_{2n+1} from A to B to C to D and back to A. In referring to the figure, we will often refer to A, B, C and D as *points* and the w, x, y, z as the lengths of *sides*, thinking of the quadrilateral $Q(A, B, C, D)$, even if there is another, out of order, quadrilateral $Q(A, B, D, C)$ or $Q(A, C, B, D)$ under consideration.

Every minimal roundness quadrilateral must be in order.

Theorem 3.3. *If Q is a minimal roundness quadrilateral in C_{2n+1} then Q is non-degenerate and its vertices are in the cyclic order given by C_{2n+1}.*

We separate the proof into five cases in which we prove that a degenerate or out of order quadrilateral in C_{2n+1} does not have minimal roundness among all quadrilaterals in C_{2n+1}. The cases are divided according to the lengths of the "sides" w, x, y, z in Figure 6.

- In Lemma 3.4, we deal with the degenerate case.
- In Lemma 3.5, we prove that an out of order quadrilateral on A, B, C, D does not have minimal roundness in the case that none of the side lengths w, x, y, z is greater than the sum of any other two consecutive side lengths.
- In Lemma 3.6, we prove that an out of order quadrilateral on A, B, C, D does not have minimal roundness in the case that the longest side is longer than the sum of any two other consecutive sides, but is shorter than the sum of lengths of the three remaining sides.
- In Lemma 3.7, we prove that an out of order quadrilateral on A, B, C, D does not have minimal roundness in the case that the longest side is longer than the

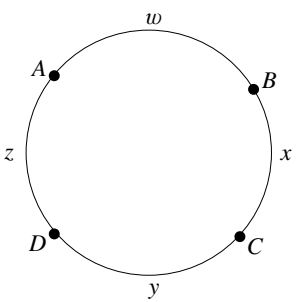

Figure 6. C_{2n+1} with four distinguished points A, B, C, D.

sum of two of the other adjacent sides, but shorter than the sum of the two others.

- In Lemma 3.8, we prove that an out of order quadrilateral on A, B, C, D does not have minimal roundness in the case that the longest side is longer than the other three combined.

Lemma 3.4. *A degenerate quadrilateral in C_{2n+1} is not a minimal roundness quadrilateral for C_{2n+1}.*

Proof. Let Q be a degenerate quadrilateral in C_{2n+1}. By Lemma 2.11, $\rho(Q) \geq 2$, but we have already observed that $\rho(C_{2n+1}) < 2$, so Q cannot be a minimal roundness quadrilateral in C_{2n+1}. □

Lemma 3.5. *Let Q' be an out of order nondegenerate quadrilateral in C_{2n+1} comprised of the vertices A, B, C, D in Figure 6. If no side length w, x, y, z is greater than the sum of the lengths of any remaining pair of adjacent sides, then Q' is not a minimal roundness quadrilateral in C_{2n+1}.*

Proof. Since Q' is nondegenerate, $w, x, y, z \neq 0$. Additionally, by our assumption on side lengths, we have:

$$\begin{array}{llll} w < x+y, & x < w+z, & y < w+x, & z < w+x, \\ w < y+z, & x < y+z, & y < w+z, & z < x+y. \end{array}$$

Consider the in-order quadrilateral $Q = Q(A, B, C, D)$. By Observation 2.4 and the symmetry of the above conditions on the lengths of the sides, we may without loss of generality assume that our out of order quadrilateral is, $Q' = Q(A, B, D, C)$. By our length conditions, these two quadrilaterals have side and diagonal lengths shown in Figure 7. Note that there are two possibilities for the lengths of some of the sides and diagonals, depending on how the two sums in question compare. But, no matter which possibilities are the actual lengths, the diagonals in Q are strictly longer than the diagonals in Q' and the vertical edges in Q are strictly shorter than the vertical edges in Q'. Therefore, by Lemma 2.5, $\rho(Q) < \rho(Q')$, finishing the proof. □

Lemma 3.6. *Let Q' be an out of order nondegenerate quadrilateral in C_{2n+1} comprised of the vertices A, B, C, D as in Figure 6. If the longest side in the in-order quadrilateral $Q = Q(A, B, C, D)$ is at least as long as any remaining pair of adjacent sides but strictly shorter than the other three sides put together, then Q' is not a minimal-roundness quadrilateral in C_{2n+1}.*

Proof. Since Q' is nondegenerate, $w, x, y, z \neq 0$. Without loss of generality, assume that w is the longest length of a side in Q. By our assumptions on lengths of sides, we have

$$w \geq x+y, \quad w \geq y+z, \quad w < x+y+z, \quad w \geq x, y, z.$$

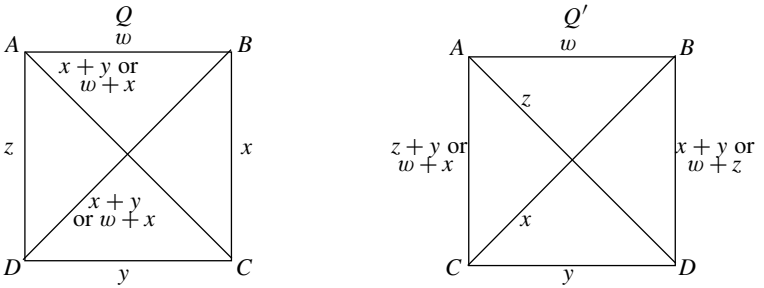

Figure 7. Quadrilaterals in Lemma 3.5. Lengths displayed inside the quadrilateral are lengths of the diagonals. Top ones for the upper-left to lower-right, bottom ones for bottom-left to upper-right.

By Observation 2.4, without loss of generality we may assume that Q' is either $Q(A, B, D, C)$ or $Q(A, C, B, D)$.

Case 1. $Q' = Q(A, B, D, C)$. In this case, we see that the diagonals of Q are longer than the diagonals of Q' and the vertical edges of Q are shorter than the vertical edges of Q' so by Lemma 2.5, $\rho(Q) < \rho(Q')$ so Q' is not a minimal length quadrilateral in C_{2n+1}.

Case 2. $Q' = Q(A, C, B, D)$. Let B' be the vertex of C_{2n+1} reached by moving one edge from B in the direction of C, as shown in Figure 8. Note that we could have $B' = C$. Let $Q'' = Q(A, C, B', D)$ We prove that if $\rho(Q')$ is finite then $\rho(Q'') < \rho(Q')$, which proves that Q' is not a minimal-roundness quadrilateral in C_{2n+1}.

There are two possibilities for the side and diagonal lengths of Q''. These are shown in Figure 9. The lengths in the right hand quadrilateral occur only when $w = x + y + z - 1$. In both possibilities, moving from Q' to Q'' increases or does

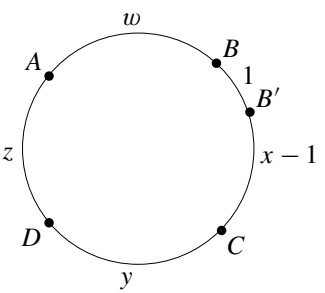

Figure 8. Forming Q'' in case 2 of Lemma 3.6.

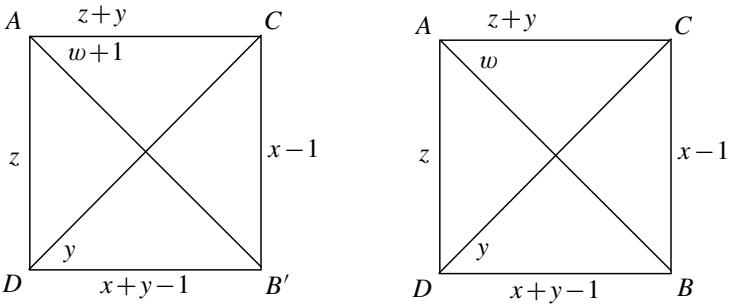

Figure 9. Possible sides and diagonals in Q''.

not change the lengths of diagonals and strictly decreased the lengths of some sides, so if $\rho(Q')$ is finite then by Lemma 2.5 $\rho(Q'') < \rho(Q')$. Since an infinite roundness quadrilateral is not of minimal roundness in C_{2n+1}, which has finite roundness, this proves that Q' is not a minimal-roundness quadrilateral in C_{2n+1}. □

Lemma 3.7. *Let Q' be an out of order nondegenerate quadrilateral in C_{2n+1} comprised of the vertices A, B, C, D as in Figure 6. If the longest side of the in-order quadrilateral $Q = Q(A, B, C, D)$ is at least as long as one of the pairs of remaining adjacent sides but no longer than the other pair of remaining adjacent sides, then Q' is not a minimal-roundness quadrilateral in C_{2n+1}.*

Proof. Without loss of generality, assume that w is the longest length of a side in Q and that $w > x + y$. By our assumptions on lengths of sides, we have

$$w \geq x + y, \quad w \leq y + z, \quad w < x + y + z, \quad w \geq x, y, z.$$

Again by Observation 2.4, without loss of generality we may assume that Q' is either $Q(A, C, B, D)$ or $Q(A, B, D, C)$.

We see the quadrilaterals $Q(A, B, C, D)$, $Q(A, C, B, D)$ and $Q(A, B, D, C)$ in Figure 10 with the lengths of their sides and diagonals. Note that $d(A, C)$ may be either $z+y$ or $w+x$, depending on which is smaller. In either case, moving from $Q(A, C, B, D)$ or $Q(A, B, D, C)$ to $Q(A, B, C, D)$ increases length of diagonals and decreases length of sides, so $\rho(Q) < \rho(Q')$ if $\rho(Q')$ is finite. This proves that Q' is not a minimal-roundness quadrilateral in C_{2n+1}. □

In the proof of the next lemma, we encounter a *linear* graph, l_m, which is a connected graph with exactly two vertices of degree one and the remaining vertices of degree two. Geometrically, a linear graph looks like a line between its two degree one vertices. By case analysis, it is not hard to show that if Q is a quadrilateral in a linear graph, then $\rho(Q) \geq 2$.

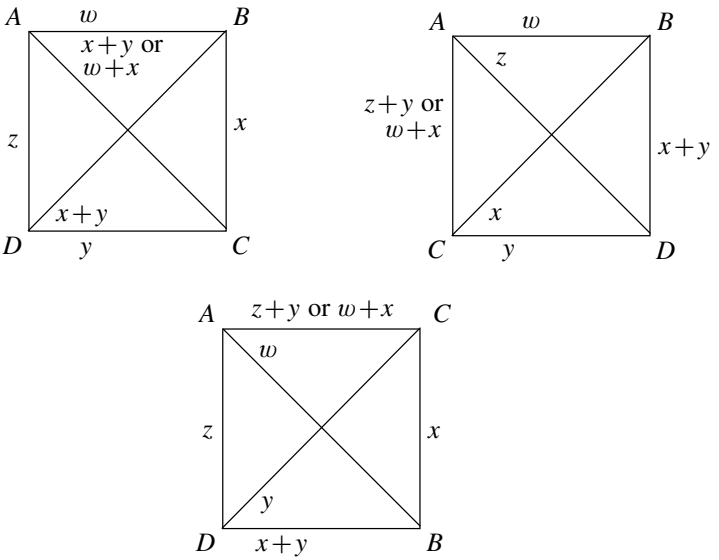

Figure 10. Quadrilaterals in Lemma 3.7.

Lemma 3.8. *Let Q' be an out of order nondegenerate quadrilateral in C_{2n+1} comprised of the vertices A, B, C, D as in Figure 6. If the longest side in the in-order quadrilateral $Q = Q(A, B, C, D)$ is at least as long as the remaining three sides put together, then Q' is not a minimal-roundness quadrilateral in C_{2n+1}.*

Proof. Since $w \geq x + y + z$, Q' actually lies in a metrically embedded linear subgraph l_m of C_{2n+1}. Therefore, $\rho(Q') \geq 2$. Since $\rho(C_{2n+1}) < 2$, Q' is not a minimal roundness quadrilateral in C_{2n+1}. □

Proof of Theorem 3.3. Let Q be a minimal roundness quadrilateral in C_{2n+1} formed from the vertices A, B, C, D as in Figure 6. By Lemma 3.4, Q is nondegenerate. Assume towards a contradiction that Q is out of order. The edge lengths w, x, y, z of Figure 6 satisfy at least one of the conditions of Lemmas 3.5 through 3.8 because these lemmas cover all the possibilities for how long the longest side is in relation to the other sides from being shorter than any pair of adjacent sides to being longer than the three other sides put together. Therefore, by these lemmas, Q is not a minimal roundness quadrilateral, contradicting the fact that it is of minimal roundness. Therefore, the assumption that Q is out of order must be false, proving that Q is in order. □

Balancing sides.

Theorem 3.9. *Let Q be a quadrilateral in C_{2n+1}. Then Q is a minimal roundness quadrilateral in C_{2n+1} if and only if Q is an in-order quadrilateral and the lengths of the longest and shortest sides of Q differ by at most* 1.

We begin with the a lemma that describes the effect of evening out the side lengths of a quadrilateral in the case that the longest side is not too long.

Lemma 3.10. *Let $Q = Q(A, B, C, D)$ be the in-order order quadrilateral in C_{2n+1} comprised of the vertices A, B, C, D as in Figure 6 and suppose that the length longest side of Q is at least two greater than the length of its shortest side. Suppose also that the longest side of Q is shorter than the remaining three sides put together. Then Q has a pair of adjacent sides whose lengths differ by at least two, and the quadrilateral Q' formed by moving the vertex separating these sides into the longer side a distance of one has roundness less than $\rho(Q)$.*

Proof. Without loss of generality, suppose that AB is a longest side, so $w \geq x, y, z$. First we prove that Q must contain a pair of adjacent sides whose lengths differ by at least two. Suppose not and let m be the length of the shortest side. Since no two adjacent side lengths differ by two or more, we must have:

$$\begin{aligned} y = m, &\quad x = w, \quad \text{or} \quad x = w - 1, \\ z = w, &\quad \text{or} \quad z = w - 1. \end{aligned}$$

Since $m \leq w-2$, and since $w \geq x \geq w-1$ and $w \geq z \geq w-1$, we actually have $y = m = w-2$ and $x = z = w-1$ because no two adjacent side lengths differ by two or more. This means that C_{2n+1} actually has $4w-4$ edges, and $2n+1 = 4w-4$, which is impossible. Therefore, Q must have two adjacent sides whose lengths differ by at least two.

To prove that evening out the lengths of two adjacent sides whose lengths differ by at least two reduces roundness, we consider two cases.

Case 1. The longest side, AB, is not adjacent to any side of length shorter than itself by at least two. Without loss of generality, suppose that side BC is the longer of the two sides adjacent to AB. Dealing with the four possible combinations for the values of x and z separately, we see that in each case the quadrilateral $Q' = Q(A, B, C', D)$ made from the points A, B, C', D shown in Figure 11 has roundness less than $\rho(Q)$.

Case 2. The longest side AB is adjacent to a side of length shorter than itself by at least two. By our assumptions on lengths, without loss of generality we have

$$w > x + 1, \quad w \geq y, \quad w \geq z, \quad z \geq x, \quad w \leq x + y + z.$$

Consider the quadrilateral $Q' = Q(A, B', C, D)$ constructed from the points A, B', C, D as shown in Figure 11. The possible side and diagonal lengths of Q and Q' are shown in Figure 12. Assume for the moment that the length of the diagonal AC is $w + x$. Let $\rho(Q) = q > 1$. Then, $(w+x)^q + (y+x)^q = w^q + x^q + y^q + z^q$ and $(w+x)^p + (y+x)^p > w^p + x^p + y^p + z^p$ if $p > q$. Additionally, for any

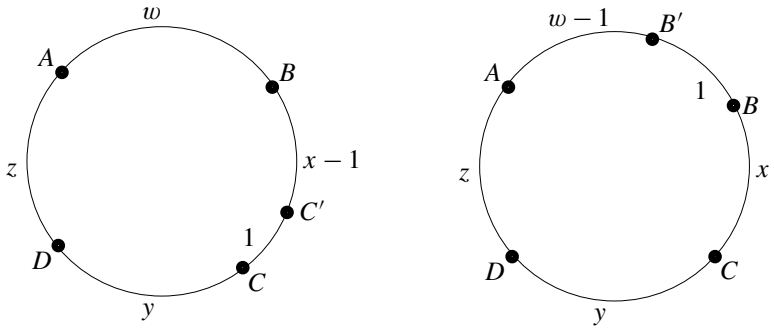

Figure 11. Case 1 (left) and case 2 (right) of Lemma 3.10.

$p > 1$, the function $f(t) = t^p - (t-1)^p$ is increasing for $t \geq 1$, which shows that $w^p + x^p > (w-1)^p + (x+1)^p$ since $w > x+1$. Therefore, if $p \geq q$, we have

$$(w+x)^p + (y+x)^p \geq w^p + x^p + y^p + z^p > (w-1)^p + (x+1)^p + y^p + z^p,$$
$$(w+x)^p + (y+x+1)^p \geq w^p + x^p + y^p + z^p > (w-1)^p + (x+1)^p + y^p + z^p.$$

Since $\rho(Q')$ is the supremum of the values p for which the sum of the p^{th} powers of the diagonals is less than or equal to the sum of the p^{th} power of the sides, we have $\rho(Q') < q = \rho(Q)$ in the case that the length of AC is equal to $w+x$. The proof that $\rho(Q') < \rho(Q)$ in the case that the length of AB is $y+z$ is similar. This finishes the proof of the lemma in case 2. □

Proof of Theorem 3.9. Let Q be a minimal roundness quadrilateral in C_{2n+1}. By Theorem 3.3, we know that Q is in cyclic order. We further know that $\rho(C_{2n+1}) < 2$ and that any quadrilateral in C_{2n+1} whose longest side is at least as long as its other three sides together has roundness greater than 2, so the longest side of Q is shorter than the other three sides together. Therefore, by Lemma 3.10, we know that the lengths of the longest and shortest sides of Q differ by a most 1, for otherwise Q

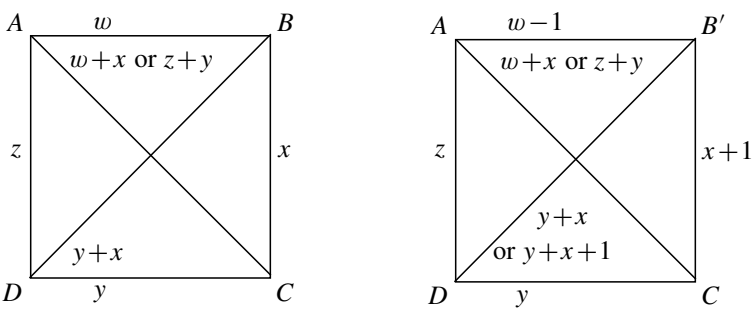

Figure 12. Sides and diagonals in case 2 of Lemma 3.10.

would not have minimal roundness. Therefore, Q is an in-order quadrilateral and the lengths of the longest and shortest sides of Q differ by at most 1.

Conversely, let Q' be an in order quadrilateral with lengths of the longest and shortest sides differing by at most 1. These conditions on Q' uniquely determine the side and diagonal lengths of Q'. Therefore, Q' has the same roundness as the minimal roundness quadrilateral Q from the first half of the proof. Therefore, Q' is itself a minimal-roundness quadrilateral in C_{2n+1}. □

Calculation of $\rho(C_{2n+1})$. Here we prove Theorem 3.1 and Corollary 3.2.

Proof of Theorem 3.1. If $2n+1$ has the form $4k+1$ for integer k then by Theorem 3.9 the diagonals of a minimal roundness quadrilateral Q in C_{2n+1} have length $2k$, one side has length $k+1$ and three sides have length k. Therefore, in this case, $\rho(C_{4k+1})$ is the supremum over all values p such that $2(2k)^p \leq 3k^p + (k+1)^p$. Define the function $f_k(p)$ by $f_k(p) = 2(2k)^p - (k+1)^p - 3k^p$. Then $f_k(1) < 0$ and $f_k(p) > 0$ for sufficiently large p. Therefore $f_k(p)$ has a zero greater than 1. Also, when arranged in decreasing order of the sizes of their bases, the exponential terms in $f_k(p)$ exhibit one "sign change", so $f_k(p)$ has at most one positive zero, (see for example [Langer 1931, p. 128]). Since $f_k(p) > 0$ for sufficiently large p values, $f_k(p)$ is positive for all p values greater than its positive zero. Therefore, $2(2k)^p > 3k^p + (k+1)^p$ for all p values greater than the solution to $2(2k)^p = 3k^p + (k+1)^p$, which proves that $\rho(C_{2n+1})$ is the positive solution of the equation $2(2k)^p = 3k^p + (k+1)^p$ in the case that $2n+1$ has the form $4k+1$. A similar argument shows that $\rho(C_{2n+1})$ is the positive solution of the equation $2(2k-1)^p = 3k^p + (k-1)^p$ if $2n+1$ has the form $4k-1$. □

Since $\rho(C_{2n}) = 1$, to prove Corollary 3.2 it suffices to show that the solutions to the equations (1) and (2) of Theorem 3.1 approach 1 as k goes to infinity. As in the proof of Theorem 3.1, the proofs in each case are similar, so we provide a rigorous proof of only (1), the case that $2n+1$ has the form $4k+1$.

Proof of Corollary 3.2. Restricting our attention to the case $2n+1 = 4k+1$, we have $\rho(C_{4k+1})$ equal to the zero of the function $f_k(p)$ from the proof of Theorem 3.1. We show that this solution can be made arbitrarily close to 1 by choosing k sufficiently large. Since $1 \leq \rho(C_{4k+1}) < \log_2 3$ for k-values greater than 2, we may restrict our attention to p values less than $\log_2 3$. Fix a real number α with $1 < \alpha < \log_2 3$. Consider the function $g(k) = f_k(\alpha) = 2(2k)^\alpha - (k+1)^\alpha - 3k^\alpha$. For all sufficiently large k, $g(k) > 0$. Therefore, for all sufficiently large k, $f_k(\alpha) > 0$. Since $f_k(1) < 0$ for all k, this proves that for all sufficiently large k, the zero of $f_k(p)$ is between 1 and α. It follows that $\lim_{k\to\infty} \rho(C_{4k+1}) = 1$. A similar argument shows that $\lim_{k\to\infty} \rho(C_{4k-1}) = 1$. Since $\rho(C_{2k}) = 1$ for all $k > 2$, this finishes the proof that $\lim_{k\to\infty} \rho(C_k) = 1$. □

4. Triangulated cycles

We now continue our investigation of roundness of finite graphs by investigating the effect of "triangulating" a cycle by connecting various of the vertices in the cycle with edges in a particular way until there are no metrically embedded cycles of length greater than 3. We focus on a particular triangulation of C_k, described below, which we simply denote by T_k.

Definition 4.1. Let C_k be the cyclic graph with vertices $v_1, v_2, \ldots, v_k$ in cyclic order. The *triangulated cycle* T_k is formed by connecting with edges the following pairs of vertices

$$(v_2, v_k), (v_k, v_3), (v_3, v_{k-1}), (v_{k-1}, v_4), \ldots$$

as shown in Figure 13.

Since the roundness of a circle is equal to 1 and the roundness of $\mathbb{R}^2$ is equal to 2, it seems reasonable that the roundness of the triangulated cycle T_n should be at least a little closer to 2 than the roundness of the nontriangulated cycle of the same length, C_n. We prove this to be true in the main theorem of this section.

Theorem 4.2. *Let T be the triangulated cycle T_{2n} or T_{2n+1}. For $n \geq 2$, $\rho(T)$ is the solution of the equation*

$$n^q = (n-1)^q + 2. \tag{4}$$

Since each T_k for $k \geq 4$ contains an metrically embedded copy of graph Δ, $\rho(T_n) \leq \log_2 3 < 2$, so no minimal roundness quadrilateral in T_n has roundness 2 or greater. This is a fact that we will frequently use without explicitly mentioning it in this section. Another fact we will use throughout is the following lemma whose proof we omit.

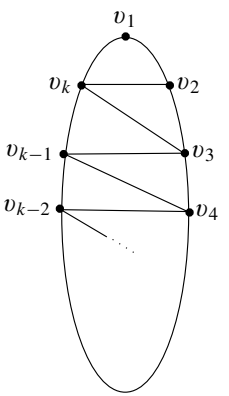

Figure 13. The triangulated cycle T_k.

Lemma 4.3. *If $r \in (0, 1]$ and $x, y > 0$ then $(x+y)^r < x^r + y^r$.*

We now prove our main theorem of this section.

Proof of Theorem 4.2. Let r_n denote the solution of Equation (4). We proceed by induction on n to prove that $\rho(T_{2n}) = \rho(T_{2n+1}) = r_n$. For the base case, $n = 2$, T_4 and T_5 are small enough that one can verify by hand that they have roundness equal to r_2.

Now assume by induction that for all $k < n$, $\rho(T_{2k}) = \rho(T_{2k+1}) = r_k$. We focus first on T_{2n} and prove that $\rho(T_{2n}) = r_n$. Note that $\rho(Q(v_1, v_2, v_{n+1}, v_{n+2})) = r_n$, so $\rho(T_{2n}) \leq r_n$. Denote by Q' the quadrilateral $Q' = Q(v_1, v_2, v_{n+1}, v_{n+2})$. Suppose now that Q is a quadrilateral in T_{2n} that does not contain both v_1 and v_{n+1}. In this case, Q is a quadrilateral in a metrically embedded subgraph of T_{2n} isomorphic to T_{2k} or T_{2k+1} for $k < n$. By our induction hypothesis, this subgraph has roundness $r_k > r_n$. So, $\rho(Q) \geq r_k > r_n = \rho(Q')$, and Q is not a minimal roundness quadrilateral in T_{2n}. Therefore, every minimal roundness quadrilateral in T_{2n} contains both v_1 and v_{n+1}. Furthermore, the greatest distance between vertices in T_{2n} is n, and this occurs only between vertices v_1 and v_{n+1}, so any minimal roundness quadrilateral in T_{2n} must be of the form $Q(v_1, u, v_{n+1}, w)$, containing the path from v_1 to v_{n+1} as a diagonal.

Now, let $Q(v_1, u, v_{n+1}, w)$ be a quadrilateral in T_{2n} with the path from v_1 to v_{n+1} on a diagonal. If both u and v occur on the same side of T_{2n} (i.e., either both have subscripts greater than $n+1$ or both have subscripts less than $n+1$), then Q lies in a metrically embedded line in T_{2n} and therefore has roundness at least 2 and is not a minimal roundness quadrilateral in T_{2n}. Therefore, assume that $u = v_{b+2}$ and $w = w_{n+2+a}$ for some a, b with $0 \leq a \leq n-2$ and $4 \leq b \leq n-2$. We prove that Q is not a minimal roundness quadrilateral in T_{2n} unless $a = b = 0$ or $a = b = n-2$. If $a + b \leq n$, then $\rho(Q)$ is the positive solution of

$$n^p + (n-a-b-1)^p = (n-1-a)^p + (a+1)^p + (n-1-b)^p + (b+1)^p, \quad (5)$$

and if $a + b > n$ then $\rho(Q)$ is the positive solution of

$$n^p + (a+b+3-n)^p = (n-1-a)^p + (a+1)^p + (n-1-b)^p + (b+1)^p. \quad (6)$$

We first deal with the case that $a + b \leq n$ and prove that the solution to (5) is greater than r_n when $a + b \leq n$ and at least one of a and b is strictly greater than 0. Assume now that $a, b \geq 0$, $a + b \leq n$ and at least one of a and b is greater than 0. Since

$$n^1 + (n-a-b-1)^1 < (n-1-a)^1 + (a+1)^1 + (n-1-b)^1 + (b+1)^1,$$

it suffices to prove that

$$n^{r_n} + (n-a-b-1)^{r_n} < (n-1-a)^{r_n} + (a+1)^{r_n} + (n-1-b)^{r_n} + (b+1)^{r_n}. \quad (7)$$

Consider the function

$$f(a,b) = n^{r_n} + (n-a-b-1)^{r_n} - (n-1-a)^{r_n} - (a+1)^{r_n} - (n-1-b)^{r_n} - (b+1)^{r_n}.$$

We prove inequality (7) by proving that $f(a,b) < 0$ for all $a, b \geq 0$ with at least one of a and b greater than 0 and $a+b \leq n$. By the symmetry between a and b, without loss of generality, we may assume that $a \geq b$. Since at least one of a and b is at least 1, we have $a \geq 1$. First consider the function $g(a) = f(a,a)$. Since r_n is the solution to (4), we have $g(0) = 0$. Now,

$$g'(a) = -2r_n(n-2a-1)^{r_n-1} + 2r_n(n-1-a)^{r_n-1} - 2r_n(a+1)^{r_n-1}.$$

By Lemma 4.3, we have

$$(n-1-a)^{r_n-1} < ((n-2a-1)+(a+1))^{r_n-1} < (n-2a-1)^{r_n-1} + (a+1)^{r_n-1}.$$

Therefore, $g'(a) < 0$ for $a > 0$ so $f(a,a) = g(a) < 0$ for all $a > 0$ and in particular for all $a \geq 1$.

A similar argument proves that $f(a,0) < 0$ for all $a \geq 1$, so we are left with proving that $f(a,b) < 0$ in the case that $a > b$ and $a, b \geq 1$ and $a+b \leq n$. Since $f(a,a) < 0$ it suffices to prove that $f_a(a,b) < 0$ for all a and b under consideration. Now, $f_a(a,b) = -r_n(n-a-b-1)^{r_n-1} + r_n(n-1-a)^{r_n-1} - r_n(a+1)^{r_n-1}$. By Lemma 4.3 and the fact that $b < a$ we have

$$(n-1-a)^{r_n-1} < ((n-a-b-1)+(a+1))^{r_n-1} < (n-a-b-1)^{r_n-1} + (a+1)^{r_n-1}.$$

Therefore, $f_a(a,b) < 0$ for all a, b under consideration, finishing the proof that Q is not a minimal roundness quadrilateral in T_{2n} in the case that $a+b \leq n$. The inequalities in case that $a+b > n$ can be reduced to the inequalities in the case $a+b \leq n$ by making the substitutions $a' = n-2-a$ and $b' = n-2-b$, so the above arguments prove that Q is not a minimal roundness quadrilateral in T_{2n} in this case, either unless $a' = b' = 0$, which is the same as $a = b = n-2$.

We have now proved that a minimal roundness quadrilateral in T_{2n} has the form $Q(v_1, u, v_{n+1}, w)$ with $u = v_{b+2}$ and $w = w_{n+2+a}$ for some $a, b \geq 0$. But, we have also proved that such a quadrilateral is not a minimal roundness quadrilateral whenever at least one of a and b is greater than 1. Therefore, the quadrilateral given when a and b are equal to 0, $Q(v_1, v_2, v_{n+1}, v_{n+2})$, is a minimal roundness quadrilateral in T_{2n}. This finishes the proof that $\rho(T_{2n}) = r_n$.

To finish the inductive step the proof, must prove that $\rho(T_{2n+1}) = r_n$ also. The details in the argument for this case are very similar to those in the proof that $\rho(T_{2n}) = r_n$, but the proof also uses the fact we just proved that $\rho(T_{2n}) = r_n$. We therefore omit the proof that $\rho(T_{2n+1}) = r_n$. This finishes the proof of the induction step and proves that $\rho(T_{2n}) = \rho(T_{2n+1}) = r_n$ for all $n \geq 2$. □

We note that it can be proved from our formulas for $\rho(T_{2n})$ and $\rho(T_{2n+1})$ that $\rho(T_{2n}) > 1 = \rho(C_{2n})$ and $\rho(T_{2n+1}) > \rho(C_{2n+1})$, as mentioned in the introduction to this section. The formulas can also be used to prove the following corollary in a way similar to the way that Corollary 3.2 was proved in the previous section.

Corollary 4.4. *Let T_k the triangulated cycle described in Definition 4.1. Then*

$$\lim_{k\to\infty} \rho(T_k) = 1.$$

5. The distribution of roundness for general graphs

As can be seen from the previous two sections, rigorously calculating the roundness of a particular graph or class of graphs can be a daunting task because the number of quadrilaterals in a graph with n vertices grows as n^4. Certainly there is a lot of duplication and some quadrilaterals can be ruled out immediately as not giving the minimal roundness, but the task is still very large. Therefore, we wrote a computer program to aid with example calculations. This program has two forms. In the first form, available at an online calculator, the user enters the adjacency matrix of a graph on 10 or fewer vertices. The program then by brute force enumerates all quadrilaterals in the graph, estimates the roundness of each one and outputs a minimal roundness quadrilateral along with its roundness. In its other form, this program reads in a file containing the adjacency matrices, formatted in a certain way, of a set of graphs on 10 or fewer vertices. The program calculates the roundness of each graph and outputs a list of all the roundness that occurred among the graphs and the number of times each roundness occurred. We ran this program on files containing the adjacency matrices of all nonisomorphic connected graphs on 7, 8 and 9 vertices that we obtained from Gordon Royle's data at the web page *Small Graphs* and found the roundness distributions among these graphs shown in Tables 1–3.

Looking at these data, one notices a number of trends that would be interesting to investigate formally. In particular, most graphs seem to have roundness equal to 1, which makes sense because any graph with a metrically embedded even cycle has roundness equal to 1. Another observation is that, after eliminating the graphs with roundness equal to 1, roundnesses tend to "bunch up" at the upper end around 1.58 and 1.39, with a tail trailing off to roundness equal to 1. It would be interesting to explore and rigorously quantify this phenomenon. One last striking feature of these distributions is that while the gap between the smallest two roundness values gets smaller as the number of vertices gets larger (as it should according to Corollaries 3.2 and 4.4), the gap between the upper two roundness values, $\log_2 3$ and 2 does not seem to shrink. This leads to the question *can any graph have roundness strictly between* $\log_2 3$ *and* 2? The answer is no:

Roundness	Number	Fraction of Total
1.00000	545	0.6389215
1.31091	2	0.0023447
1.39495	26	0.0304807
1.58497	221	0.2590856
2.00000	58	0.0679953
∞	1	0.0011723
Total number of graphs: 853		

Table 1. Roundness distribution: 7 vertices.

Roundness	Number	Fraction of Total
1.00000	9170	0.824862823
1.23336	1	8.99523E-05
1.31091	21	0.001888999
1.32766	4	0.000359809
1.39495	361	0.032472789
1.58497	1395	0.125483494
2.00000	164	0.014752181
∞	1	8.99523E-05
Total number of graphs: 11117		

Table 2. Roundness distribution: 8 vertices.

Roundness	Number	Fraction of Total
1.00000	245324	0.9396507
1.21258	2	7.66E-06
1.23336	16	6.128E-05
1.27156	3	1.149E-05
1.31091	375	0.0014363
1.32766	94	0.00036
1.39495	4844	0.0185537
1.58497	9926	0.038019
2.00000	495	0.001896
∞	1	3.83E-06
Total number of graphs: 261080		

Table 3. Roundness distribution: 9 vertices.

Theorem 5.1. *For any finite graph G, $\rho(G) \notin (\log_2 3, 2)$.*

We call the interval between $\log_2 3$ and 2 a *gap* in the roundness spectrum for finite graphs. Theorem 5.1 and the fact that the data in Tables 1–2 seem to exhibit other gaps suggests the following question:

Are there any other gaps in the roundness spectrum for finite graphs? In particular, does any finite graph have roundness between 1.58497 *and* 1.39495?

We suspect that the answer is yes there are other gaps, including one between 1.58497 and 1.39495, but we do not have a proof at present. For now, we prove Theorem 5.1, beginning with the following lemma. This lemma is the key that allows us to severely restrict the kinds of quadrilaterals that could appear in a graph with roundness between $\log_2 3$ and 2.

Lemma 5.2. *If G is a graph with $\rho(G) > \log_2 3$, every closed nonrepeating path in G is contained in a subgraph of G that is a complete graph.*

Proof. First note that if C_n for $n \geq 4$ or Graph Δ is metrically embedded in a graph, then the graph's roundness is less than or equal to $\log_2 3$. Therefore, G has no metrically embedded subgraph isomorphic to C_n for $n \geq 4$ or Δ. Let γ be a closed nonrepeating path in G of length k. We proceed by induction on k to show that γ is contained in a complete subgraph. The base case $k = 3$ is trivial because in this case, γ itself is a complete graph on 3 vertices. Now assume that every closed nonrepeating path in G of length less at most $n-1$ is contained in a complete subgraph. Consider a closed nonrepeating path γ with length $k = n \geq 4$. If γ is metrically embedded, then γ is a metrically embedded C_n for $n \geq 4$, which is impossible since $\rho(G) < \log_2 3$. Therefore two nonadjacent vertices v and w in γ must be connected by a path in G shorter than the shortest path between them within γ. Let τ be such a path between v and w in G and let γ_1 and γ_2 be the two paths between v and w described by γ. We now have two closed paths, $\gamma' = \tau \cup \gamma_1$ and $\gamma'' = \tau \cup \gamma_2$, both of which have length less than n and which together contain all vertices of γ. The only repetition possible in these paths is in τ. Therefore, by eliminating repetition in τ, or by replacing τ with a segment of τ between two consecutive intersections of τ with γ and choosing new vertices v and w in γ, we may assume that γ' and γ'' are also nonrepeating closed paths of length less that n. By our induction hypothesis both of these paths lie in complete subgraphs of G.

To see that all of γ lies in a single complete subgraph, let G_0 be the subgraph of G consisting of all of the vertices in γ together with all edges between these vertices. Choose vertices s and t in γ. If s and t both lie together in γ' or in γ'', then by fact just proved that both γ' and γ'' lie in complete subgraphs, s and t span an edge in G. If they do not lie together in γ' or γ'' and they do not span an edge in G, then the vertices v, s, w, t span a metrically embedded subgraph isomorphic to

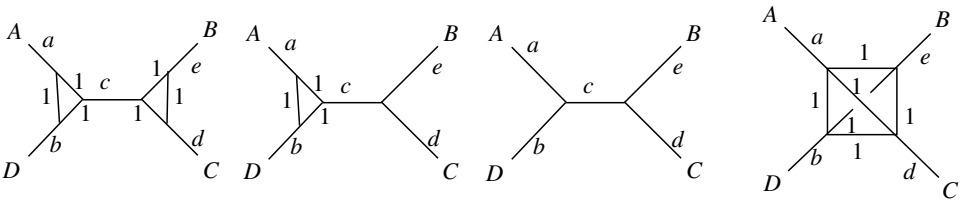

Figure 14. Possible shapes for a quadrilateral in G.

graph Δ, which is impossible since $\rho(G) > \rho(\Delta)$. Therefore, s and t must span an edge in G. This proves that the subgraph G_0 that contains γ is a complete graph, finishing the inductive step. Therefore every closed nonrepeating path in G lies in a complete subgraph of G. □

Using Lemma 5.2, we show that the geodesics comprising any quadrilateral $Q(A, B, C, D)$ in G must fit together into one of the four "shapes" in Figure 14. In this figure, we are considering fixed shortest paths, *geodesics*, between the points A, B, C, D in G. The lines in the figure represent parts of the fixed geodesics, and the lower case letters a, b, c, d and e are the lengths of subpaths of these paths. Paths of length 1 indicate edges connecting nonintersecting subpaths of the geodesics. We note that there may be many geodesics in G between any two points, but for the following arguments, we arbitrarily fix one distinguished geodesic between each pair of vertices that we consider throughout all the proofs.

Lemma 5.3. *If G is a graph with $\rho(G) > \log_2 3$ and if Q is a quadrilateral in G with vertices A, B, C, D then, after possibly renaming A, B, C, D, the geodesics forming Q take on one of the four shapes in Figure 14.*

Proof. First consider the fixed geodesics, X_1 from A to B, X_2 from B to C, and X_3 from A to C. Let A_1 be the vertex at which X_1 and X_3 last agree, A_2 the last vertex at which X_1 and X_2 last agree and let A_3 be the last vertex at which X_2 and X_3 agree. If the A_i are all distinct then these vertices and geodesics must lie as in Figure 15. Otherwise (for example if A_2 were to lie closer along X_1 to A than A_1 lies to A), by making replacements of subpaths, we could shorten at least one of the geodesics X_1, X_2 or X_3. The closed path formed by α followed by β followed by γ in Figure 15 is nonrepeating path, for otherwise we could shorten one of the geodesic paths α, β or γ. By Lemma 5.2 and the fact that each of these is a geodesic, they all must have length 1. Therefore, for any three points in the quadrilateral Q the geodesics between them must form a *degenerate* triangle as in Figure 16, with length ϵ being equal to either 0 or 1. Combining the possibilities for the triangle formed by A, B, C with the possibilities for the triangle formed by A, C, D, and remembering that graph Δ cannot metrically embed in G leads to only the four possible configurations in Figure 14, after possibly renaming the vertices. □

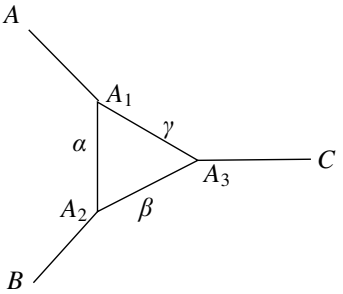

Figure 15. Orientation of vertices in the proof of Lemma 5.3.

Proof of Theorem 5.1. Let G be a finite graph with roundness strictly greater than $\log_2 3$, and let Q be a quadrilateral in G formed with vertices A, B, C, D of G. Fix geodesics in G between each pair of these vertices. By Lemma 5.3, after a possible renaming of the vertices, A, B, C and D and the corresponding geodesics fall into one of the shapes in Figure 14. To prove that $\rho(G) \notin (\log_2 3, 2)$ it suffices to verify that $q = 2$ satisfies the inequality in Definition 2.1 for quadrilateral Q. By Observation 2.4, this amounts to verifying the inequality for quadrilaterals $Q(A,B,C,D)$, $Q(A,B,D,C)$ and $Q(A,C,B,D)$ in all four shapes of Figure 14. All of the verifications are performed similarly, so we show the proof only for $Q(A,B,C,D)$ in the first shape. This amounts to proving that

$$(a+c+d+2)^2 + (b+c+e+2)^2 \\ \leq (a+c+e+2)^2 + (a+b+1)^2 + (d+e+1)^2 + (b+c+d+2)^2.$$

This can be verified through the following sequence of inequalities:

$$0 \leq (a-e)^2 + (b-d)^2 + 2ab + 2ad + 2be + 2de + a + b + d + e + 2,$$
$$0 \leq a^2 + b^2 + d^2 + e^2 + 2ab + 2ad - 2ae - 2bd + 2be + 2de + a + b + d + e + 2,$$

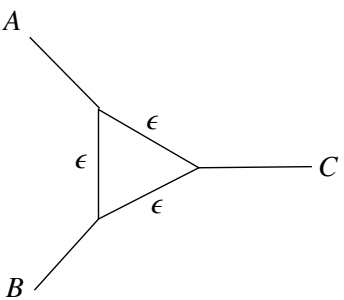

Figure 16. Degenerate triangle in the proof of Lemma 5.3.

$$\begin{aligned}a^2+b^2+2c^2+d^2+e^2+2ac+2ae+2bc+2bd+2cd+2ce+4a+4b+8c+4d+4e+8 \\ \le 2a^2+2b^2+2c^2+2d^2+2e^2+2ab+2ac+2ad+2bc+2be \\ +2cd+2ce+2de+5a+5b+8c+5d+5e+10,\end{aligned}$$

$$\begin{aligned}(a+c+d+2)^2+(b+c+e+2)^2 \\ \le (a+c+e+2)^2+(a+b+1)^2+(d+e+1)^2+(b+c+d+2)^2. \quad \square\end{aligned}$$

We finish this section by noting that the roundness of an infinite connected graph is the infimum of the roundnesses of all of its metrically embedded finite connected subgraphs. Since none of these finite subgraphs can have roundness between $\log_2 3$ and 2, it follows that no graph, finite or infinite, can have roundness between $\log_2 3$ and 2. We record this as our final corollary.

Corollary 5.4. *If G is a connected graph then $\rho(G) \notin (\log_2 3, 2)$.*

References

[Enflo 1970a] P. Enflo, "On a problem of Smirnov", *Ark. Mat.* **8** (1970), 107–109. MR 54 #3661 Zbl 0196.14003

[Enflo 1970b] P. Enflo, "On the nonexistence of uniform homeomorphisms between L_p-spaces", *Ark. Mat.* **8** (1970), 103–105. MR 42 #6600 Zbl 0196.14002

[Jaudon 2008] G. Jaudon, "Some remarks on generalized roundness", *Geom. Dedicata* **135** (2008), 23–27. MR 2009e:20092 Zbl 1152.20037

[LaFont and Passidis 2006] J.-F. LaFont and S. Passidis, "Roundness properties of groups", *Geom. Dedicata* **117** (2006), 137–160.

[Langer 1931] R. E. Langer, "On the zeros of exponential sums and integrals", *Bull. Amer. Math. Soc.* **37**:4 (1931), 213–239. MR 1562129 Zbl 0001.34403

Received: 2009-07-27 Revised: 2009-12-28 Accepted: 2009-12-29

horakm@uwstout.edu *Mathematics, Statistics and Computer Science Department, University of Wisconsin – Stout, Menomonie, WI 54751, United States*
http://faculty.uwstout.edu/horakm/

larosee@uwstout.edu *Mathematics, Statistics and Computer Science Department, University of Wisconsin – Stout, Menomonie, WI 54751, United States*

moorej@uwstout.edu *Mathematics, Statistics and Computer Science Department, University of Wisconsin – Stout, Menomonie, WI 54751, United States*

rooneym@uwstout.edu *Mathematics, Statistics and Computer Science Department, University of Wisconsin – Stout, Menomonie, WI 54751, United States*

rosenthalh@uwstout.edu *Mathematics, Statistics and Computer Science Department, University of Wisconsin – Stout, Menomonie, WI 54751, United States*

On (2, 3)-agreeable box societies

Michael Abrahams, Meg Lippincott and Thierry Zell

(Communicated by Arthur T. Benjamin)

The notion of a (k, m)-agreeable society was introduced by Berg, Norine, Su, Thomas and Wollan: a family of convex subsets of $\mathbb{R}^d$ is called (k, m)-*agreeable* if any subfamily of size m contains at least one nonempty k-fold intersection. In that paper, the (k, m)-agreeability of a convex family was shown to imply the existence of a subfamily of size βn with a nonempty intersection, where n is the size of the original family and $\beta \in [0, 1]$ is an explicit constant depending only on k, m and d. The quantity $\beta(k, m, d)$ is called the minimal *agreement proportion* for a (k, m)-agreeable family in $\mathbb{R}^d$.

If we assume only that the sets are convex, simple examples show that $\beta = 0$ for (k, m)-agreeable families in $\mathbb{R}^d$ where $k < d$. In this paper, we introduce new techniques to find positive lower bounds when restricting our attention to families of d-boxes, that is, cuboids with sides parallel to the coordinates hyperplanes. We derive explicit formulas for the first nontrivial case: (2, 3)-agreeable families of d-boxes with $d \geq 2$.

1. Introduction

Berg et al. [2010] introduced the concept of geometric approval voting, where a *platform* is a point in $\mathbb{R}^d$ and a *vote* can be any convex subset, representing all the platforms deemed acceptable by that particular voter. (The convexity assumption is a way to require our voters to be reasonable: the fact that all votes contain every point on a segment with both endpoints in the vote means that any platform obtained as a compromise between two acceptable positions is again deemed acceptable.) The main question addressed in [Berg et al. 2010] was, given a collection of votes, to find the largest number of overlapping votes, and thus the largest number of voters that could be satisfied by the adoption of any single platform.

More specifically, the authors concentrated on what they termed (k, m)-*agreeable societies*, where any group of m voters contains k or more who can agree on a common platform. Their main goal was to obtain lower bounds on the *agreement proportion* (the ratio of satisfied voters to total number of voters) in terms of k, m

MSC2000: primary 52C45; secondary 91B12.

Keywords: boxicity, arrangements of boxes, agreement proportion, voting, Helly's theorem.

and d only. Using the version of the fractional Helly theorem due to Kalai [1984], they showed that if a (k, m)-agreeable society contains $n \geq m$ votes, all of which are convex subsets of $\mathbb{R}^d$, then there exists a platform contained in at least $\beta(k, m, d)\, n$ votes, where the *proportion* $\beta(k, m, d)$ satisfies:

$$\beta(k, m, d) \geq 1 - \left[1 - \frac{\binom{k}{d+1}}{\binom{m}{d+1}}\right]^{\frac{1}{d+1}}. \tag{1}$$

Given that the fractional Helly theorem makes no reference to k-fold intersections when $k \leq d$, it is no surprise that this lower bound is positive only when $k \geq d+1$.

If the general convex case requires detailed information about the whole intersection pattern of the arrangement of votes, the *intersection graph* does capture the structure of the whole arrangement in the special case when the votes are *boxes*, that is, cuboids with sides parallel to the coordinate axes. This case was also addressed in [Berg et al. 2010], and purely graph-theoretic considerations yielded a sharp bound of k/m for the agreement proportion in the *strong agreement case:* the situation of (k, m)-agreeability where $m \leq 2k-2$. (The result proved there for this case $m \leq 2k-2$ is in fact substantially stronger: if the number of boxes is n, there is an overlap of at least $n - m + k$ boxes, so the actual agreement proportion *starts* at k/m and *increases* to 1 as the number n of boxes goes to infinity.)

The case of $(2, m)$-agreeable societies of d-boxes does not fall in the strong agreement category, and it is left essentially open in [Berg et al. 2010]. In fact, it is not even clear at the outset that there is a positive agreement proportion for $(2, m)$-agreeable arrangements of d-boxes when $m \geq 3$ and $d \geq 2$, since the lower bound given by (1) is zero in that case. In this paper we tackle the $(2, 3)$-agreeable case and prove the following result.

Theorem 1.1. *For any $d \geq 1$, any $(2, 3)$-agreeable d-box society has an agreement proportion of at least $(2d)^{-1}$.*

The remainder of the paper is organized as follows.

The material in Section 2 is independent from the rest of the paper: it presents an elementary proof of the fact that $(2, 3)$-agreeable arrangements of intervals have an agreement proportion of at least $\frac{1}{2}$. Section 3 is devoted to preliminaries. It introduces notation and definitions regarding arrangements of boxes and their intersection graphs. Section 4 establishes upper and lower bounds on the degrees of vertices in a $(2, 3)$-agreeable graph G with bounded clique number. A classification of the small cases is given, and we prove that positive lower bounds do exist for all d. In Section 5, we establish the specific values of the lower bound stated in Theorem 1.1. The proof uses a lower bound on boxicity taken from [Adiga et al. 2008]. Section 6 relates $(2, 3)$-agreeability to Ramsey numbers and presents a few questions left open by our work.

Throughout the paper, all arrangements of boxes are assumed to be $(2, 3)$-agreeable. Many of the definitions and results could easily be extended to the (k, m)-agreeable case; this level of generality was eschewed in order to keep notations simple and legible. The only step for which $(2, 3)$-agreeability is crucial is in establishing the lower bound of Section 4.

Notation 1.2. Throughout this paper, G denotes a simple, undirected graph. The sets $V(G)$ and $E(G)$ are respectively the sets of vertices and edges of G, and we let $n = \#V(G)$. Recall that any subset W of $V(G)$ gives rise to the subgraph $G[W]$ *induced* by W, which is the graph that has W as its set of vertices, and has for edges all the edges of $E(G)$ with both endpoints in W.

A *clique* in G is any subset of $V(G)$ that induces a complete subgraph, and the size of the largest clique is called the *clique number* of G and denoted by $\omega(G)$.

2. The linear case

The intersection graphs associated to arrangements of intervals in the line are *perfect graphs*. This allowed Berg et al. [2010] to prove the nontrivial fact: for any (k, m)-agreeable arrangement of intervals, the agreement number is at least $(n - R)/Q$, where Q and R denote respectively the quotient and the remainder of the Euclidean division of $m - 1$ by $k - 1$. This lower bound is sharp and it implies that any (k, m)-agreeable collection of intervals must have an agreement proportion

$$\beta(k, m, 1) \geq \frac{k-1}{m-1}.$$

In particular, the above implies that any $(2, 3)$-agreeable collection of intervals has agreement proportion at least $\frac{1}{2}$. This substantially improves the general case bound given in formula (1), which for $d = 1$ in the $(2, 3)$-agreeable setting yields an agreement proportion of

$$1 - \sqrt{\tfrac{2}{3}} \approx 0.1835.$$

We reprove the lower bound of $\frac{1}{2}$ using only elementary means. First we need to know when the agreement proportion equals 1.

Lemma 2.1. *A linear society has agreement proportion* 1 *if and only if every pair of votes intersects. In the terminology of* [Berg et al. 2010], *such an arrangement is called* super-agreeable.

Proof. This is a special case of Helly's theorem [Matoušek 2002], which states that for any arrangement of convex sets in $\mathbb{R}^d$, the sets have a nonempty intersection if and only if all $(d + 1)$-fold intersections are nonempty. □

Theorem 2.2. [Berg et al. 2010, Theorem 1] *The minimal agreement proportion of a linear* $(2, 3)$*-agreeable society is* $\frac{1}{2}$.

Proof. If every pair of votes intersects, Helly's theorem for intervals implies that the agreement proportion is 1. So, without loss of generality, we can assume that in our one-dimensional $(2, 3)$-agreeable society, there are two nonintersecting intervals A (Alice's vote) and B (Bob's vote), with A to the left of B.

The remaining voters can be divided into three categories: those who agree only with Alice, those who agree only with Bob, and those who agree with both Alice and Bob. (There are no voters who agree with neither since that would violate $(2, 3)$-agreeability.) These three categories of voters — call them friends of Alice, friends of Bob and friends of both — form super-agreeable groups, where all voters can agree pairwise and thus, by Helly's theorem, all the votes in each group overlap. Indeed, friends of Alice must agree with each other, because if two of them did not agree, then taken together with Bob, we would have three votes containing no intersecting pair, violating the condition of $(2, 3)$-agreeability. Similarly, voters who only agree with Bob must also agree with each other. As for votes which overlap with both Alice and Bob's vote, they all meet in the interval $[\max(A), \min(B)]$ between A and B (Figure 1). If one of the three categories is empty, we have two super-agreeable groups, one of which must account for at least one half of the voters, and the result holds.

Suppose that all three categories are nonempty, and let C be a vote containing $[\max(A), \min(B)]$, D be a vote intersecting A but not B, and E be a vote intersecting B but not A. The three votes must share at least one intersection to respect the $(2, 3)$-agreeable condition; and note that if $D \cap E \neq \varnothing$, it implies that the two intersections with C are also nonempty (all meet in the middle region). If we can find a vote D from a friend of Alice such that $C \cap D = \varnothing$, then we must have $C \cap E \neq \varnothing$, and, replacing E by any other vote E' intersecting B, the same reasoning shows that $C \cap E' \neq \varnothing$, too. Thus any vote C bridging the gap between

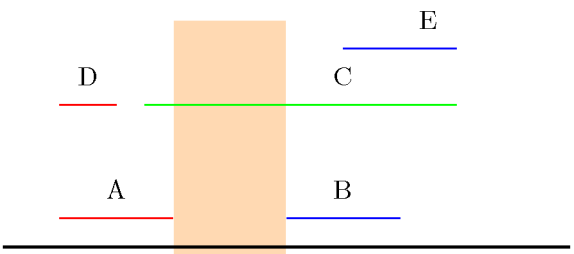

Figure 1. Alice, Bob, and their friends. The shaded area in the middle is shared by all the friends of Bob and Alice, such as C.

Alice and Bob must either meet all the votes that intersect A or all the votes that intersect B. Thus, we can assign those bridging votes to Alice or Bob, since they have to overlap with all of the friends of at least one. We can divide the votes into two super-agreeable groups once again. One of those must account for at least half the voters, proving the result. □

Remark 2.3. This theorem is sharp: any society formed by taking r copies of A and r copies of B is $(2, 3)$-agreeable with an agreement proportion of exactly $\frac{1}{2}$.

Remark 2.4. The result of the previous theorem only holds in dimension 1. For instance, Figure 2 shows five votes in dimension 2 arising from $(2, 3)$-agreeable voters, yet the agreement proportion is only $\frac{2}{5}$.

3. Boxes and agreeable graphs

We introduce some definitions and notation for the two main objects of study: arrangements of boxes and their associated intersection graphs.

3.1. ***Arrangements of boxes and intersection graphs.*** A *d-box* is a subset of $\mathbb{R}^d$ given by the Cartesian product of d closed intervals. A collection $\mathcal{B}$ of boxes gives rise to a graph in the following fashion.

Definition 3.1. The *intersection graph* $G_{\mathcal{B}}$ associated to an arrangement $\mathcal{B} = \{B_1, \ldots, B_n\}$ of d-boxes is the graph with vertices $V = \{1, \ldots, n\}$ such that $\{i, j\}$ is an edge if and only if $B_i \cap B_j \neq \varnothing$.

Conversely, given a simple, undirected graph G, we can define its *boxicity* $\mathrm{box}(G)$: it is the smallest integer d such that there exists an arrangement of d-boxes $\mathcal{B}$ whose intersection graph is G.

Roberts [1969] showed that this number is always finite, and that $\mathrm{box}(G) \leq \lfloor \#V/2 \rfloor$. (Graphs for which this bound is tight are classified in [Trotter 1979].)

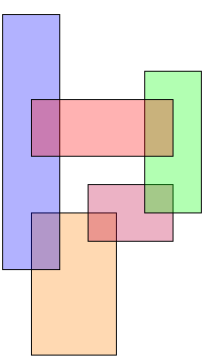

Figure 2. A $(2, 3)$-agreeable society of 2-boxes with agreement proportion $\frac{2}{5}$.

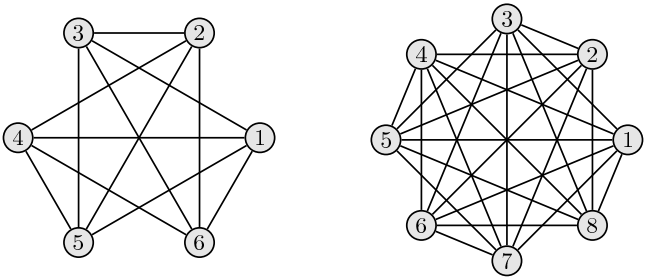

Figure 3. The complete partite graphs $K_3(2)$ (left) and $K_4(2)$ (right).

Remark 3.2. By convention we let $\mathrm{box}(K_n) = 0$ for all n (a 0-box would be a point). This shows that boxicity does not behave nicely with respect to taking subgraphs. On the other hand, it is clear that boxicity can only decrease when taking *induced subgraphs*, since for any arrangement of d-boxes $\mathcal{B} = \{B_1, \ldots, B_n\}$ and any subset $I \subseteq \{1, \ldots, n\}$, the intersection graph of the subarrangement $\{B_i \mid i \in I\}$ is simply the graph $G_{\mathcal{B}}[I]$ induced by the vertices I in $G_{\mathcal{B}}$.

Example 3.3. Note that the bound $\mathrm{box}(G) \leq \lfloor \#V/2 \rfloor$ remains sharp, *even if we restrict our attention to* $(2, 3)$*-agreeable graphs.* Indeed, for any $d \geq 1$, let $K_d(2)$ be the complete d-partite graph on d pairs of vertices, that is, the graph with $V = \{1, 2, \ldots, 2d\}$ and where E contains all possible edges except those of the form $\{i, i+1\}$ for i odd (see Figure 3). The graph $K_d(2)$ is $(2, 3)$-agreeable, and by [Roberts 1969, Theorem 7], we have $\mathrm{box}(K_d(2)) = d = \#V/2$.

Remark 3.4. Graphs with $\mathrm{box}(G) \leq 1$ are *interval graphs*, which can be easily identified in linear time [Booth and Lueker 1976; Habib et al. 2000]. Algorithms exist to test if $\mathrm{box}(G) \leq 2$ [Quest and Wegner 1990] or to compute boxicity in general [Cozzens and Roberts 1983], but they are a lot more cumbersome. The task of testing if $\mathrm{box}(G) \leq d$ is known to be NP-complete for all $d \geq 2$ [Cozzens and Roberts 1983].

The definition of $(2, 3)$-agreeability as it appears in [Berg et al. 2010] can be reformulated in terms of intersection graphs.

Definition 3.5. An arrangement $\mathcal{B} = \{B_1, \ldots, B_n\}$ of d-boxes is $(2, 3)$-agreeable if and only if any one of the three equivalent properties holds:

(1) For any $1 \leq i < j < k \leq n$, one at least of the intersections $B_i \cap B_j$, $B_i \cap B_k$ or $B_j \cap B_k$ is nonempty.

(2) For any three vertices in the intersection graph $G_{\mathcal{B}}$, the graph induced by these vertices contains at least one edge.

(3) The graph complement $\overline{G_{\mathcal{B}}}$ of the intersection graph satisfies $\omega(\overline{G_{\mathcal{B}}}) \leq 2$.

3.2. ***Agreement number and agreement proportion.*** Since any simple, undirected graph can be realized as the intersection graph of an arrangement of boxes, it will be convenient to blur the distinction between the two notions. In particular, we can use properties (2) and (3) in Definition 3.5 to define (2, 3)-agreeability for graphs rather than arrangements.

Another good reason to identify arrangements and their graphs is that the intersection graph encodes all the information about arrangements of boxes (this fails for arrangements of more general convex sets). Indeed, in such an arrangement, having nonempty pairwise intersection and having a point common to all the boxes are equivalent. In particular, the maximal number of overlapping boxes (or *agreement number* of the society) is simply the clique number $\omega(G_{\mathcal{B}})$ of the intersection graph.

Notation 3.6. We denote by $\mathcal{G}$ the set of all (2, 3)-agreeable graphs, and, for any $d \geq 0$, denote by $\mathcal{G}_d$ the subset of those graphs with boxicity at most d. Given $r \geq 1$, we let $\mathcal{G}(r)$ and $\mathcal{G}_d(r)$ respectively be the subsets of $\mathcal{G}$ and $\mathcal{G}_d$ formed by graphs G with $\omega(G) \leq r$. Note that for any $G \in \mathcal{G}_d(r)$ and any subset of vertices $W \subseteq V(G)$, the subgraph $G[W]$ induced by W is also in $\mathcal{G}_d(r)$: (2, 3)-agreeability is preserved by taking induced graphs, and both clique size and boxicity can only decrease (Remark 3.2).

We define the associated vertex sizes for all $r \geq 1$ and all $d \geq 0$,

$$\eta(r, d) = \max\{\#V(G) \mid G \in \mathcal{G}_d(r)\},$$
$$\eta(r) = \max\{\#V(G) \mid G \in \mathcal{G}(r)\}.$$

These quantities are related by the inequalities

$$2r = \eta(r, 1) \leq \eta(r, 2) \leq \cdots \leq \eta(r).$$

We will show in Proposition 4.5 that $\eta(r) \leq r(r + 3)/2$ for all $r \geq 1$, and thus all sets $\mathcal{G}_d(r)$ are finite. This is not a surprising result since it is the expected behavior brought on by (k, m)-agreeability, but note that in our case of interest, (2, 3)-agreeability, the very existence of a positive lower bound on the agreement proportion was left open in [Berg et al. 2010].

For any graph, the *agreement proportion* is defined as $\omega(G)/\#V(G)$. Once we prove that the set $\mathcal{G}_d(r)$ is finite for all $r \geq 1$ and $d \geq 1$, we can define

$$\rho(r, d) = \min\{\omega(G)/\#V(G) \mid G \in \mathcal{G}_d(r)\}, \tag{2}$$

that is, the *minimal agreement proportion* that can be obtained from a (2, 3)-agreeable graph with boxicity at most d and clique number at most r.

4. Upper and lower bounds on degrees

Throughout this section, $G = (V, E)$ denotes a $(2, 3)$-agreeable graph on n vertices. We show that a $(2, 3)$-agreeable graph with low clique number must have many edges. The results obtained here are purely combinatorial: in this section, we ignore the geometry of the problem and the boxicity of G.

4.1. ***Lower bound on the degree.*** The following trivial observation is the key to establishing lower bounds on the degrees of vertices.

Lemma 4.1. *If G is a $(2, 3)$-agreeable graph, then for any vertex $v \in V$, we have* $\deg(v) \geq n - \omega(G) - 1$.

Note that the inequality in this lemma may be strict, even if v is of minimal degree. We can see this by considering $G = W_4$, the wheel with four spokes, which is a $(2, 3)$-agreeable graph with $n = 5$ and $\omega(G) = 3$.

Proof. The vertex $v \in V$ is connected to $\deg(v)$ vertices. The other $n - \deg(v) - 1$ vertices must form a clique W. Indeed, if W were not a clique, it would contain two nonadjacent vertices, u and w. The subgraph induced by the three vertices $\{u, v, w\}$ would be empty, which would contradict the fact that G is $(2, 3)$-agreeable. Thus, $\omega(G) \geq |W| = n - \deg(v) - 1$, and the result follows. □

Using the formula

$$|E| = \tfrac{1}{2} \sum_{v \in V} \deg(v),$$

Lemma 4.1 yields the following lower bound on $|E|$.

Corollary 4.2. *For any $(2, 3)$-agreeable graph G, we have*

$$|E| \geq \tfrac{n}{2}(n - \omega(G) - 1).$$

Equality can occur in Corollary 4.2, for example, for the 5-cycle that appeared in Remark 2.4.

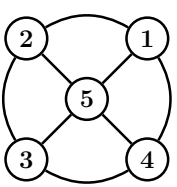

Figure 4. The wheel with four spokes W_4 is an example of a graph for which the inequality in Lemma 4.1 is strict.

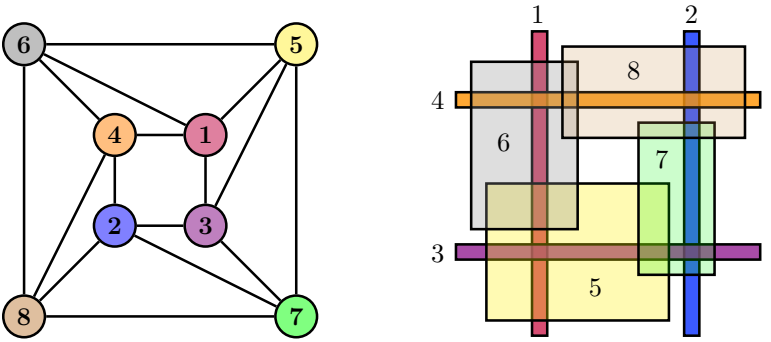

Figure 5. A (2, 3)-agreeable graph G with $|V(G)| = 8$, $\omega(G) = 3$ and $\mathrm{box}(G) = 2$, together with a family of 2-boxes whose intersection graph is G. This graph is 4-regular, $|E| = 16$.

4.2. ***Examples with low agreement proportion.*** The conclusion of [Berg et al. 2010] mentioned the existence of (2, 3)-agreeable families of 2-boxes with agreement $\frac{3}{8}$. (The example, credited to Rajneesh Hegde, was not given in the paper.) We give a few examples.

Case $n = 8$, $\mathrm{box}(G) = 2$. Figures 5 and 6 give two nonisomorphic examples of families of eight 2-boxes with no more than triple intersections. The corresponding intersection graphs have respectively 8 and 10 triangles.

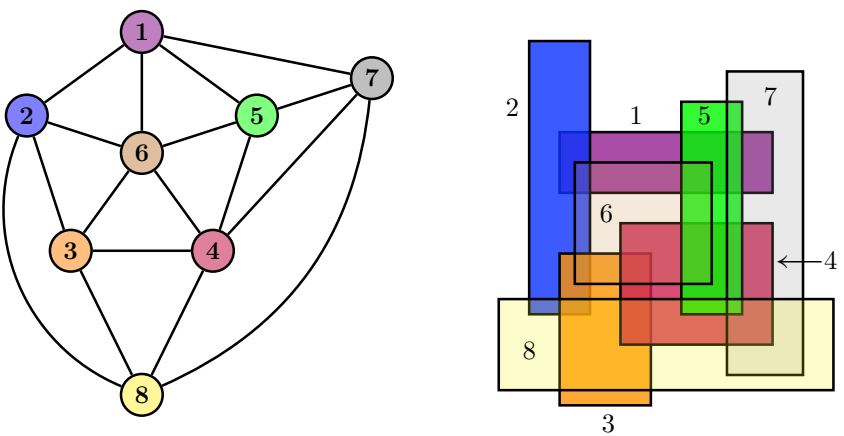

Figure 6. Another (2, 3)-agreeable graph G with $|V(G)| = 8$, $\omega(G) = 3$ and $\mathrm{box}(G) = 2$. Like the example in the previous figure, this graph also has boxicity 2, but $|E| = 17$.

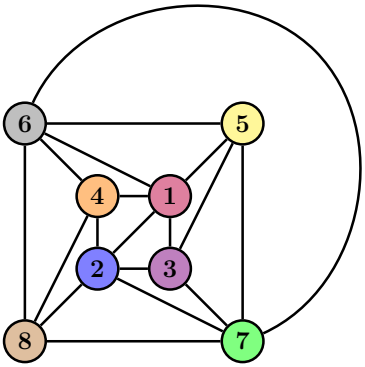

Figure 7. A $(2,3)$-agreeable graph with $|V(G)| = 8$, $\omega(G) = 3$, but $\mathrm{box}(G)$ unknown. Modifying the arrangement of Figure 5 so $B_1 \cap B_2 \neq \varnothing$ and $B_6 \cap B_7 \neq \varnothing$ creates more intersections, so it is not obvious whether a 2-box arrangement can realize this graph.

Case $n = 8$, $\mathrm{box}(G) =$?. Figure 7 presents a third example of a $(2,3)$-agreeable graph with agreement proportion $\frac{3}{8}$, obtained from Figure 5 by adding two edges. This graph has 12 triangles; its boxicity may be more than 2 (and we conjecture that it is).

Case $n = 13$, $\omega(G) = 4$. Figure 8 presents (the complement of) a $(2,3)$-agreeable graph on 13 vertices with unknown boxicity and agreement proportion $\frac{4}{13} \approx 0.31$. There are 39 cliques of size 4 in that example. We prove in Proposition 4.4 that 13 is the maximum number of vertices for a $(2,3)$-agreeable graph with no 5-cliques.

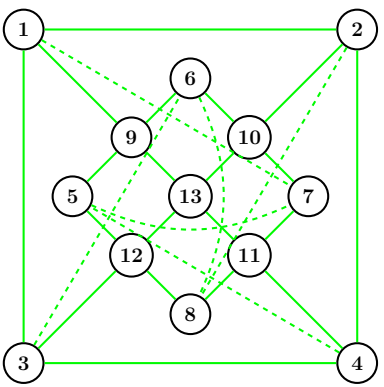

Figure 8. A graph whose *complement* is a $(2,3)$-agreeable 8-regular graph with $\omega = 4$.

4.3. ***Upper bounds on degree and graph size.*** We now give upper bounds on the degrees of vertices in (2, 3)-agreeable graphs, and deduce an upper bound on the number of vertices of such graphs with a given clique number.

Lemma 4.3. *Let $G \in \mathcal{G}_d(r)$, where $r \geq 2$ and $d \geq 1$. Then for any $v \in V$, we have*

$$\deg(v) \leq \eta(r-1, d) \leq \eta(r-1).$$

Proof. The neighbors of v induce a (2, 3)-agreeable graph H. If there are more than $\eta(r-1, d)$ vertices in the graph H, it must contain an r-clique, which together with v forms an $(r+1)$-clique in G, contradicting the hypothesis $\omega(G) \leq r$. □

The inequality in the lemma can be sharp, but it is not always so, even if G has the maximum possible number of vertices $\eta(r)$: in the case $r = 3$, we have $\eta(r-1) = 5$ and $\eta(r) = 8$ (see Proposition 4.4). The graphs in Figures 5 and 6 both have the maximum number of vertices (8) for their clique number of 3, but the maximum degree is 4 in the first graph, and 5 (the maximum possible) in the second example.

With Lemma 4.1 giving a lower bound on the number of edges which increases with the number of vertices, and Lemma 4.3 giving an upper bound which depends only on the clique number, this suggests that the graphs which maximize $\eta(r)$ must be regular or almost-regular. We can use this idea to establish step-by-step the first few values of $\eta(r)$.

Proposition 4.4. *We have the following table for the maximal size of* (2, 3)*-agreeable graphs with $\omega(G) = r$.*

r	1	2	3	4	5
$\eta(r)$	2	5	8	13	≤ 18

Proof. By definition of (2, 3)-agreeability, any graph with at least three vertices must have an edge, and thus $\eta(1) = 2$. The examples we've seen so far give the following lower bounds:

$$\eta(2) \geq 5, \quad \eta(3) \geq 8, \quad \eta(4) \geq 13.$$

Suppose that one of these lower bounds is not sharp: in other words, there exists at least one (2, 3)-agreeable graph with one of the following.

$\omega(G)$	2	3	4	5
$\#V$	6	9	14	19

Let $\delta(G)$ and $\Delta(G)$ denote respectively the minimum and the maximum degree for vertices in G. The case $|V(G)| = 6$ and $\omega(G) = 2$ is clearly impossible, since Lemma 4.1 implies $\delta(G) \geq 3$, and Lemma 4.3 implies $\Delta(G) \leq \eta(1) = 2$, giving the contradiction $\delta(G) > \Delta(G)$.

Thus we have proved that $\eta(2) = 5$, which combined with Lemma 4.3 implies that for any $G \in \mathcal{G}$ with $\omega(G) = 3$ we must have $\Delta(G) \leq 5$. In the case $|V(G)| = 9$ with $\omega(G) = 3$, Lemma 4.1 yields $\delta(G) \geq 5$. Since the graph G cannot be 5-regular (the sum of all degrees must be even), this yields in turn $\Delta(G) \geq 6$, which is again a contradiction.

This proves $\eta(3) = 8$, which implies that $\Delta(G) \leq 8$ for any $G \in \mathcal{G}$ with $\omega(G) = 4$. The other cases are similar. □

The method used in the proof of the above proposition could be extended indefinitely, provided one can construct examples that provide lower bounds on η. Even without a battery of examples, we can prove that the function $\eta(r)$ has at most quadratic growth, and thus that the sets $\mathcal{G}_d(r)$ are finite for any $d \geq 1$ and $r \geq 1$.

Proposition 4.5. *For all $r \geq 1$, the maximal number of vertices $\eta(r)$ for a $(2, 3)$-agreeable graph G with $\omega(G) \leq r$ satisfies $\eta(r) \leq r(r+3)/2$.*

Proof. Let G be a $(2, 3)$-agreeable graph such that $\omega(G) = r$ and $|V(G)| = \eta(r)$. If v is a vertex of G, Lemmas 4.1 and 4.3 imply the inequalities

$$\eta(r) - r - 1 \leq \deg(v) \leq \eta(r-1).$$

Solving the recurrence $\eta(r) - r - 1 - \eta(r-1) \leq 0$ with the initial condition $\eta(1) = 2$ gives the result. □

5. Lower bound on boxicity and the main result

Given a simple graph G on n vertices, call a vertex $v \in V(G)$ *universal* if $\deg(v) = n - 1$. [Adiga et al. 2008] presents several lower bounds on the boxicity of a graph; we need the following.

Theorem 5.1. [Adiga et al. 2008, Theorem 9] *Let G be a graph with no universal vertices and minimum degree δ. Then the boxicity of G has the lower bound*:

$$\operatorname{box}(G) \geq \frac{n}{2(n - \delta - 1)}.$$

The theorem above only applies to graphs with no universal vertices. Fortunately the lemma below shows that graphs minimizing the agreement proportion satisfy this property. Recall that for all $r \geq 1$ and $d \geq 1$, the quantity $\rho(r, d)$ denotes the minimum agreement proportion that can be achieved by a graph $G \in \mathcal{G}_d(r)$.

Lemma 5.2. *Given $r \geq 1$ and $d \geq 1$, consider a graph $G \in \mathcal{G}_d(r)$ such that the agreement proportion of G is equal to $\rho(r, d)$. Then G has no universal vertices.*

Proof. Suppose $G \in \mathcal{G}_d(r)$ is a graph with universal vertices, $G \neq K_n$. We construct from G a graph $\widehat{G} \in \mathcal{G}_d(r)$ without universal vertices and with a lower agreement proportion. Let Ω be the set of universal vertices,

$$\Omega = \{v \in V(G) \mid \deg(v) = n-1\};$$

define $W = V(G)\backslash\Omega$, and let $\widehat{G} = G[W]$ be the graph induced by W. Since we assumed $G \neq K_n$, the graph $\widehat{G}$ is nonempty. Note that $\mathrm{box}(\widehat{G}) \leq \mathrm{box}(G) \leq d$, since boxicity can only decrease when considering induced graphs (Remark 3.2). Letting $k = |\Omega|$, we have for any vertex in $w \in W$,

$$\deg_{\widehat{G}}(w) = \deg_G(w) - k < n - 1 - k = |W| - 1,$$

so that no vertex in $\widehat{G}$ is universal. Moreover, we have

$$\omega(\widehat{G}) = \omega(G) - k,$$

since any maximal clique in G must contain all the vertices in Ω. Thus, the agreement proportion for $\widehat{G}$ is

$$\frac{\omega(\widehat{G})}{\#V(\widehat{G})} = \frac{\omega(G)-k}{n-k} < \frac{\omega(G)}{n};$$

thus, any graph which minimizes agreement proportion does not have any universal vertices. □

Proof of Theorem 1.1. Consider a graph $G \in \mathcal{G}_d(r)$ on n vertices such that the agreement proportion of G is equal to the minimum $\rho(r, d)$. By Lemma 5.2, G does not contain a universal vertex. Theorem 5.1 applies so that

$$d \geq \mathrm{box}(G) \geq \frac{n}{2\,(n-\delta-1)},$$

where δ denotes the minimum degree in G. Since G is $(2, 3)$-agreeable, Lemma 4.1 yields

$$\omega(G) \geq n - \delta - 1.$$

Combining the two inequalities, we get

$$\rho(r, d) = \frac{\omega(G)}{n} \geq \frac{n-\delta-1}{n} \geq \frac{1}{2\,d}.$$

This completes the proof of the main theorem. □

6. Discussion

6.1. ***Ramsey numbers and agreement.*** Recall that the Ramsey number $R(k, m)$ is the smallest number such that any simple undirected graph G with $|V(G)| \geq R(k, m)$ contains either a clique of size at least k or an independent set of vertices

of size at least m. Ramsey numbers are notoriously difficult to study, and few precise results are known about them. Fortunately, one of the sharper known bounds applies directly to the study of $(2, 3)$-agreeable graphs.

Ajtai et al. [1980] (upper bound) and Kim [1995] (lower bound) proved the existence of positive constants c_1 and c_2 such that, for all $k \geq 2$,

$$c_1 \frac{k^2}{\log k} \leq R(k, 3) \leq c_2 \frac{k^2}{\log k}. \tag{3}$$

The connection to $(2, 3)$-agreeability is the following: recall that we denote by $\eta(r)$ the maximum number of vertices for a $(2, 3)$-agreeable graph with clique number r. Thus any graph G with $\eta(r)+1$ vertices either contains a clique of size $r+1$ or is not $(2, 3)$-agreeable, that is, $\overline{G}$ contains a triangle. It follows that we have, for all $r \geq 2$,

$$\eta(r) + 1 = R(r + 1, 3). \tag{4}$$

The quantity $r/\eta(r)$ is the minimum agreement proportion for $(2, 3)$-agreeable graphs G with $\omega(G) \leq r$. Since $\eta(r)$ can be expressed in terms of $R(r + 1, 3)$, Kim's lower bound allows us to conclude that the agreement proportion satisfies

$$\lim_{r\to\infty} \frac{r}{\eta(r)} = 0.$$

6.2. ***Agreement proportion and boxicity.*** The above argument indicates that, for any infinite family of $(2, 3)$-agreeable graphs that minimizes the agreement proportion, the boxicity must go to infinity, since Theorem 1.1 shows that the agreement proportion is bounded away from zero when the boxicity is bounded.

We do not know of any explicit version of this result. Constructing a family of $(2, 3)$-agreeable graphs whose agreement proportion goes to zero would be of great interest.

6.3. ***Asymptotics of $\eta(r)$ and*** **box**(G)**.** In Proposition 4.5 we showed that $\eta(r) \leq r(r + 3)/2$. Equation (4) shows that $\eta(r)$ follows an inequality similar to (3), and in particular, it does grow almost quadratically. We can use Theorem 1.1 to relate these estimates to the boxicity of the graphs: if G is a graph of boxicity at most d, with $\omega(G) = r$ and $|V(G)| = \eta(r)$, then we must have

$$d \geq \frac{\eta(r)}{2r} \geq c \frac{r}{\log r} \tag{5}$$

for some positive constant c. Having sharp bounds for the value of c could be of considerable practical interest.

6.4. ***Exposed boxes.*** Our work originally established weaker lower bounds by borrowing the exposed boxes techniques used by Eckhoff [1988]. These allowed us to

establish inequalities between face vectors of arrangements of d-boxes and $(d-1)$-boxes. The bounds were much weaker than Theorem 1.1 for $d \geq 4$, but these ideas might still produce interesting results for $(2, m)$-agreeability with $m \geq 4$.

Acknowledgements

This paper originated with a research project that took place during the 2008 Undergraduate Research Summer Institute at Vassar College, where the first two authors were students and the last author was a visiting professor. The authors are grateful to the Institute for its support, and extend special thanks to Professor Frank and her own URSI group for helping to foster a stimulating mathematical environment.

The software Mathematica and especially the Combinatorica package proved invaluable in the study of examples for this paper.

The authors are also thankful for the conscientious work of the anonymous referee, whose suggestions were instrumental in clarifying the exposition of some important points in the paper.

References

[Adiga et al. 2008] A. Adiga, L. S. Chandran, and N. Sivadasan, "Lower bounds for boxicity", Preprint, 2008. arXiv 0806.3175v1

[Ajtai et al. 1980] M. Ajtai, J. Komlós, and E. Szemerédi, "A note on Ramsey numbers", *J. Combin. Theory Ser. A* **29**:3 (1980), 354–360. MR 82a:05064 Zbl 0455.05045

[Berg et al. 2010] D. E. Berg, S. Norine, F. E. Su, R. Thomas, and P. Wollan, "Voting in agreeable societies", *Amer. Math. Monthly* **117**:1 (2010), 27–39.

[Booth and Lueker 1976] K. S. Booth and G. S. Lueker, "Testing for the consecutive ones property, interval graphs, and graph planarity using PQ-tree algorithms", *J. Comput. System Sci.* **13**:3 (1976), 335–379. MR 55 #6932 Zbl 0367.68034

[Cozzens and Roberts 1983] M. B. Cozzens and F. S. Roberts, "Computing the boxicity of a graph by covering its complement by cointerval graphs", *Discrete Appl. Math.* **6**:3 (1983), 217–228. Zbl 0524.05059

[Eckhoff 1988] J. Eckhoff, "Intersection properties of boxes. I. An upper-bound theorem", *Israel J. Math.* **62**:3 (1988), 283–301. MR 90a:52016

[Habib et al. 2000] M. Habib, R. McConnell, C. Paul, and L. Viennot, "Lex-BFS and partition refinement, with applications to transitive orientation, interval graph recognition and consecutive ones testing", *Theoret. Comput. Sci.* **234**:1-2 (2000), 59–84. MR 2000m:68131 Zbl 0945.68189

[Kalai 1984] G. Kalai, "Intersection patterns of convex sets", *Israel J. Math.* **48**:2-3 (1984), 161–174. MR 86c:52002 Zbl 0557.52005

[Kim 1995] J. H. Kim, "The Ramsey number $R(3, t)$ has order of magnitude $t^2/\log t$", *Random Structures Algorithms* **7**:3 (1995), 173–207. MR 96m:05140 Zbl 0832.05084

[Matoušek 2002] J. Matoušek, *Lectures on discrete geometry*, Springer, New York, 2002. Zbl 0999.52006

[Quest and Wegner 1990] M. Quest and G. Wegner, "Characterization of the graphs with boxicity ≤ 2", *Discrete Math.* **81**:2 (1990), 187–192. Zbl 0725.05070

[Roberts 1969] F. S. Roberts, "On the boxicity and cubicity of a graph", pp. 301–310 in *Recent progress in combinatorics: proceedings of the 3rd Waterloo Conference on Combinatorics* (Waterloo, ON, 1968), edited by W. T. Tutte, Academic Press, New York, 1969. MR 40 #5489 Zbl 0193.24301

[Trotter 1979] W. T. Trotter, Jr., "A characterization of Roberts' inequality for boxicity", *Discrete Math.* **28**:3 (1979), 303–313. MR 81a:05118

Received: 2009-08-25 Revised: 2010-01-27 Accepted: 2010-02-09

miabraha@gmail.com *Vassar College, Poughkeepsie, NY 12604, United States*

meg.lippincott@gmail.com *Vassar College, Poughkeepsie, NY 12604, United States*

thierry.zell@lr.edu *The Donald and Helen Schort School of Mathematics and Computing Sciences, Lenoir-Rhyne University, Hickory NC 28603, United States*
http://mat.lr.edu/faculty/zell

Nontrivial solutions to a checkerboard problem

Meaghan Heires, Ryan Jones, Futaba Okamoto,
Willem Renzema and Matthew Roberts

(Communicated by Ron Gould)

The squares of an $m \times n$ checkerboard are alternately colored black and red. It has been shown that for every pair m, n of positive integers, it is possible to place coins on some of the squares of the checkerboard (at most one coin per square) in such a way that for every two squares of the same color the numbers of coins on neighboring squares are of the same parity, while for every two squares of different colors the numbers of coins on neighboring squares are of opposite parity. All solutions to this problem have been what is referred to as trivial solutions, namely, for either black or red, no coins are placed on any square of that color. A nontrivial solution then requires at least one coin to be placed on a square of each color. For some pairs m, n of positive integers, however, nontrivial solutions do not exist. All pairs m, n of positive integers are determined for which there is a nontrivial solution.

1. Introduction

Suppose that the squares of an $m \times n$ checkerboard (m rows and n columns), where $1 \leq m \leq n$ and $n \geq 2$, are alternately colored black and red. Figure 1 shows a 4×5 checkerboard (where a shaded square represents a black square). Two squares are said to be *neighboring* if they belong to the same row or to the same column and there is no square between them. Thus every two neighboring squares are of different colors.

The checkerboard conjecture [Okamoto et al. 2010]. *For every pair m, n of positive integers, it is possible to place coins on some of the squares of an $m \times n$ checkerboard (at most one coin per square) in such a way that for every two squares of the same color the numbers of coins on neighboring squares are of the same parity, while for every two squares of different colors the numbers of coins on neighboring squares are of opposite parity.*

MSC2000: 05C15.
Keywords: $m \times n$ checkerboard, coin placement, trivial solution, nontrivial solution.

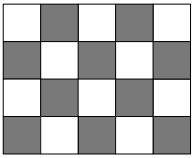

Figure 1. A 4×5 checkerboard.

Figure 2 shows a placement of 5 coins on the 4×5 checkerboard such that the number of coins on neighboring squares of every black square is even and the number of coins on neighboring squares of every red square is odd. Thus for every two squares of different colors, the numbers of coins on neighboring squares are of opposite parity. Consequently, the checkerboard conjecture is true for a 4×5 checkerboard. Observe that each of the five coins on the 4×5 checkerboard of Figure 2 is placed on a black square. Thus the number of coins on neighboring squares of each black square is 0, while the number of coins on neighboring squares of each red square is either 1 or 3. For a given checkerboard, if it is possible to place all coins on squares of one of the two colors, say black, in such a way that the number of coins on neighboring squares of a square is even if and only if that square is black; such a coin placement is called a *trivial solution*. Hence, the coin placement for the 4×5 checkerboard in Figure 2 is a trivial solution. In [Okamoto et al. $\geq$ 2010] it is shown that every $m \times n$ checkerboard has a trivial solution, through the analysis of a vertex coloring of graphs called the *modular coloring*.

The checkerboard theorem. *Every $m \times n$ checkerboard has a trivial solution.*

A *nontrivial solution* to the $m \times n$ checkerboard problem requires at least one coin to be placed on a square of each color. As we will see in this work, some $m \times n$ checkerboards have no nontrivial solution. For an $m \times n$ checkerboard C, we consider the following two related problems.

Problem 1.1. Place coins on some of the red squares of C (at most one coin per square) in such a way that the number of coins on neighboring squares of every black square is even.

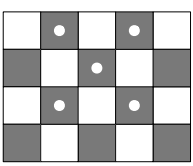

Figure 2. A trivial solution for a 4×5 checkerboard.

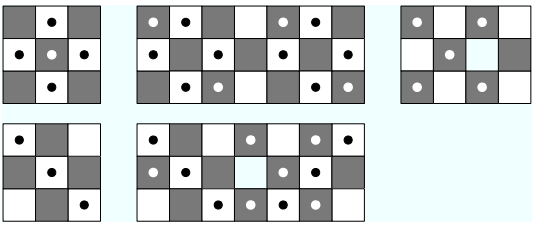

Figure 3. Some $3 \times n$ checkerboards for $n = 3, 4, 7$.

Problem 1.2. Place coins on some of the black squares of C (at most one coin per square) in such a way that the number of coins on neighboring squares of every red square is odd.

Note that in Problem 1.1 there is no restriction on whether or not there are coins on black squares, since coins on black squares do not affect the number of coins on neighboring squares of each black square. Similarly, in Problem 1.2 placing coins on red squares is allowed. Of course, every solution to Problem 1.2 must place at least one coin on a black square of C; while Problem 1.1 has a trivial solution of placing no coins at all on the red squares of C.

In Figure 3, the checkerboards of size 3×3 and 3×7 are shown with coins placed on some of the squares. Since both m and n are odd, every square on the four corners must be of the same color. Observe that the 3×3 checkerboard whose four corner squares are all black has a nontrivial solution to each of Problems 1.1 and 1.2, while the 3×3 checkerboard having four red corner squares has no solution to Problem 1.2. On the other hand, each of the two 3×7 checkerboards has a nontrivial solution to each of Problems 1.1 and 1.2 regardless of the color of the corner squares. As another example, consider the 3×4 checkerboard, which must have two black corner squares and two red corner squares. In this case, the only possible solution to Problem 1.1 is the trivial solution, while there is a solution to Problem 1.2 as shown in Figure 3.

Next consider a checkerboard of size $1 \times n$ with $n \geq 2$. The following is easy to verify.

Observation 1.3. *A $1 \times n$ checkerboard ($n \geq 2$) has a nontrivial solution to* Problem 1.1 *if and only if the two corner squares are both red. Also, there is a solution to* Problem 1.2 *if and only if $n \not\equiv 1 \pmod 4$ or at least one of the two corner squares is black.*

As a result, every $1 \times n$ checkerboard belongs to one of the three categories described in the next corollary.

Corollary 1.4. *For every integer $n \geq 2$, a $1 \times n$ checkerboard has a nontrivial solution to at least one of* Problems 1.1 *and* 1.2. *In particular*:

(A) *There is a nontrivial solution to each of* Problems 1.1 *and* 1.2 *if and only if* $n \equiv 3 \pmod 4$ *and the two corner squares are both red.*

(B) *There is a nontrivial solution to* Problem 1.1 *but not to* Problem 1.2 *if and only if* $n \equiv 1 \pmod 4$ *and the two corner squares are both red.*

(C) *There is a nontrivial solution to* Problem 1.2 *but not to* Problem 1.1 *if and only if at most one of the two corner squares is red.*

Let $\mathcal{C} = \mathcal{C}_R \cup \mathcal{C}_B$ be the set of $m \times n$ checkerboards with $mn \geq 2$, where $C \in \mathcal{C}_R$ if C contains a red corner square; while $C \in \mathcal{C}_B$ if C contains a black corner square. Hence, a checkerboard belongs to $\mathcal{C}_R \cap \mathcal{C}_B$ if and only if the number of squares is even. Our goal in this paper is to classify all checkerboards (size and color configuration) for which (A) there is a nontrivial solution to each of Problems 1.1 and 1.2; (B) there is a nontrivial solution to Problem 1.1 but not to Problem 1.2; (C) there is a nontrivial solution to Problem 1.2 but not to Problem 1.1; and (D) there is a nontrivial solution to neither Problem 1.1 nor Problem 1.2.

2. Even and odd extensions

Definitions and notation. Before considering checkerboards having multiple rows and multiple columns, we give additional definitions and notation. For an $m \times n$ checkerboard C, let $S = B \cup R$ be the set of mn squares in C, where B and R are the sets of black squares and red squares, respectively, and let $s_{i,j} \in S$ be the square in the i-th row and j-th column for $1 \leq i \leq m$ and $1 \leq j \leq n$.

We express a coin placement for C using a coin placement function $f : S \to \{0, 1\}$ defined by $f(s) = 1$ if and only if there is a coin placed on the square s. The corresponding *neighbor sum* of a square s, denoted by $\sigma_f(s)$ (or simply $\sigma(s)$), is the number of coins placed on the neighboring squares of s. For simplicity, we further assume that $\sigma(s)$ is expressed as one of 0 and 1 modulo 2.

An *even placement* f is a coin placement such that $f(s) = \sigma(s) = 0$ for every $s \in B$. Hence, a checkerboard C has a solution to Problem 1.1 if and only if C has an even placement. In particular, C has a nontrivial solution to Problem 1.1 if and only if C has a nontrivial even placement. An *odd placement* g is a coin placement such that $g(s) = 0$ and $\sigma(s) = 1$ for every $s \in R$. Then a checkerboard C has a solution to Problem 1.2 if and only if C has an odd placement. Recall that every solution to Problem 1.2 must place at least one coin on a black square, implying that there is no trivial odd placement.

To achieve the goal described in the first section, therefore, we investigate the conditions on the size and color configuration of checkerboards under which (A) there are a nontrivial even placement and an odd placement; (B) there is a nontrivial

even placement but no odd placement; (C) there is an odd placement but no nontrivial even placement; and (D) there is neither an odd placement nor a nontrivial even placement.

Let $S = S_1 \cup S_2 \cup \cdots \cup S_n$, where $S_j = \{s_{i,j} : 1 \le i \le m\}$ for $1 \le j \le n$. Hence, S_j is the set of the m squares in the j-th column. Further, let $S'_i = S_1 \cup S_2 \cup \cdots \cup S_i$ for $1 \le i \le n$. (Hence $S'_1 = S_1$ and $S'_n = S$.) Let $f_1 : S'_1 \to \{0, 1\}$ be an arbitrary coin placement for the squares in S'_1 such that $f_1(s) = 0$ for every $s \in B \cap S'_1$. Observe then that there exists a unique coin placement $f_2 : S'_2 \to \{0, 1\}$ such that $f_2(s) = 0$ for every $s \in B \cap S'_2$; f_2 restricted to S'_1 equals f_1; and $\sigma(s) = 0$ for every $s \in S'_1$. After finding such a coin placement f_2, observe further that there exists a unique coin placement $f_3 : S'_3 \to \{0, 1\}$ such that $f_3(s) = 0$ for every $s \in B \cap S'_3$; f_3 restricted to S'_2 equals f_2; and $\sigma(s) = 0$ for every $s \in S'_2$. In general, for every integer j $(1 \le j \le n-1)$, suppose that $f_j : S'_j \to \{0, 1\}$ is a coin placement such that $f_j(s) = 0$ for every $s \in B \cap S'_j$ and $\sigma(s) = 0$ for every $s \in S'_{j-1}$ (if $j \ge 2$). Then there exists a unique coin placement $f_{j+1} : S'_{j+1} \to \{0, 1\}$ such that $f_{j+1}(s) = 0$ for every $s \in B \cap S'_{j+1}$; f_{j+1} restricted to S'_j equals f_j; and $\sigma(s) = 0$ for every $s \in S'_j$.

Similarly, let $g_1 : S'_1 \to \{0, 1\}$ be an arbitrary coin placement for the squares of S'_1 such that $g_1(s) = 0$ for every $s \in R \cap S'_1$. Then there exists a unique coin placement $g_2 : S'_2 \to \{0, 1\}$ such that $g_2(s) = 0$ for every $s \in R \cap S'_2$; g_2 restricted to S'_1 equals g_1; and $\sigma(s) = 1$ for every $s \in R \cap S'_1$. In general, for every integer j $(1 \le j \le n-1)$, suppose that $g_j : S'_j \to \{0, 1\}$ is a coin placement such that $g_j(s) = 0$ for every $s \in R \cap S'_j$ and $\sigma(s) = 1$ for every $s \in R \cap S'_{j-1}$ (if $j \ge 2$). Then there exists a unique coin placement $g_{j+1} : S'_{j+1} \to \{0, 1\}$ such that $g_{j+1}(s) = 0$ for every $s \in R \cap S'_{j+1}$; g_{j+1} restricted to S'_j equals g_j; and $\sigma(s) = 1$ for every $s \in R \cap S'_j$.

These observations yield the following two lemmas.

Lemma 2.1. *For each coin placement $f_1 : S_1 \to \{0, 1\}$ such that $f_1(s) = 0$ for every $s \in B \cap S_1$, there exists a unique coin placement $F : S \to \{0, 1\}$ such that* (i) *$F(s) = 0$ for every $s \in B$,* (ii) *F restricted to S_1 equals f_1, and* (iii) *$\sigma(s) = 0$ for every $s \in S'_{n-1} (= S - S_n)$. Furthermore, F is nontrivial if and only if f_1 is nontrivial.*

Lemma 2.2. *For each coin placement $g_1 : S_1 \to \{0, 1\}$ such that $g_1(s) = 0$ for every $s \in R \cap S_1$, there exists a unique coin placement $G : S \to \{0, 1\}$ such that* (i) *$G(s) = 0$ for every $s \in R$,* (ii) *G restricted to S_1 equals g_1, and* (iii) *$\sigma(s) = 1$ for every $s \in R \cap S'_{n-1}$.*

For the coin placements f_1 and F for a checkerboard C described in Lemma 2.1, we say that F is the *even extension* of f_1; while for the coin placements g_1 and G of C described in Lemma 2.2, G is said to be the *odd extension* of g_1. We also say that F and G are the even and odd extensions for C, respectively.

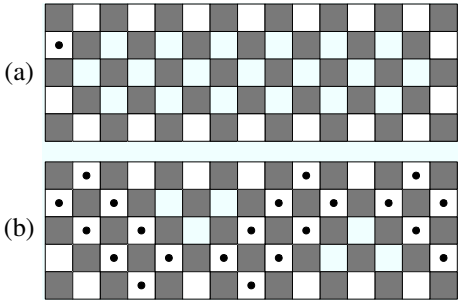

Figure 4. An even extension for a 5×15 checkerboard.

Properties of even extensions. Consider an $m \times n$ checkerboard, where n is sufficiently large. Let $f_1 : S_1 \to \{0, 1\}$ be an arbitrary coin placement such that $f_1(s) = 0$ for every $s \in B \cap S_1$. Obtain the unique even extension F of f_1. We will next show that $F(s) = 0$ for every $s \in S_j$ whenever $j \equiv 0 \pmod{m+1}$. Before we verify this, let us consider an example. In Figure 4(a), there is a 5×15 checkerboard in $\mathcal{C}_B - \mathcal{C}_R$ with coins placed on some of the red squares in S_1. Figure 4(b) shows its even extension and observe that there are no coins placed on the squares in $S_6 \cup S_{12}$.

Proposition 2.3. *For an $m \times n$ checkerboard with $2 \le m \le n$, let $f_1 : S_1 \to \{0, 1\}$ be an arbitrary coin placement with $f_1(s) = 0$ for every $s \in B \cap S_1$. Then for every $j \equiv 0 \pmod{m+1}$, the unique even extension of f_1 assigns 0 to every square in S_j.*

Proof. We begin by assuming that m is even. Furthermore, we may assume that $s_{1,1} \in R$. Therefore, $s_{i,j} \in R$ if and only if $i + j$ is even. Let $f_1 : S_1 \to \{0, 1\}$ be given by

$$f_1(s_{i,1}) = \begin{cases} a_{(i+1)/2} & \text{if } i \text{ is odd,} \\ 0 & \text{if } i \text{ is even,} \end{cases}$$

for $1 \le i \le m$. Furthermore, for each integer j $(1 \le j \le m/2)$ let $A_j = \sum_{i=1}^{j} a_i$ while $A_0 = 0$. Now define a coin placement $F_1 : S \to \{0, 1\}$ by $F_1(s) = 0$ if $s \in B$ and

$$F_1(s_{i,j}) = \begin{cases} A_{(i+j)/2} + A_{(i-j)/2} & \text{if } j \le i \text{ and } i + j \le m, \\ F_1(s_{(m+1)-j,(m+1)-i}) & \text{if } j \le i \text{ and } i + j \ge m + 2, \\ F_1(s_{j,i}) & \text{if } i + 2 \le j \le m, \\ 0 & \text{if } j = m + 1, \\ F_1(s_{(m+1)-i,j-(m+1)}) & \text{if } m + 2 \le j \le 2m + 2, \\ F_1(s_{i,j-(2m+2)}) & \text{if } j \ge 2m + 3, \end{cases}$$

if $s_{i,j} \in R$ (and so $i + j$ is even), where addition is performed modulo 2 except on the subscripts. Note that $F_1(s_{i,2m+2}) = F_1(s_{(m+1)-i,m+1}) = 0$ and so $F_1(s_{i,j}) = 0$

whenever $j \equiv 0 \pmod{m+1}$. Also, $F_1(s_{i,1}) = A_{(i+1)/2} + A_{(i-1)/2} = a_{(i+1)/2} = f_1(s_{i,1})$ for $i = 1, 3, \ldots, m-1$, so F_1 restricted to S_1 equals f_1.

We now show that F_1 is the even extension of f_1, that is, $F_1 = F$. To do this, we need only verify that $\sigma(s) = 0$ for every $s \in B \cap S'_{n-1}$. Hence, we show that $\sigma(s_{i,j}) = 0$ for integers i and j with $1 \le i \le m$ and $1 \le j \le n-1$ such that $i+j$ is odd. By symmetry, we may further suppose that either $1 \le j < i \le m$ or $j = m+1$.

***Case 1*: $1 \le j < i \le m$.** First suppose that $j = 1$. If $2 \le i \le m-2$, then

$$\begin{aligned}\sigma(s_{i,1}) &= F_1(s_{i,2}) + F_1(s_{i-1,1}) + F_1(s_{i+1,1}) \\ &= \left(A_{(i+2)/2} + A_{(i-2)/2}\right) + \left(A_{i/2} + A_{(i-2)/2}\right) + \left(A_{(i+2)/2} + A_{i/2}\right) = 0,\end{aligned}$$

while

$$\sigma(s_{m,1}) = F_1(s_{m,2}) + F_1(s_{m-1,1}) = F_1(s_{m-1,1}) + F_1(s_{m-1,1}) = 0.$$

Next suppose that $i = m$ and $3 \le j \le m-1$. Then

$$\begin{aligned}\sigma(s_{m,j}) &= F_1(s_{m,j-1}) + F_1(s_{m,j+1}) + F_1(s_{m-1,j}) \\ &= F_1(s_{m-j+2,1}) + F_1(s_{m-j,1}) + F_1(s_{m-j+1,2}) \\ &= (A_{(m-j+3)/2} + A_{(m-j+1)/2}) + (A_{(m-j+1)/2} + A_{(m-j-1)/2}) \\ &\qquad + (A_{(m-j+3)/2} + A_{(m-j-1)/2}) = 0.\end{aligned}$$

Hence, suppose next that $2 \le j < i \le m-1$. If $i + j \le m-1$, then

$$\begin{aligned}\sigma(s_{i,j}) &= F_1(s_{i,j-1}) + F_1(s_{i,j+1}) + F_1(s_{i-1,j}) + F_1(s_{i+1,j}) \\ &= (A_{(i+j-1)/2} + A_{(i-j+1)/2}) + (A_{(i+j+1)/2} + A_{(i-j-1)/2}) \\ &\quad + (A_{(i+j-1)/2} + A_{(i-j-1)/2}) + (A_{(i+j+1)/2} + A_{(i-j+1)/2}) = 0.\end{aligned}$$

For $i + j = m+1$,

$$\begin{aligned}\sigma(s_{i,j}) &= F_1(s_{i,j-1}) + F_1(s_{i,j+1}) + F_1(s_{i-1,j}) + F_1(s_{i+1,j}) \\ &= F_1(s_{i,j-1}) + F_1(s_{m-j,m-i+1}) + F_1(s_{i-1,j}) + F_1(s_{m-j+1,m-i}) \\ &= (A_{m/2} + A_{(i-j+1)/2}) + (A_{m/2} + A_{(i-j-1)/2}) \\ &\qquad + (A_{m/2} + A_{(i-j-1)/2}) + (A_{m/2} + A_{(i-j+1)/2}) = 0.\end{aligned}$$

Similarly, if $i + j \ge m+3$, then

$$\begin{aligned}\sigma(s_{i,j}) &= F_1(s_{i,j-1}) + F_1(s_{i,j+1}) + F_1(s_{i-1,j}) + F_1(s_{i+1,j}) \\ &= F_1(s_{m-j+2,m-i+1}) + F_1(s_{m-j,m-i+1}) + F_1(s_{m-j+1,m-i+2}) + F_1(s_{m-j+1,m-i}) \\ &= (A_{(2m-i-j+3)/2} + A_{(i-j+1)/2}) + (A_{(2m-i-j+1)/2} + A_{(i-j-1)/2}) \\ &\quad + (A_{(2m-i-j+3)/2} + A_{(i-j-1)/2}) + (A_{(2m-i-j+1)/2} + A_{(i-j+1)/2}) = 0.\end{aligned}$$

***Case 2*: $j = m+1$.** Then i is even and $2 \le i \le m$. If $2 \le i \le m-2$, then

$$\begin{aligned}\sigma(s_{i,m+1}) &= F_1(s_{i,m}) + F_1(s_{i,m+2}) + F_1(s_{i-1,m+1}) + F_1(s_{i+1,m+1}) \\ &= F_1(s_{m,i}) + F_1(s_{m-i+1,1}) + 0 + 0 \\ &= F_1(s_{m-i+1,1}) + F_1(s_{m-i+1,1}) = 0.\end{aligned}$$

Finally,

$$\begin{aligned}\sigma(s_{m,m+1}) &= F_1(s_{m,m}) + F_1(s_{m,m+2}) + F_1(s_{m-1,m+1}) \\ &= F_1(s_{1,1}) + F_1(s_{1,1}) + 0 = 0.\end{aligned}$$

Therefore, F_1 is the even extension of f_1 as claimed.

Next we assume that m is odd. If $\{s_{1,1}, s_{m,1}\} \subseteq R$, then let $f_1 : S_1 \to \{0,1\}$ be given by

$$f_1(s_{i,1}) = \begin{cases} a_{(i+1)/2} & \text{if } i \text{ is odd,} \\ 0 & \text{if } i \text{ is even,} \end{cases}$$

for $1 \le i \le m$. For each integer j $(1 \le j \le (m+1)/2)$ let $A_j = \sum_{i=1}^{j} a_i$, while $A_0 = 0$. Then define a coin placement $F_2 : S \to \{0,1\}$ by $F_2(s) = 0$ if $s \in B$ and

$$F_2(s_{i,j}) = \begin{cases} A_{(i+j)/2} + A_{(i-j)/2} & \text{if } j \le i \text{ and } i+j \le m+1, \\ F_2(s_{(m+1)-j,(m+1)-i}) & \text{if } j \le i \text{ and } i+j \ge m+3, \\ F_2(s_{j,i}) & \text{if } i+2 \le j \le m, \\ 0 & \text{if } j = m+1, \\ F_2(s_{(m+1)-i,j-(m+1)}) & \text{if } m+2 \le j \le 2m+2, \\ F_2(s_{i,j-(2m+2)}) & \text{if } j \ge 2m+3, \end{cases}$$

if $s_{i,j} \in R$ (and so $i+j$ is even), where addition is performed modulo 2 except on the subscripts. Then it can be verified that $F_2 = F$ in a manner similar to that used to show that $F_1 = F$ when m is even.

Similarly, if $\{s_{1,1}, s_{m,1}\} \subseteq B$, then let $f_1 : S_1 \to \{0,1\}$ be given by

$$f_1(s_{i,1}) = \begin{cases} a_{i/2} & \text{if } i \text{ is even,} \\ 0 & \text{if } i \text{ is odd,} \end{cases}$$

for $1 \le i \le m$. For each integer j $(1 \le j \le (m-1)/2)$ let $A_j = \sum_{i=1}^{j} a_i$ while $A_0 = 0$. Then define a coin placement $F_3 : S \to \{0,1\}$ by $F_3(s) = 0$ if $s \in B$ and

$$F_3(s_{i,j}) = \begin{cases} A_{(i+j-1)/2} + A_{(i-j-1)/2} & \text{if } j \le i-1 \text{ and } i+j \le m, \\ F_3(s_{(m+1)-j,(m+1)-i}) & \text{if } j \le i-1 \text{ and } i+j \ge m+2, \\ F_3(s_{j,i}) & \text{if } i+1 \le j \le m, \\ 0 & \text{if } j = m+1, \\ F_3(s_{(m+1)-i,j-(m+1)}) & \text{if } m+2 \le j \le 2m+2, \\ F_3(s_{i,j-(2m+2)}) & \text{if } j \ge 2m+3, \end{cases}$$

if $s_{i,j} \in R$ (and so $i + j$ is odd), where addition is performed modulo 2 except on the subscripts. Then again it can be verified that $F_3 = F$. □

Properties of odd extensions. Next we present some properties of odd extensions. Again consider an $m \times n$ checkerboard, where n is sufficiently large, and let $g_1 : S_1 \to \{0, 1\}$ be an arbitrary coin placement such that $g_1(s) = 0$ for every $s \in R \cap S_1$. Obtain the unique odd extension G of g_1. It turns out that the behavior of odd extensions can be sometimes different from that of even extensions, depending on the size and color configuration of checkerboards. Before continuing our discussion, we first define a special odd extension.

Definition 2.4. For the trivial coin placement $g_1 : S_1 \to \{0, 1\}$, its unique odd extension is called the trivial odd extension and denoted by G_0.

See Figure 5 for examples of the trivial odd extensions. We state the following observation without a proof.

Observation 2.5. *If G_0 is the trivial odd extension for an $m \times n$ checkerboard, then $G_0(s) = 0$ for every $s \in S_j$, where $j \equiv 0 \pmod{2m+2}$. Furthermore, if $j \equiv m+1 \pmod{2m+2}$, then* (i) *$G_0(s) = 0$ for every $s \in S_j$ if $\{s_{1,1}, s_{m,1}\} \not\subseteq R$, while* (ii) *$G_0(s) = 1$ for every $s \in B \cap S_j$ if $\{s_{1,1}, s_{m,1}\} \subseteq R$.*

In fact, *every* odd extension has the property described in Observation 2.5, as shown in the next result.

Proposition 2.6. *For an $m \times n$ checkerboard with $2 \le m \le n$, let $g_1 : S_1 \to \{0, 1\}$ be an arbitrary coin placement with $g_1(s) = 0$ for every $s \in R \cap S_1$. Then for every $j \equiv 0 \pmod{2m+2}$, the unique odd extension G of g_1 assigns 0 to every square in S_j. Furthermore, if $j \equiv m+1 \pmod{2m+2}$, then* (i) *$G(s) = 0$ for every $s \in S_j$ if $\{s_{1,1}, s_{m,1}\} \not\subseteq R$, while* (ii) *$G(s) = 1$ for every $s \in B \cap S_j$ if $\{s_{1,1}, s_{m,1}\} \subseteq R$.*

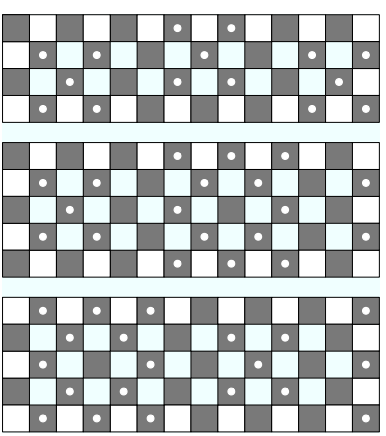

Figure 5. Trivial odd extensions.

Proof. First suppose that m is even. We may assume that $s_{1,1} \in B$. Therefore, $s_{i,j} \in B$ if and only if $i + j$ is even. Let $g_1 : S_1 \to \{0, 1\}$ be given by

$$g_1(s_{i,1}) = \begin{cases} a_{(i+1)/2} & \text{if } i \text{ is odd,} \\ 0 & \text{if } i \text{ is even,} \end{cases}$$

for $1 \le i \le m$. Also, for each integer j $(1 \le j \le m/2)$ let $A_j = \sum_{i=1}^{j} a_i$ while $A_0 = 0$. Then define the coin placement $G_1 : S \to \{0, 1\}$ by $G_1 = F_1 + G_0$, where F_1 is the even extension defined in the proof of Proposition 2.3 and G_0 is the trivial odd extension. (See Figure 6 for an example.)

If m is odd and $\{s_{1,1}, s_{m,1}\} \subseteq B$, then let $g_1 : S_1 \to \{0, 1\}$ be given by

$$g_1(s_{i,1}) = \begin{cases} a_{(i+1)/2} & \text{if } i \text{ is odd,} \\ 0 & \text{if } i \text{ is even,} \end{cases}$$

for $1 \le i \le m$. For each integer j $(1 \le j \le (m+1)/2)$ let $A_j = \sum_{i=1}^{j} a_i$ while $A_0 = 0$. Then let $G_2 : S \to \{0, 1\}$ be a coin placement such that $G_2 = F_2 + G_0$, where F_2 is the even extension defined in the proof of Proposition 2.3.

Finally, if m is odd and $\{s_{1,1}, s_{m,1}\} \subseteq R$, then let $g_1 : S_1 \to \{0, 1\}$ be given by

$$g_1(s_{i,1}) = \begin{cases} a_{i/2} & \text{if } i \text{ is even,} \\ 0 & \text{if } i \text{ is odd,} \end{cases}$$

for $1 \le i \le m$. For each integer j $(1 \le j \le (m-1)/2)$ let $A_j = \sum_{i=1}^{j} a_i$ while $A_0 = 0$. Then consider the coin placement $G_3 = F_3 + G_0$, where again F_3 is the even extension defined in the proof of Proposition 2.3.

Observe that G_1, G_2, and G_3 are the odd extensions of g_1 depending on the parity of m and color configuration of the checkerboard. Furthermore, each G_i $(1 \le i \le 3)$ has the desired properties by Proposition 2.3 and Observation 2.5. □

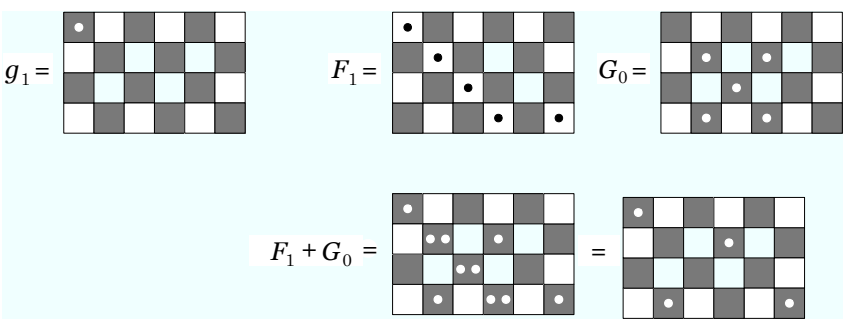

Figure 6. Illustrating F_1, G_0, and $G_1 = F_1 + G_0$.

3. Extensions and reductions of checkerboards

In this section we explore possibilities of obtaining an even (odd) placement for a checkerboard of a certain size and color configuration from an even (odd) placement for another checkerboard of a different size and color configuration.

For example, a 5×8 checkerboard with an even placement is shown in Figure 7(a). Extending this coin placement, we are able to obtain an even placement for a 5×11 checkerboard as well as an even placement for an 8×11 checkerboard, as shown in Figure 7(b). Therefore, the even placement for the 5×8 checkerboard in Figure 7(a) can be *extended* to even placements for a 5×11 checkerboard and an 8×11 checkerboard. On the other hand, we may also say that the even placement for the 5×11 checkerboard shown in Figure 7(b) can be *reduced* to an even placement for a 5×8 checkerboard.

The following observation describes a fact on this process of extending and reducing even (odd) placements. Recall that if f is an even placement for an $m \times n$ checkerboard, then $\sigma_f(s) = 0$ for every $s \in B$; while if F is an even extension for an $m \times n$ checkerboard, then $\sigma_F(s) = 0$ for every $s \in B$ except possibly for those in $B \cap S_n$. Similarly, if g is an odd placement for an $m \times n$ checkerboard, then $\sigma_g(s) = 1$ for every $s \in R$; while if G is an odd extension for an $m \times n$ checkerboard, then $\sigma_G(s) = 1$ for every $s \in R$ except possibly for those in $R \cap S_n$.

Observation 3.1. *Suppose that ℓ, m, and n are positive integers such that $m \leq n$ and $\ell < n$. Then there exists an even (odd) placement for an $m \times \ell$ checkerboard in $\mathcal{C}_R$ if and only if there exists an even (odd) extension F for an $m \times n$ checkerboard in $\mathcal{C}_R$ such that $F(s) = 0$ for every $s \in S_{\ell+1}$. Similarly, there exists an even (odd) placement for an $m \times \ell$ checkerboard in $\mathcal{C}_B$ if and only if there exists an even (odd) extension F for an $m \times n$ checkerboard in $\mathcal{C}_B$ such that $F(s) = 0$ for every $s \in S_{\ell+1}$.*

As a consequence of Propositions 2.3 and 2.6 and Observation 3.1, we obtain a result for $m \times m$ checkerboards.

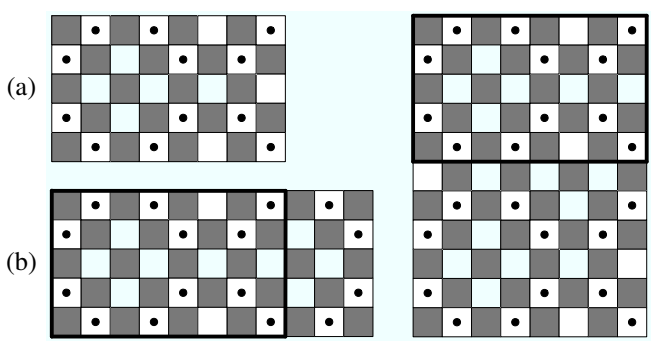

Figure 7. Examples of extension and reduction of checkerboards.

Corollary 3.2. *For every integer $m \geq 2$, an $m \times m$ checkerboard C has a nontrivial even placement. Furthermore, C has an odd placement if and only if $C \in \mathcal{C}_B$.*

In the following subsections we discuss in more detail a way to extend or to reduce a given even (odd) placement for a checkerboard to obtain even (odd) placements for checkerboards of different sizes and color configurations.

Determining the existence of even placements. By Observation 3.1, we take a closer look at the even extensions for checkerboards. Recall the construction of an even extension $F \in \{F_1, F_2, F_3\}$ described in Proposition 2.3. We make the following observation on F.

Observation 3.3. *Let F be an even extension for an $m \times n$ checkerboard with $2 \leq m \leq n$.*

(a) *Suppose that $F(s) = 0$ for every $s \in S_k$ for some k. Then $F(s) = 0$ for every $s \in S_\ell$ whenever $\ell \equiv \pm k \pmod{m+1}$. Also, $F(s) = 0$ for every $s \in S_\ell$ whenever ℓ is a multiple of k.*

(b) *Suppose that $F(s) = 1$ for some $s \in S_k$ for some k. Then $F(s) = 1$ for some $s \in S_\ell$ whenever $\ell \equiv \pm k \pmod{m+1}$. In particular, if F is nontrivial, then $F(s) = 1$ for some $s \in S_\ell$ whenever $\ell \equiv \pm 1 \pmod{m+1}$.*

The following is a consequence of Observations 3.1 and 3.3 and Corollary 3.2.

Corollary 3.4. *Let C be an $m \times n$ checkerboard with $1 \leq m \leq n$ and $n \geq 2$.*

(a) *If $n \equiv m \pmod{m+1}$, then C has a nontrivial even placement.*

(b) *Suppose that ℓ is a positive integer with $\ell \equiv n \pmod{\ell+1}$. If there exists an $\ell \times m$ checkerboard C' such that either $\{C, C'\} \subseteq \mathcal{C}_R$ or $\{C, C'\} \subseteq \mathcal{C}_B$ and there exists a nontrivial even placement for C', then there exists a nontrivial even placement for C.*

(c) *If $n \equiv 0 \pmod{m+1}$ or $n \equiv m-1 \pmod{m+1}$, then C has no nontrivial even placement.*

We are now prepared to present a complete result on even placements.

Theorem 3.5. *Let C be an $m \times n$ checkerboard with $1 \leq m \leq n$ and $n \geq 2$. Then C has a nontrivial even placement if and only if either* (i) *$m \equiv n \equiv \ell \pmod{\ell+1}$ for some integer $\ell \geq 2$, or* (ii) *$C \in \mathcal{C}_R - \mathcal{C}_B$.*

Proof. We may assume that $m \geq 2$ since the result holds for $m = 1$ by Corollary 1.4. If (i) occurs, then first suppose that $C \in \mathcal{C}_R$ and consider an $\ell \times \ell$ checkerboard $C' \in \mathcal{C}_R$. By Corollary 3.2, there exists a nontrivial even placement for C'. Then by Corollary 3.4(a) there exists a nontrivial even placement for an $\ell \times m$ checkerboard $C'' \in \mathcal{C}_R$, which in turn implies that there exists a nontrivial even placement for C by Corollary 3.4(b). Observe also that the same argument holds if $C \in \mathcal{C}_B$. If (ii)

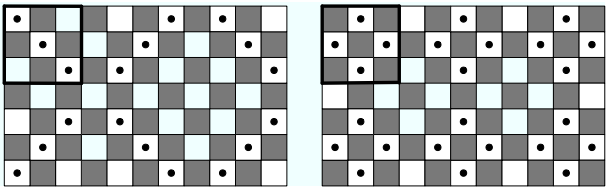

Figure 8. Two 7×11 checkerboards.

occurs, then observe that the coin placement $f : S \to \{0, 1\}$ defined by $f(s_{i,j}) = 1$ if and only if both i and j are odd is an even placement for C.

For the converse, assume, to the contrary, that there exists an $m \times n$ checkerboard in $\mathcal{C}_B$ having a nontrivial even placement with no integer $\ell \geq 2$ such that $m \equiv n \equiv \ell \pmod{\ell + 1}$. In particular, $n \not\equiv m \pmod{m + 1}$. Suppose that C is such a checkerboard with the smallest number of squares. Since $C \in \mathcal{C}_B$, we may assume that $s_{1,n} \in B$. Let f be a nontrivial even placement for C. Hence, $n \not\equiv 0, m - 1 \pmod{m + 1}$ by Corollary 3.4(c). This implies that there exists an integer k with $1 \leq k \leq m-2$ such that $n \equiv k \pmod{m+1}$. However then, f restricted to $S - S'_{n-k}$ induces an even placement for an $k \times m$ checkerboard belonging to $\mathcal{C}_B$, which is impossible since $km < mn$. □

Figure 8 shows even placements for the two 7×11 checkerboards. Note that $7 \equiv 11 \equiv 3 \pmod 4$, so we use an even placement for a 3×3 checkerboard as a building block.

Determining the existence of odd placements for checkerboards in $\mathcal{C}_B$. We now show that every checkerboard in $\mathcal{C}_B$ has an odd placement. We start with:

Proposition 3.6. *An $m \times \ell$ checkerboard in $\mathcal{C}_B$, where $\ell \in \{1, m, m \pm 1\}$, has an odd placement.*

Proof. Since the result holds for $\ell \in \{1, m\}$ by Corollaries 1.4 and 3.2, we first assume that $\ell = m - 1$. Let C be an $m \times m$ checkerboard, where $s_{1,1} \in B$. If m is odd, then the trivial odd extension assigns 0 to every $s \in S_m$. If m is even, then define $g_1 : S_1 \to \{0, 1\}$ by $g_1(s) = 0$ if and only if $s \in R \cap S_1$ and observe that the odd extension of g_1 assigns 0 to every $s \in S_m$. Therefore, an $m \times (m - 1)$ checkerboard in $\mathcal{C}_B$ has an odd placement by Observation 3.1. This also implies that an $m \times (m + 1)$ checkerboard in $\mathcal{C}_B$ has an odd placement. □

Let us also recall the construction of an odd extension $G \in \{G_1, G_2\}$ for checkerboards in $\mathcal{C}_B$ described in Proposition 2.6. We saw that $G(s) = 0$ for every $s \in S_j$ whenever $j \equiv 0 \pmod{m + 1}$. This together with Observation 3.1 leads to:

Proposition 3.7. *Let ℓ, m, and n be integers with $1 \leq \ell \leq m + 1$ and $n \equiv \ell \pmod{m + 1}$. If an $m \times n$ checkerboard in $\mathcal{C}_B$ has an odd placement, then so does*

an $m \times \ell$ checkerboard in $\mathscr{C}_B$. Conversely, if an $m \times \ell$ checkerboard in $\mathscr{C}_B$ has an odd placement, then so does an $m \times n$ checkerboard in $\mathscr{C}_B$.

Proof. First suppose that g is an odd placement for an $m \times n$ checkerboard with $s_{1,n} \in B$. Then $g(s) = 0$ for every $s \in S_j$ whenever $j \equiv 0 \pmod{m+1}$ by Proposition 2.6. This implies that g restricted to the set $S - S'_{n-\ell}$ induces an odd placement for an $m \times \ell$ checkerboard in $\mathscr{C}_B$.

Conversely, suppose that g is an odd placement for an $m \times \ell$ checkerboard with $s_{1,\ell} \in B$. Then extending g to the right, we obtain an odd placement for an $m \times n$ checkerboard C. Furthermore, at least one of $s_{1,n}$ and $s_{m,n}$ belongs to B. Therefore, $C \in \mathscr{C}_B$. □

We state the following as a corollary of Propositions 3.6 and 3.7.

Corollary 3.8. *Let C be an $m \times n$ checkerboard in $\mathscr{C}_B$. If $n \equiv \ell \pmod{m+1}$, where $\ell \in \{1, m, m+1\}$, then C has an odd placement.*

We are now prepared to show that every checkerboard in $\mathscr{C}_B$ has an odd placement. We first introduce the following algorithm that allows us to obtain a sequence $X = \langle \ell_0, \ell_1, \ldots, \ell_k \rangle$ of positive integers for each $m \times n$ checkerboard $(2 \le m < n)$ in $\mathscr{C}_B$, where $\ell_0 = n$ and $\ell_1 = m$. For a sequence X, we denote the sequence X followed by ℓ by $\langle X, \ell \rangle$.

Algorithm 3.9.

Input: Two integers m and n with $2 \le m < n$.

Output: A sequence $X = \langle \ell_0, \ell_1, \ldots, \ell_k \rangle$ of positive integers with $\ell_0 = n$ and $\ell_1 = m$.

Step 1. Let $\ell_0 \leftarrow n$, $\ell_1 \leftarrow m$, and $X_1 \leftarrow \langle \ell_0, \ell_1 \rangle$. Let $i \leftarrow 1$.

Step 2. Let ℓ_{i+1} be the integer with $1 \le \ell_{i+1} \le \ell_i + 1$ such that

$$\ell_{i+1} \equiv \ell_{i-1} \pmod{\ell_i + 1}.$$

Step 3. If $\ell_{i+1} \in \{1, \ell_i, \ell_i \pm 1\}$, then go to Step 4. Otherwise, let $i \leftarrow i + 1$ and $X_i \leftarrow \langle X_{i-1}, \ell_i \rangle$. Return to Step 2.

Step 4. Output $X = \langle X_i, \ell_{i+1} \rangle$.

As an example, consider a 12×23 checkerboard in $C \in \mathscr{C}_B$. Then $X = \langle 23, 12, 10, 1 \rangle$. Let C_1, C_2, and C_3 be checkerboards in $\mathscr{C}_B$, whose sizes are 1×10, 10×12, and 12×23, respectively. We saw that C_1 has an odd placement by Corollary 3.8 (or by Corollary 1.4). Then by Proposition 3.7, so does C_2, which in turn implies that so does $C_3 = C$. We illustrate how we obtain an odd placement for each of C_1, C_2, and C_3 in Figure 9.

We have proved the result for checkerboards having some black corner squares:

Theorem 3.10. *Every checkerboard in $\mathscr{C}_B$ has an odd placement.*

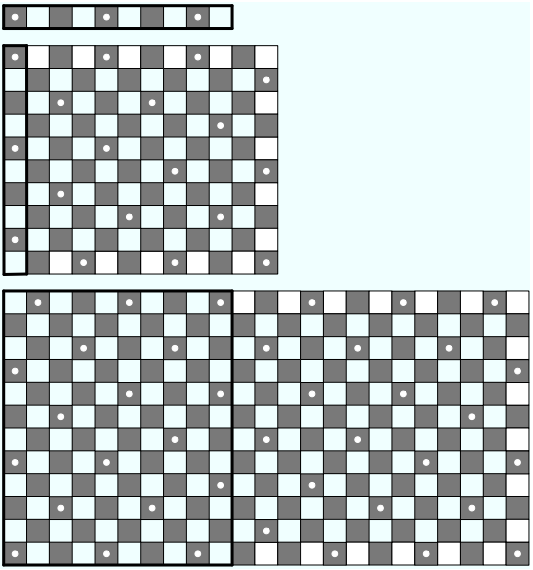

Figure 9. Obtaining odd placements for C_1, C_2, and C_3.

Determining the existence of odd placements for checkerboards in $\mathcal{C}_R - \mathcal{C}_B$. Finally, we consider those checkerboards in $\mathcal{C}_R - \mathcal{C}_B$, whose corner squares are all red. Note that if C is an $m \times n$ checkerboard in $\mathcal{C}_R - \mathcal{C}_B$, then both m and n are odd. We have seen in Figure 3 that the 3×7 checkerboard in $\mathcal{C}_R - \mathcal{C}_B$ has an odd placement while the 3×3 checkerboard in $\mathcal{C}_R - \mathcal{C}_B$ does not. Hence, our goal here is to characterize the checkerboards in $\mathcal{C}_R - \mathcal{C}_B$ for which there are odd placements.

Recall the construction of the odd extension G_3 described in Proposition 2.6. We saw that

$$G(s) = 0 \text{ for every } s \in S_j \quad \text{whenever } j \equiv 0 \pmod{2m+2}. \tag{1}$$

As a consequence of (1) with Observation 3.1, we state the following. Note also that the result holds for $m = 1$ by Corollary 1.4.

Corollary 3.11. *An $m \times (2m+1)$ checkerboard in $\mathcal{C}_R - \mathcal{C}_B$ has an odd placement for every $m \geq 1$.*

Here is another useful fact.

Proposition 3.12. *Let ℓ and m be odd integers with $m \geq 3$ and $1 \leq \ell \leq 2m-1$. Then an $m \times \ell$ checkerboard in $\mathcal{C}_R - \mathcal{C}_B$ has an odd placement if and only if an $m \times (2m-\ell)$ checkerboard in $\mathcal{C}_R - \mathcal{C}_B$ has an odd placement.*

Proof. Let C be an $m \times \ell$ checkerboard in $\mathcal{C}_R - \mathcal{C}_B$ and let g be an odd placement for C. Let G be the odd extension of g for an $m \times (2m+3)$ checkerboard in $\mathcal{C}_R - \mathcal{C}_B$ and observe that $\{s_{1,\ell+2}, s_{m,\ell+2}, s_{1,2m+1}, s_{m,2m+1}\} \subseteq R$. By Proposition 2.6 and Observation 3.1, $G(s) = 0$ for every $s \in S_{\ell+1} \cup S_{2m+2}$. This implies that G restricted to the set $S'_{2m+1} - S'_{\ell+1}$ induces an odd placement for an $m \times (2m-\ell)$ checkerboard in $\mathcal{C}_R - \mathcal{C}_B$. The converse can be verified in the same manner. □

The following is another consequence of (1) and Observation 3.1, stated without a proof since it will be almost identical to that of Proposition 3.7.

Proposition 3.13. *Let ℓ, m, and n be odd integers with $1 \le \ell \le 2m+1$ and $n \equiv \ell \pmod{2m+2}$. Then an $m \times n$ checkerboard in $\mathcal{C}_R - \mathcal{C}_B$ has an odd placement if and only if an $\ell \times m$ checkerboard in $\mathcal{C}_R - \mathcal{C}_B$ has an odd placement.*

By Proposition 3.13 with Corollaries 3.2 and 3.11, we have the following. Note again that the result holds for $m = 1$ as well.

Corollary 3.14. *Let C be an $m \times n$ checkerboard in $\mathcal{C}_R - \mathcal{C}_B$.*

(a) *If $n \equiv 2m+1 \pmod{2m+2}$, then C has an odd placement.*

(b) *If $n \equiv m \pmod{2m+2}$, then C does not have an odd placement.*

We now present an algorithm that finds a sequence Y of positive integers for each $m \times n$ checkerboard C in $\mathcal{C}_R - \mathcal{C}_B$, where m and n are positive odd integers with $m \le n$. We then use Y to determine whether or not C has an odd placement.

Algorithm 3.15.

Input: Two odd integers m and n with $1 \le m \le n$ and $n \ge 3$.

Output: A sequence $Y = \langle \ell_0, \ell_1, \ldots, \ell_k \rangle$ of positive integers with $\ell_0 = n$ and $\ell_1 = m$.

Step 1. Let $\ell_0 \leftarrow n$, $\ell_1 \leftarrow m$, and $Y_1 = \langle \ell_0, \ell_1 \rangle$. Let $i \leftarrow 1$.

Step 2. Let ℓ'_{i+1} be the odd integer with $1 \le \ell'_{i+1} \le 2\ell_i + 1$ such that $\ell'_{i+1} \equiv \ell_{i-1} \pmod{2\ell_i + 2}$.

Step 3. If $\ell'_{i+1} \in \{\ell_i, 2\ell_i + 1\}$, then let $\ell_{i+1} = \ell'_{i+1}$ and go to Step 4. Otherwise, let ℓ_{i+1} be the odd integer with $1 \le \ell_{i+1} \le \ell_i - 2$ such that either $\ell_{i+1} \equiv \ell'_{i+1} \pmod{2\ell_i}$ or $\ell_{i+1} \equiv -\ell'_{i+1} \pmod{2\ell_i}$. Let $i \leftarrow i+1$ and $Y_i \leftarrow \langle Y_{i-1}, \ell_i \rangle$. Return to Step 2.

Step 4. Output $Y = \langle Y_i, \ell_{i+1} \rangle$.

We present the result on odd placements for checkerboards in $\mathcal{C}_R - \mathcal{C}_B$ as a consequence of Propositions 3.12 and 3.13 and Corollary 3.14.

Theorem 3.16. *Let $C \in \mathcal{C}_R - \mathcal{C}_B$ and obtain the sequence $Y = \langle \ell_0, \ell_1, \ldots, \ell_k \rangle$ for C. Then C has an odd placement if and only if $\ell_{k-1} \neq \ell_k$.*

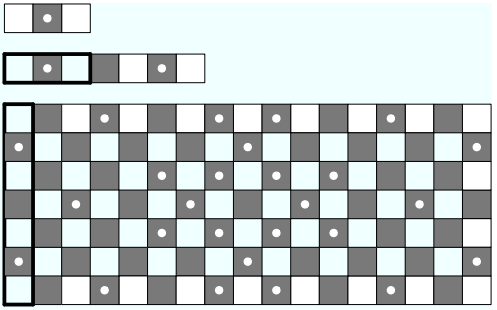

Figure 10. An odd placement for the 7×17 checkerboard in $\mathcal{C}_R - \mathcal{C}_B$.

For example, the 1×9 checkerboard in $\mathcal{C}_R - \mathcal{C}_B$ has no odd placement, as verified in Corollary 1.4, since $Y = \langle 9, 1, 1 \rangle$. Also, the 5×29 checkerboard in $\mathcal{C}_R - \mathcal{C}_B$ has no odd placement since $Y = \langle 29, 5, 5 \rangle$.

On the other hand, the 7×17 checkerboard in $\mathcal{C}_R - \mathcal{C}_B$, whose associated sequence is $Y = \langle 17, 7, 1, 3 \rangle$, has an odd placement. To actually build an odd placement using Y, we start with the 1×3 checkerboard C_1 in $\mathcal{C}_R - \mathcal{C}_B$ with an odd placement g_1. (Note also that this is the unique odd placement for C_1.) Since $7 \equiv 3 \pmod{(2 \cdot 1 + 2)}$, obtain an odd placement g_2 for the 1×7 checkerboard in $\mathcal{C}_R - \mathcal{C}_B$ by extending g_1. Since $17 \equiv 1 \pmod{(2 \cdot 7 + 2)}$, we can extend g_2 to obtain an odd placement for the 7×17 checkerboard in $\mathcal{C}_R - \mathcal{C}_B$, as shown in Figure 10.

As another example, let us consider the 7×21 checkerboard in $\mathcal{C}_R - \mathcal{C}_B$. Then $Y = \langle 21, 7, 5, 3, 1, 3 \rangle$. We again start with the 1×3 checkerboard C_1 in $\mathcal{C}_R - \mathcal{C}_B$ with the unique odd placement g_1 for C_1. Since $5 \equiv -1 \pmod{(2 \cdot 3)}$, we can obtain an odd placement g_2 for the 3×5 checkerboard in $\mathcal{C}_R - \mathcal{C}_B$ from the odd placement for the $3 \times (2 \cdot 3 + 1)$ checkerboard in $\mathcal{C}_R - \mathcal{C}_B$ obtained by extending g_1 (see Figure 11 on the next page). Similarly, since $7 \equiv -3 \pmod{(2 \cdot 5)}$, obtain an odd placement g_3 for the 5×7 checkerboard in $\mathcal{C}_R - \mathcal{C}_B$ from the odd placement for the $5 \times (2 \cdot 5 + 1)$ checkerboard in $\mathcal{C}_R - \mathcal{C}_B$ obtained by extending g_2 (again see Figure 11). Finally, since $21 \equiv 5 \pmod{(2 \cdot 7 + 2)}$, we obtain an odd placement for the 7×21 checkerboard in $\mathcal{C}_R - \mathcal{C}_B$ by simply extending g_3.

4. Conclusion

The following two theorems summarize the results obtained in the previous sections.

Theorem 4.1. *Every checkerboard in $\mathcal{C}$ has a nontrivial solution to at least one of* Problems 1.1 *and* 1.2.

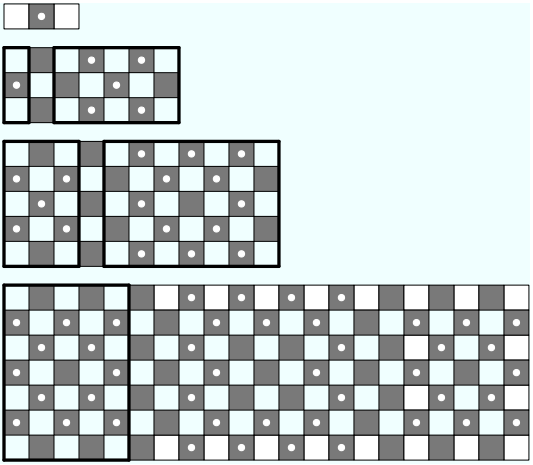

Figure 11. An odd placement for the 7×21 checkerboard in $\mathcal{C}_R - \mathcal{C}_B$.

Proof. If $C \in \mathcal{C}_R - \mathcal{C}_B$, then C has a nontrivial even placement. If $C \in \mathcal{C}_B$, then C has an odd placement. □

Theorem 4.2. *Let C be an $m \times n$ checkerboard, where $1 \leq m \leq n$ and $n \geq 2$. If $C \in \mathcal{C}_R - \mathcal{C}_B$, then let Y be the associated sequence obtained by Algorithm 3.15.*

(A) *C has a nontrivial solution to each of* Problems 1.1 *and* 1.2 *if and only if either* (i) *$C \in \mathcal{C}_R - \mathcal{C}_B$ and the last two terms in Y are not equal or* (ii) *$C \in \mathcal{C}_B$ and $m \equiv n \equiv \ell \pmod{\ell + 1}$ for some integer $\ell \geq 2$.*

(B) *C has a nontrivial solution to* Problem 1.1 *but not to* Problem 1.2 *if and only if $C \in \mathcal{C}_R - \mathcal{C}_B$ and the last two terms in Y are equal.*

(C) *C has a nontrivial solution to* Problem 1.2 *but not to* Problem 1.1 *if and only if $C \in \mathcal{C}_B$ and there is no integer $\ell \geq 2$ such that $m \equiv n \equiv \ell \pmod{\ell + 1}$.*

We conclude this paper with related open questions.

Problem 4.3. If a checkerboard has a nontrivial solution to Problem 1.1 (or 1.2), how many solutions (up to symmetry) are there? Which checkerboards have unique nontrivial solutions?

Problem 4.4. If a checkerboard has a nontrivial solution to Problem 1.1 (or 1.2), what is the minimum number of coins necessary to construct such a solution? Also, what is the maximum number of coins that can be used in a solution?

Acknowledgments

We are grateful to the referee whose valuable suggestions resulted in an improved paper.

References

[Okamoto et al. 2010] F. Okamoto, E. Salehi, and P. Zhang, "A checkerboard problem and modular colorings of graphs", *Bull. Inst. Combin. Appl.* **58** (2010), 29–47.

[Okamoto et al. $\geq$ 2010] F. Okamoto, E. Salehi, and P. Zhang, "A checkerboard theorem", preprint.

Received: 2009-09-13 Revised: 2009-12-23 Accepted: 2009-12-29

meaghan.m.heires@wmich.edu *Department of Mathematics, Western Michigan University, Kalamazoo, MI 49008, United States*

ryan.c47.jones@wmich.edu *Department of Mathematics, Western Michigan University, Kalamazoo, MI 49008, United States*

okamoto.futa@uwlax.edu *Mathematics Department, University of Wisconsin, La Crosse, WI 54601, United States*

willem.a.renzema@wmich.edu *Department of Mathematics, Western Michigan University, Kalamazoo, MI 49008, United States*

matthew.j.roberts@wmich.edu *Department of Mathematics, Western Michigan University, Kalamazoo, MI 49008, United States*

Guidelines for Authors

Authors may submit manuscripts in PDF format on-line at the Submission page at the Involve website.

Originality. Submission of a manuscript acknowledges that the manuscript is original and and is not, in whole or in part, published or under consideration for publication elsewhere. It is understood also that the manuscript will not be submitted elsewhere while under consideration for publication in this journal.

Language. Articles in *Involve* are usually in English, but articles written in other languages are welcome.

Required items. A brief abstract of about 150 words or less must be included. It should be self-contained and not make any reference to the bibliography. If the article is not in English, two versions of the abstract must be included, one in the language of the article and one in English. Also required are keywords and subject classifications for the article, and, for each author, postal address, affiliation (if appropriate), and email address.

Format. Authors are encouraged to use LaTeX but submissions in other varieties of TeX, and exceptionally in other formats, are acceptable. Initial uploads should be in PDF format; after the refereeing process we will ask you to submit all source material.

References. Bibliographical references should be complete, including article titles and page ranges. All references in the bibliography should be cited in the text. The use of BibTeX is preferred but not required. Tags will be converted to the house format, however, for submission you may use the format of your choice. Links will be provided to all literature with known web locations and authors are encouraged to provide their own links in addition to those supplied in the editorial process.

Figures. Figures must be of publication quality. After acceptance, you will need to submit the original source files in vector graphics format for all diagrams in your manuscript: vector EPS or vector PDF files are the most useful.

Most drawing and graphing packages (Mathematica, Adobe Illustrator, Corel Draw, MATLAB, etc.) allow the user to save files in one of these formats. Make sure that what you are saving is vector graphics and not a bitmap. If you need help, please write to graphics@mathscipub.org with details about how your graphics were generated.

White Space. Forced line breaks or page breaks should not be inserted in the document. There is no point in your trying to optimize line and page breaks in the original manuscript. The manuscript will be reformatted to use the journal's preferred fonts and layout.

Proofs. Page proofs will be made available to authors (or to the designated corresponding author) at a Web site in PDF format. Failure to acknowledge the receipt of proofs or to return corrections within the requested deadline may cause publication to be postponed.

involve
2010 vol. 3 no. 1